Trabecular ontogeny of the gorilla third metacarpal

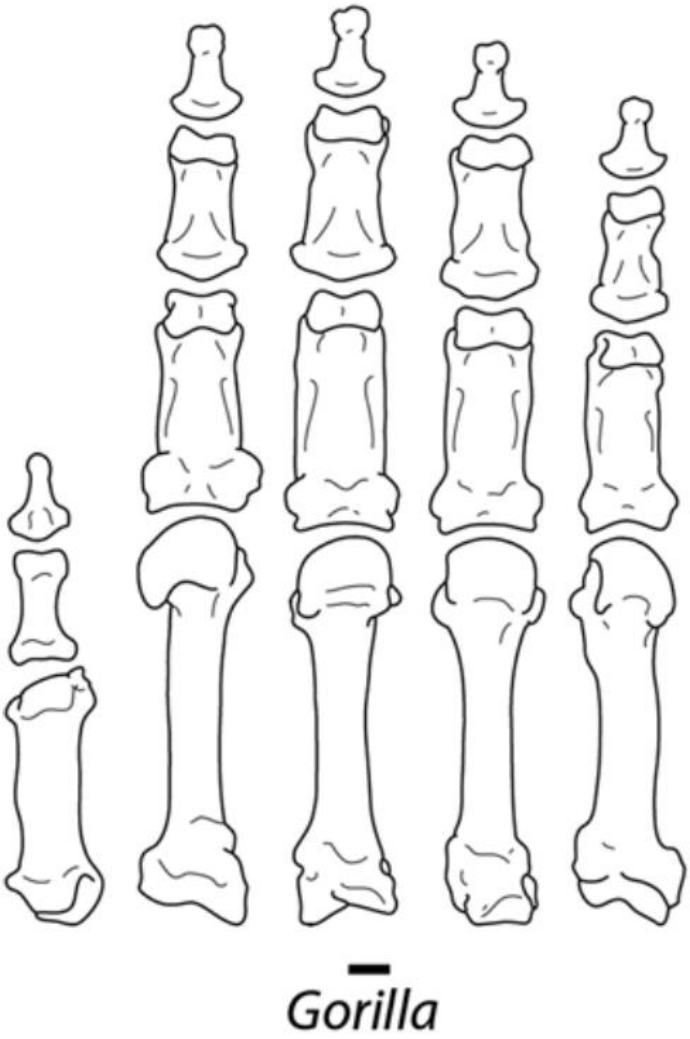

By Kim Deckers

SBRC
Skeletal Biology Research Centre

University of Kent

Trabecular ontogeny and morphology of the gorilla third metacarpal

Kim Antonia Paulina Maria Deckers

Student ID – 17902978

kapd2@kent.ac.uk

School of Anthropology and Conservation

University of Kent

Project supervisors – Dr. Tracy Kivell

Dr. Matthew Skinner

Cover picture (Patel and Maiolino 2016)

Acknowledgements

I would like to start by thanking Dr. Tracy Kivell and Dr. Matthew Skinner for accepting me as their student five years ago and for giving me the opportunity to have access to their resources and laboratories to learn new imaging and analysis techniques. I also want to thank them for their support and guidance while I was undertaking my own research and for their support and understanding when my research was interrupted by health issues. I could not have finished this project without their support and will be forever grateful for it.

Thanks also to Inbal Livne (Powell-Cotton Museum) and Frieder Mayer and Christiane Funk (Museum für Naturkunde Berlin) for access to the western lowland gorilla specimens. I am also grateful to Dr. Shannon McFarlin for facilitating access to the Virunga mountain gorilla specimens and to the Rwandan government for permission to study skeletal remains curated by the Mountain Gorilla Skeletal Project (MGSP).

I would also like to thank Dr. Chris Dunmore and Dr. Zewdi Tsegai for their instruction on how to use medtool, and for being my continued technical support when something with the program went wrong. I would also like to than Zewdi for being willing to CT scan a part of my data sample when I was unable to.

Thanks also to my mother, Marina de Blok, for being my biggest fan during my academic journey and especially this year. None of this would have been possible without her past financial and moral support.

Finally, I would also like to thank the University of Kent for awarding me the Vice Chancellor's Research Scholarship, without which I could not have undertaken this research.

Abstract

The trabecular bone morphology of adult extant primates has been shown to reflect mechanical loading patterns related to locomotion. However, ontogenetic studies of humans and other mammal species has shown that there may be an adaptive lag between trabecular response and current mechanical loading patterns, which could result in adult trabecular bone morphology reflecting juvenile behaviours. This study investigated ontogenetic changes in the trabecular bone structure of the third metacarpal of mountain (n = 26) and western lowland gorillas (n = 26) and its relationship to changes in loading patterns. Results show that trabecular bone reflects mechanical loading throughout ontogeny. Bone volume fraction, trabecular thickness, and trabecular number are low at birth and increase with age. Degree of anisotropy was variable throughout ontogeny and showed no clear pattern. A high concentration of bone volume fraction can be observed on the palmar side of the third metacarpal in early life, reflecting the high frequency of climbing, suspensory, and play behaviours of young gorillas. This concentration moves to the dorsal side as terrestrial knuckle-walking becomes the primary form of locomotion around 5 years of age. Fusion of the epiphysis often did not take place until 8 – 12 years of age, and overall trabecular patterning did not fully reflect adult patterns until fusion was complete, suggesting there is a lag between adult-like behaviours and adult-like trabecular morphology. No differences were found between mountain and western lowland gorillas.

Table of Contents

1. Introduction

Modern humans are the only living primate species to practice habitual bipedalism as their main form of locomotion and to use their upper limbs primarily for manipulation. This unique locomotory pattern has been used to define whether specific fossil specimens should be included or excluded from the hominin lineage. However, differing interpretations of fossil hominin external skeletal morphology have proven it difficult to reconstruct the behaviour of some of these fossil species. Debate continues over the ancestral locomotion pattern of the last common ancestor of chimpanzees and humans. Some have argued that features such as limited wrist extension in *Australopithecus anamensis* and *Australopithecus afarensis*, as well as chimpanzees and gorillas, suggests that the last common ancestor practiced knuckle-walking (Richmond and Strait, 2000; Richmond 2006), while others have suggested that the differing ontogenetic development of gorilla and chimpanzee carpal bones, combined with the lack of evidence of knuckle-walking features in early hominin upper limb morphology, indicate that the last common ancestor was more arboreal (Dainton and Macho, 1999; Kivell and Schmitt, 2009). Another cause for debate has been the exact timeline in which habitual bipedalism developed and all arboreal behaviours ceased. The persistence of skeletal features related to arboreal locomotion and climbing in the upper limb of hominins such as *Au. afarensis* and *Australopithecus sediba* has been interpreted by some researchers to show that these species were both bipeds and arborealists (Stern 2000; Green et al. 2007; Green and Alemseged, 2012; Churchill et al. 2013), while others argue that the presence of arboreal features in bipedal species is merely a retention of an ancestral skeletal pattern and not related to their locomotion patterns or behaviour (Haile-Selassie *et al.* 2010; Latimer and Lovejoy, 1990; Ruff et al. 2016; Ward et al. 2011). Lastly, uncertainty has also been

stated over the timing of when the upper limb, and especially the hand, developed the manipulative dexterity required to make tools. Evidence suggests that the first stone tools appeared around 3.3 million years ago (Harmand et al. 2015). However, recent finds of apparent tool use on bone in strata related to *Australopithecus* instead of *Homo habilis* have indicated that the advent of tool use may have occurred much earlier (Panger *et al.* 2002; McPherron et al. 2010; 2011; but see Dominguez-Rodrigo et al. 2012). This is supported by evidence of the internal bone structure of the hand of *Australopithecus africanus* (Skinner et al. 2015), as well as the scapular morphology of *Australopithecus afarensis* (Young et al. 2015). Though debate persists, as both these studies have been criticized by others in the field that have argued these features are not indicators of tool use, but merely artefacts of increased bipedal terrestriality (Almecija et al. 2015; Melillo, 2015), or that overall outer bone morphology limits hand use in these species (Rolian et al. 2011).

Recent advances in imaging techniques have increased the interest of palaeoanthropologists of the trabecular bone structure of living humans and non-human primates to reconstruct fossil hominin behavior. Trabecular bone has been shown to respond to mechanical loads exerted on it during locomotion (Rafferty and Ruff, 1994; Majumdar et al. 1998; Ulrich et al. 1999; Müller, 2005; Bevill et al. 2006; Pontzer et al. 2006). Furthermore, trabecular bone has a faster remodeling rate than cortical bone (Mullender et al. 1998; Ortner, 2003), which means that its morphology will reflect changes in mechanical loading faster than cortical bone would and may be less constricted by phylogeny (Skinner et al. 2015). This would suggest that variation in trabecular architecture between fossil and extant primate species may be especially useful when reconstructing behaviour from skeletal elements. However, studies focused on the reconstruction of behaviour using trabecular architecture in living

primates have shown varying results, with some showing that trabecular morphology of the hind limbs can be used to distinguish between different locomotory categories (Ryan and Ketcham 2002; Ryan and Shaw 2012 (extant); Barak et al. 2013b;Su et al. 2013 (fossil)), while others show no such distinction (Ryan and Walker, 2010 (extant); DeSilva and Devlin, 2012 (fossil)). The primate upper limb has been especially problematic with regards to using trabecular bone to reconstruct behaviour, as findings have not been consistent with predictions of loading and locomotion during life (Ryan and Walker, 2010; Ryan and Shaw, 2012; Scherf et al. 2013; Schilling et al. 2014) A more detailed discussion of these findings can be found later in the chapter.

Trabecular bone morphology is not only determined by mechanical loads during life; its development is also influenced by a number of factors, such as metabolic rates, phylogenetic constriction, diet and hormone levels (Mullender et al. 1998; Seto et al. 1999; Eckstein et al. 2007; Cunningham and Black, 2009; Tsegai et al. 2018b; Ferretti et al. 2019), any of which may be an explanation for the discrepancy in results found in studies of extant primate trabecular bone. Another complicating factor may be ontogeny. Loading during ontogeny has been shown to influence epiphyseal morphology (Carter, 1987; Carter et al. 1989), cortical bone morphology (Ruff, 2003), femoral bicondylar angle (Tardieu, 1999), and phalangeal curvature (Richmond, 2007). During ontogeny primates undergo not only physical changes as they grow, but also behavioural changes. Mechanical loading patterns begin influencing skeletal development in the very early stages of ossification (Carter et al. 1991). In non-human primates, grasping abilities play a major role throughout ontogeny (Doran, 1997; Thorpe and Crompton, 2006; Sarringhaus et al. 2014). In early life, non-human primates mainly use their hands to grab onto their mother's body, but after the shift to autonomy the hands are used for many more activities, such as feeding

and locomotion (Druelle et al. 2017). Almost all studies reconstructing behaviour from primate trabecular bone morphology are done on adult specimens. This may be problematic, as bone remodels at a much faster rate during early ontogeny than it does in adulthood (Currey, 2002). Thus, the trabecular microarchitecture observed in adult specimens may in fact be reflecting the mechanical response of trabecular bone to juvenile behaviours, instead of adult locomotion patterns. Despite the influence of ontogenetic patterns on mechanical adaptation, very little attention has been given to the trabecular morphology of immature primates. This is unfortunate, as studies of trabecular ontogeny in sheep (Nafei et al. 2000), pigs (Tanck et al. 2001), dogs (Wolschrijn and Weijs, 2004), and humans (Ryan and Krovitz, 2006; Gosman and Ketcham, 2009; Raichlen et al. 2015; Saers et al. 2020) have shown that loading patterns during development influence trabecular bone remodelling and that juvenile behaviours can influence adult trabecular bone morphology (Pettersson et al. 2010; Deckers, 2017) as well as adulthood (Best et al. 2017). So far, only two studies have focused on the juvenile primate upper limb (Tsegai et al. 2018a; Ragni, 2020), both of which found that trabecular bone morphology reflected mechanical loading during ontogeny, but that the ontogenetic development differed to the pattern found in humans (Ryan and Krovitz, 2006; Gosman and Ketcham, 2009; Raichlen et al. 2015; Saers et al. 2020). Understanding the development of the primate hand and upper limb during ontogeny is incredibly important, as the upper limb plays a pivotal role in locomotion, food acquisition, manipulation, and interactions with co-specifics (Pouydebat 2017). Furthermore, adult trabecular morphology of great apes is often used as a comparative sample to ascertain behavioural patterns in fossil hominins (e.g. Barak et al. 2013; Zeininger et al. 2016; Su and Carlson 2017; Chirchir 2019; Dunmore et al. 2020). However, without a thorough understanding of the ontogenetic influence

on juvenile and adult trabecular bone architecture, it is problematic to use variations in its morphology as a means of reconstructing fossil hominin behaviour, as extant primate trabecular morphology provides the necessary comparative context. This study attempts to rectify this gap in knowledge by analysing how the ontogenetic development of trabecular bone in the hand, specifically the third metacarpal, relates to known changes in frequency of locomotor behaviours of two gorilla species.

1.1 Study aims and hypotheses

The purpose of this study is to provide new data on the changes in trabecular bone variables during ontogeny in two gorilla species (western lowland and mountain gorillas) using a whole-bone approach. This study will focus on the internal bone structure of the third metacarpal. The third metacarpal was chosen as its central position within the hand means it experiences mechanical loading during most locomotor and manipulative activities (Tuttle 1969; Susman 1979; Sarmiento 1994; Matarazzo 2013; Neufuss et al. 2017). Furthermore, the third metacarpal has been comparatively well-studied in adult great apes (e.g. Chirchir et al; 2017; Dunmore et al. 2019; Matarazzo, 2015, Tsegai et al. 2013), which allows for a comparison of adult trabecular morphology to the juvenile data collected here. Using a whole-bone approach, this study will investigate if changes in trabecular bone structure reflect changes in the frequency of locomotor behaviour throughout ontogeny in gorillas. This study further aims to test whether small differences in behavioural frequencies, such as degree of arboreality, during the juvenile period between two gorilla subspecies (*Gorilla gorilla* and *Gorilla beringei*) can be detected in trabecular bone. This study predicts that:

1. Changes in trabecular bone morphology in the third metacarpal will follow the same pattern in ontogeny as have been previously observed in the upper limb of chimpanzees (Tsegai et al 2018a). This means that we expect that bone volume fraction (ratio of bone volume to total volume) will initially be low and increase throughout ontogeny. We expect the degree of anisotropy (preferred orientation of individual trabeculae) to remain relatively constant throughout life in the base, as observed by Ragni (2020), and for anisotropy in the epiphysis to be initially isotropic (symmetry of orientation of individual trabeculae in all directions) as new bone is deposited and become more anisotropic as variation in locomotion decreases throughout ontogeny.

If changes in locomotor behaviour through ontogeny are reflected in the trabecular structure, we predict that:

2. During early ontogeny bone volume fraction will be highest in the palmar region of the metacarpal epiphysis, which reflects flexion on the third metacarpal during clinging and arboreal behaviours that dominate the early juvenile gorilla activity pattern (Doran, 1997). As knuckle-walking becomes the more dominant locomotor style, the third metacarpal is loaded in a hyperextended joint posture, which we predict to be reflected in the trabecular bone by a greater bone volume fraction being present in the dorsal region of the metacarpal epiphysis.

3. We expect to see the same shift from a palmar to dorsal concentration of bone volume fraction in the distal metaphysis and the metacarpal base. However, any changes related to locomotor behaviours in the trabecular bone will be less pronounced in these regions than in the epiphysis given the limited mobility at the

carpometacarpal joint (base) and the influence of bone modelling and remodelling occurring at the growth plate (distal metaphysis) during ontogeny.

4. Trabecular structure will begin to differ between species around 4 years of age, when mountain gorillas shift from a mixture of arboreal and terrestrial locomotor behaviours to mainly terrestrial knuckle-walking (Doran, 1997), while western lowland gorillas maintain some arboreal behaviour throughout ontogeny (Remis, 1995; Ruff et al. 2013). This shift will be reflected in relatively greater BV/TV and DA in the dorsal region of the mountain gorilla metacarpal epiphysis compared with western lowland gorillas.

2. Literature Review

This literature review is divided into three main sections. As this study focuses on the locomotor and positional behavioural changes that occur throughout the life of western lowland (*Gorilla gorilla)* and mountain gorillas (*Gorilla beringei*) and its effect on trabecular bone, an understanding of not only behavioural ontogeny, but also of biomechanics and trabecular bone development, is necessary to understand the aims of this research.

The first section focuses on the changes in behaviour, both locomotory and positional, in both gorilla species. This will include descriptions of different types of locomotion practiced by *Gorilla* species, their biomechanics on the relevant bones, and detailed descriptions of activity patterns and behavioural frequencies for each age category.

The second section will lay the groundwork necessary to understand the ontogenetic analysis of trabecular bone by outlinng the overall processes involved in bone modelling and remodelling.

The third section will give a very brief overview of the morphology of the third metacarpal.

The fourth and final section will discuss previous studies of trabecular bone morphology in primates, and how these findings inform the aims and hypotheses of this study.

2.1 Behaviour and Biomechanics

2.1.1 Ontogeny of Gorilla Locomotor Behaviour

Terrestrial knuckle-walking is the most frequently used form of locomotion for all *Gorilla* species (Doran 1997; Remis 1995; Remis 1998) but there is substantial variation in the degree of aboreality among individuals within and between each species. Unfortunately, detailed data on changes to locomotion and activity patterns during ontogeny has only been published (Fig. 1) for the mountain gorilla (*Gorilla beringei*) populations located in the Virunga Mountains of Rwanda (Doran 1997) and the information relayed below is thus based solely on the observations of this species. However, until approximately 4 years of age, when terrestrial knuckle-walking frequency increases, the ontogenetic behavioural pattern of western lowland gorillas (*Gorilla gorilla*) is thought to be remarkably similar to that of mountain gorillas (Remis 1995). However, small differences in other factors which may influence behaviour and locomotion have been observed. For example, western lowland gorillas are generally weaned a year later than mountain gorillas (Breuer et al 2008; Stoinski et al 2013), which extends the period of which the former is dependent on the mother and would most likely remain close to her. Furthermore, it has been shown that in general females experience skeletal growth spurt (both the initial one at age 1-2 years) and the prepubescent spurt) before males in both species (Shea 1981; Leigh and Shea 1996; Taylor 1997), but that these growth spurtsalso occurs earlier in mountain gorillas than western lowland gorillas. This may have some influence on the timing and appearance of certain behaviours, such as the time when terrestrial knuckle-walking becomes dominant. As there is currently no data available on ontogenetic behaviour for western lowland gorillas, this study has worked under the assumption that these differences would not make a large impact on the results and uses the

mountain gorilla behavioural data (Doran 1997) to inform its age and behavioural categories.

Gorillas spend the first six months of their life clinging to their mother and thus do not engage in independent locomotor behaviour (Doran 1997). During the first months of life, positional behaviour is forelimb dominated and characterised by crawling and climbing on the mother's abdomen. Between approximately six and 10 months of age, locomotor activity increases significantly with nearly 60% of all locomotion occurring above ground, and 39% of this being primarily palmigrade quadrupedal locomotion (Doran, 1997). Palmigrade quadrupedal locomotion refers to using a flat hand, where the palm touches the substrate, to move around. By 6 months of age, locomotion activity of infant gorillas begins to expand, occurs on a number of substrates (ground, branches, rocks, etc), and includes quadrupedal locomotion. However, at this time a gorilla's quadrupedalism is almost entirely palmigrade. Aside from being weight-bearing during quadrupedalism, the forelimbs are now also frequently used by infants to pull themselves up into a bipedal stance (Doran, 1997).

Between 10 and 15 months of age, knuckle-walking becomes increasingly more frequent (and palmigrady less frequent) and arboreal behaviours (suspension and vertical climbing) become more frequent as well. By 15 months, quadrupedal locomotion is the most practised locomotor activity and knuckle-walking quadrupedalism becomes more frequent. During this time behaviours such as climbing, rolling, arm-hanging, and jumping also become more frequent (5.9% of overall behaviour). Although the degree of terrestrial quadrupedalism is increasing, almost 40% of locomotion is undertaken in an arboreal environment (Doran 1997). Suspension and vertical climbing increases until approximately two years of age, when

knuckle-walking then becomes the primary form of quadrupedal locomotion and climbing behaviours start to decrease (though still much higher than in adults).

A significant decrease in arboreal locomotion behaviours can be observed by 4 years of age and terrestrial knuckle-walking reaches adult-like frequency at this time (85% of all locomotion). After age 4, locomotion is similar to that observed in adult gorillas (Doran, 1997).

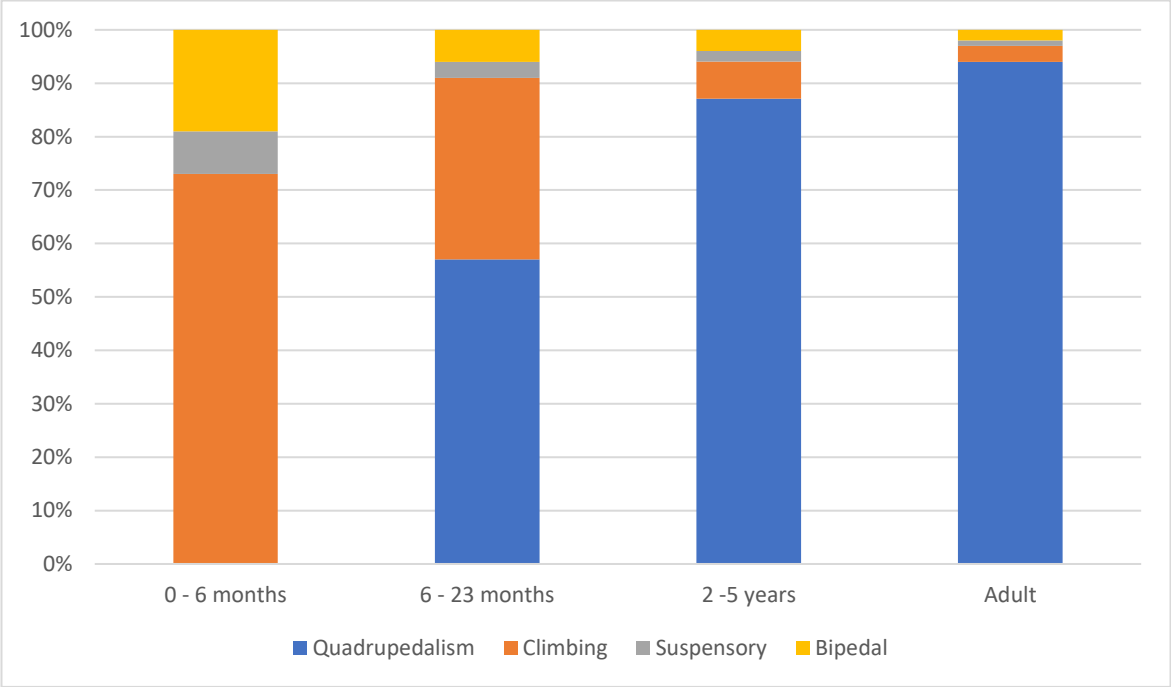

Figure 1. Simplified locomotor activity budget of *Gorilla beringei beringei* throughout ontogeny (based on Doran, 1997)

While there is little information on ontogenetic behaviours of immature western lowland gorillas (*Gorilla gorilla*), observations of adult individuals have shown that adult western lowland gorillas are more arboreal than adult mountain gorillas (*Gorilla beringei*). Remis (1995;1998) has reported that western lowland gorillas spend at least 20 percent of their time engaging in arboreal behaviours, while adult mountain gorillas spend at least 90% of their time practicing terrestrial knuckle-walking (Doran 1997), and up to 98% in male adults in particular (Doran 1997). These

differences in arboreality are most likely driven by differences in diet. Mountain gorillas are mainly herbivorous, choosing to mainly eat plants and herbs that are readily available in their habitat year-round (Doran and McNeilage 1998). In contrast. Western lowland gorillas are more frugivorous, choosing to eat high quality fruits when available and relying on other plant material when fruits are not in season (Remis et al. 2001; Doran et al. 2002). The frugivorous diet of western lowland gorillas would not only cause this species to be more arboreal, but to also have larger home ranges due to the spacing of fruit throughout the habitat (Doran and McNeilage 2001), which would cause adult individuals and independent juvenile western lowland gorillas to perhaps spend more time practicing vertical climbing, as well as terrestrial knuckle-walking. If western lowland gorillas do have a higher frequency of these behaviours, it may influence trabecular bone structure. Due to a lack of ontogenetic data for western lowland gorillas, it is currently unclear at what life stage these differences in frequency of arboreality and other locomotion occur.

2.1.2. Third Metacarpal Morphology

This study focuses on the third metacarpal. This is a small long bone located in the third ray of the primate hand (Figure 2). In general, the third metacarpal can be divided into three main sections: the base, the shaft, and the head (Patel and Maiolino 2016). In adult gorilla, all metacarpals are relatively short compared to modern humans, and the third metacarpal is the second largest of the five rays. The head and base of the metacarpal are of relatively the same size, but have different shapes. Overall, the base of the gorilla third metacarpal is more rectangular in shape, while the head is more circular (Patel and Maiolino 2016). The base articulates with the second metacarpal on its lateral surface and the fourth metacarpal on its medial side, and the capitate on its inferior surface. The head articulates with the proximal third phalange. In gorilla the head tends to show a compression on the dorsal surface compared to the palmar surface (Susman 1979). The shaft tends to be straight on the dorsal surface and concave on the palmar. Muscle entheses on the palmar surface of the gorilla third metacarpal also give a more triangular appearance to the palmar aspect of the shaft (Susman 1979).

In immature individuals, the appearance of the metacarpal is slightly different. The shaft is straight and narrow, with a less concave appearance palmarly. The base is less defined and does not yet show the inferior protrusion of the articular surface with the second metacarpal (figure 2) (Baker et al. 2005). The epiphysis is not yet present, thus the metacarpal head is absent. Instead, the shaft ends at the epiphyseal growth plate, which causes the distal metacarpal to have a flat horizontal surface distally.

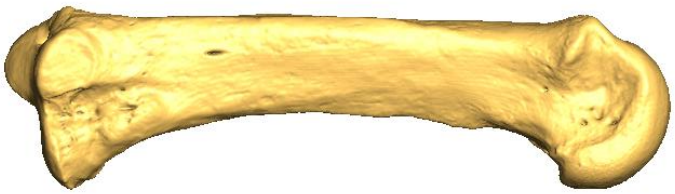

Figure 2. 3D Surface model of an adult mountain gorilla third metacarpal. The base is left, the head is right, the dorsal surface is superior, the palmar inferior.

2.1.3 Biomechanics of Adult Gorilla Locomotion

To adequately study the link between trabecular morphology and mechanical loading throughout life, it is important to understand the locomotor behaviours of the primate species under study, and how these behaviours may change (both in posture and frequency) throughout ontogeny. The type of locomotion practised by primate species often influences the degree of motion that their joints are capable of, and thus influences how weight will be transferred throughout the skeleton during movement.

The main type of locomotion of gorillas after the age of four years is terrestrial knuckle-walking. As in other quadrupedal primates, knuckle-walkers bear weight on both their forelimbs and hindlimbs. During knuckle-walking, the upper limb is held in an extended position, while the hand makes contact with the substrate. A simplified illustration of the forces acting on the hand during knuckle-walking can be seen in figure 3.

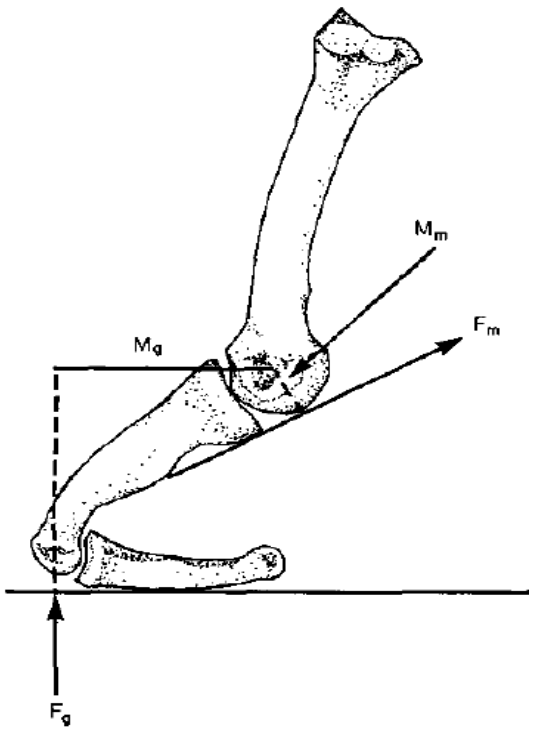

Figure 3. The third metacarpal and phalanges of gorilla in knuckle-walking position. F_g refers to ground reaction force, F_m is the muscle force, M_g and M_m are the respective moment arms of those forces. As seen in Inouye (1994).

Weight is borne by the dorsal side of the intermediate phalanges II-V of the fingers, while metacarpophalangeal joints are held in a hyperextended position in line with the other wrist bones (Aiello and Dean 1990; Wunderlich and Jungers 2009; Kivell et al. 2016). The central position of the third metacarpal within the hand means that it is regularly used during most locomotor and manipulative activities, and thus it directly or indirectly experiences external reaction forces and is somewhat buffered from radioulnar forces. A study of pressure distribution during terrestrial knuckle-walking in captive lowland gorillas showed that peak pressures were highest on the third digit (Matarazzo, 2013). During knuckle-walking, the metacarpophalangeal joint is hyperextended (Matarazzo, 2013; Susman, 1979; Tuttle, 1969). The central position of the third metacarpal within the hand means that it is regularly used during most locomotor and manipulative activities, and thus it directly or indirectly experiences

external reaction forces and is somewhat buffered from radioulnar forces. A study of pressure distribution during terrestrial knuckle-walking in captive lowland gorillas showed that peak pressures were highest on the third digit (Matarazzo, 2013). Trabecular bone density and bone volume fraction on the dorsal side of the metacarpal head indicates that this region undergoes significant compressive forces in the metacarpophalangeal joint during knuckle-walking (Zeininger et al 2011; Tsegai et al. 2013). The base is aligned with the rest of the wrist in a proximodistal direction (Sarmiento 1985) and has two ligamentous attachments, and mainly undergoes compressive forces in the same direction during knuckle-walking.

While the wrist is in a close-packed position, the metacarpophalangeal joints hyperextend. The dorsal sides of the metacarpal heads of knuckle-walking species have often developed transverse ridges. These ridges are especially prominent on the third and fourth digit, as these transfer the most weight to the rest of the upper limb during locomotion (Aiello and Dean 1990; Inouye 1992; Wunderlich and Jungers 2009; Kivell et al. 2016). This is reflected in the robusticity of the metacarpals. When comparing robusticity of metacarpals of knuckle-walking species to other non-human primates, it has been shown that the third and fourth metacarpals of knuckle-walkers are much more robust than seen in orangutan and humans (Marchi 2005). The shortened appearance of the proximal phalanges, compared to other quadrupedal species, may be beneficial to reducing joint and ground reaction forces in knuckle-walking species (Aiello and Dean 1990).

Aside from knuckle-walking, gorillas also frequently participate in vertical climbing (though their behaviour is not limited to these two behaviours). During vertical climbing the forelimb is mainly involved in positioning the trunk close to the substrate, and aiding in pulling up the body, while the hind limb provides most of the

propulsive power during climbing (Neufuss et al. 2017). The upper limb's main movement during vertical climbing is elbow flexion, though this changes to extension on larger substrates (Hunt et al. 1996). A comparison of vertical climbing in bonobos and gorillas showed that bonobos pulled their humerus closer to their trunk, and increased flexion in their elbow joint than gorillas (Isler 2005). A separate comparison of vertical descent between chimpanzees and gorillas showed that gorillas show a greater degree of ulnar deviation at the wrist. These differences in position of the joint during locomotion could affect joint loading patterns and weight transfer, and may ultimately influence trabecular morphology. During climbing or manipulative grasping, the metacarpophalangeal joint is typically flexed to varying degrees depending on the size of the substrate or object (Neufuss et al. 2017; Sarmiento 1994) This results in tensile forces at the head of the metacarpal, as well as the base, though the latter has less freedom of movement and may also experience some compressive force, depending on the wrist posture during climbing (Figure 4).

Figure 4. Hand posture of gorilla while grasping. Arrow shows directionality of the force acting on the metacarpophalangeal joint. As seen in Zeininger et al. (2011).

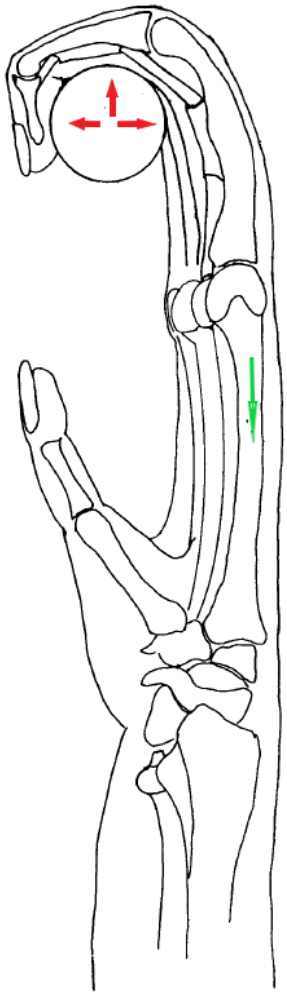

Arboreal behaviour does not only include climbing, but also suspension. This is when the hand is elevated above the body and carries all the body weight and is hooked over the supporting substrate (See Fig 5). During suspensory behaviour the centre of mass of the gorilla is below the structural support, which causes tensile forces in the hand and upper limb of the animal (Schwartz et al 1989). During suspensory hand postures, the phalanges make contact with the substrate while the metacarpals do not (Fleagle 2013). While compressive forces act on the phalanges as they hold on to the substrate (Richmond 2006), the third metacarpal (both base and head) mainly experiences proximodistal tensile forces, and the metacarpophalangeal joint experiences flexion (Schmitt et al. 2016).

Figure 5. The hand during suspensory locomotion. The red arrows reflect the reaction forces from the substrate, while the green arrow shows the tensile forces acting on the third metacarpal. Modified from Sarmiento (1988).

2.2 Bone Development

Reconstructing behavioural patterns through trabecular bone variables does not only require an underlying understanding of the types of locomotion and biomechanical influences that a juvenile primate undergoes throughout life, it also requires an understanding of how bone itself develops. The following section briefly summarises the process of bone development and remodeling in modern humans, which has been shown to be very similar to remodeling in other animals (Christen et al. 2015). Finally, a short overview is given of the ontogenetic development of the long bones of modern humans (Scheuer et al. 2000), and the current information available about great ape bone development.

2.2.1 Trabecular Bone Modelling

To understand how changes in locomotion during ontogeny affect trabecular microarchitecture, it is necessary to understand how bone develops and remodels throughout life. Compared to other mammals, the primate upper limb is relatively primitive in its anatomy and development. Most of the research on the early development of primates has been done on humans. Bone modelling refers to the process where osteoblasts and osteoclasts work to shape or reshape bone. This process is what allows for skeletal development and longitudinal long bone growth during ontogeny, while being responsible for periosteal expansion in adult life (Langdahl et al. 2016). The development of human limb buds occurs during the embryonic period (0 – 2 weeks prenatally). During the first weeks after conception the mesenchyme (matrix undifferentiated connective tissue) initiates limb bud outgrowth by secreting

human growth factor. During the formation of the upper limb, elements form in a conserved sequence from most proximal to most distal (Rolian 2016).

The earliest ossification processes occur prenatally. By week seven of fetal life, most of the rudimentary musculoskeletal elements have formed, though ossification is often just beginning (Carter et al. 1991). Trabecular bone develops through two types of ossification processes; intramembranous ossification and endochondral ossification. Intramembranous ossification mainly occurs through the transformation of mesenchymal tissue (Scheuer et al. 2000). During intramembranous ossification, mesenchymal cells differentiate into osteoblasts which cluster together to form the ossification centre. The osteoblasts secrete bone matrix and osteoid, which then calcifies. The periosteum, as well as trabecular bone, is formed through the accumulation of osteoid. Finally, the trabecular bone adjacent to the periosteum is replaced with lamellar bone, while the trabeculae in the internal bone structure remain and become oriented to loading directions. Endochondral ossification occurs by the transformation of cartilage (figure 6). During this process, a bone collar forms around the diaphysis, which mainly consists of hyaline cartilage and is responsible for the formation of cortical bone (Rolian 2016). Slowly, the cartilage in the centre of the diaphysis begins to calcify (Huiskes 2000). Subsequently, osteocytes begin to invade the internal cavities created during the calcification of the internal diaphysis and trabecular bone starts to form. As the ossification process continues, the diaphysis elongates, secondary ossification centres begin to form in epiphyses, and a medullary cavity begins to take shape. Lastly, the epiphyses ossify, leaving only cartilage in the epiphyseal growth plates between the shaft and the epiphyses (Marieb et al. 2014).

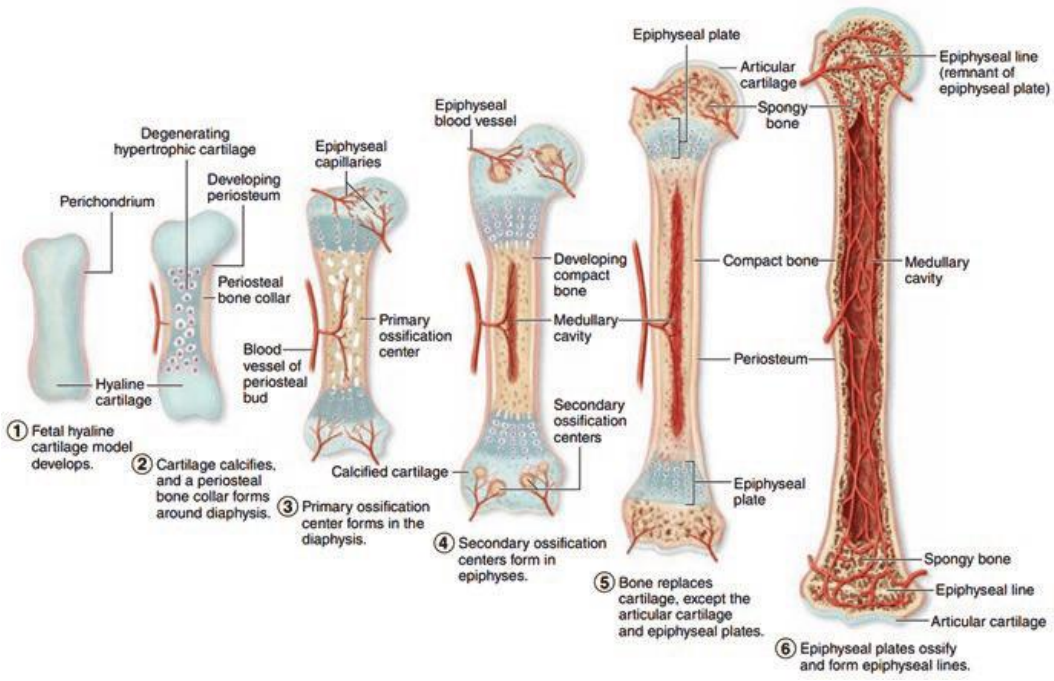

Figure 6. Endochondral ossification process of human long bones (Gasser and Kneissel 2017)

In foetuses and subadult humans, growth is mainly realised by changes to the cartilaginous tissue near the epiphyseal growth plate (Byers et al. 2000) (Figure 7) . The cartilage cells in the resting zone, the area closest to the epiphysis, are small and inactive (Scheuer et al. 2000). The shape of the cartilage cells changes as they enter the proliferation zone. Here, the cartilage cells stack on top of each other, creating columns through miotic division. Chrondroblasts at the top of these stacks divide at high speed, which pushes the epiphyses away from the diaphysis. The next zone of the epiphyseal plate is called the hypertrophic zone. In this zone chondrocytes cause the surrounding matrix to ossify. Finally, in the calcification zone, the chondrocytes die. This process leaves trabeculae-like spindles of calcified cartilage on the diaphysis side of the epiphyseal plate. In time, osteoclasts will partly erode these cartilaginous trabeculae, before osteoblasts deposit bone and the mature trabecular structure is created (Marieb et al. 2014). Bone morphology at the epiphyseal growth plate seems to be heavily influenced by the mechanical stresses it incurs during the process of bone formation. The newly forming trabeculae in the epiphyseal growth plate are oriented

to withstand the mechanical stress it is undergoing during the ossification process (Bertram and Schwartz 1991).

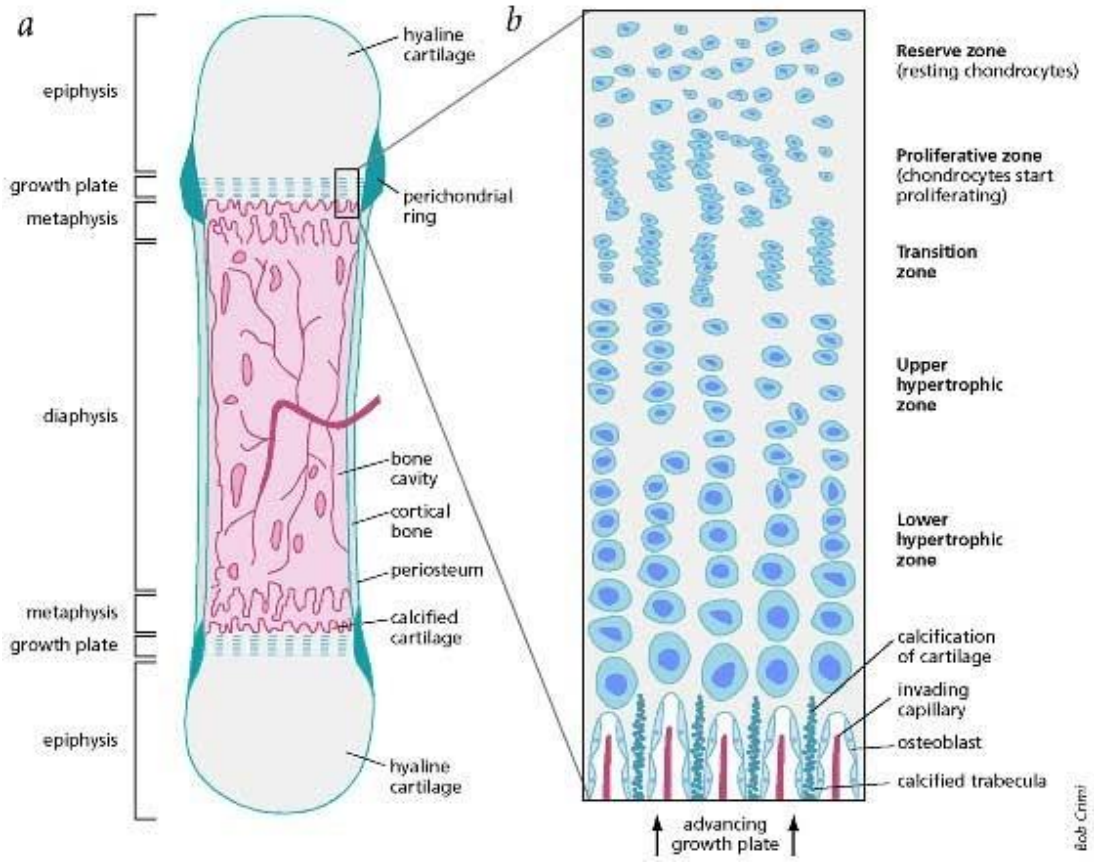

Figure 7. Schematic of the changes in chrondroblast morphology and ossification processes occurring at the epiphyseal or growth plate (As seen in Stickens and Evans 1998).

2.2.2 Trabecular Bone Remodelling

Bone remodelling is a homeostatic process. Bone mass is balanced through the resorption of bone by osteoclasts and the formation of bone by osteoblasts. Around 25% of trabecular bone is renewed every year by basic multicellular units, or BMU's (Huiskes et al. 2000; Ortner, 2003). BMU's consist of osteoclasts and osteoblasts. One of the main instigators of trabecular bone remodelling is changes in mechanical stress put on bone throughout ontogeny (Carter, 1987). The main purpose of bone is to be a stiff structure that supports the rest of the body, and it thus needs to be strong enough to withstand applied loads (Pearson and Lieberman, 2004). Mechanical loading causes

stress on the skeleton, which subsequently generates compressive or tensile strains within individual bones. The most common strains in long bones are compressive, and consist of axial compression, bending, twisting, and shearing forces (Pearson and Lieberman, 2004) (Figure 8). In mechanical loading from locomotion, a combination of these stresses usually occurs, and external and internal bone morphology influence how well a specific skeletal element can distribute the stresses it is under.

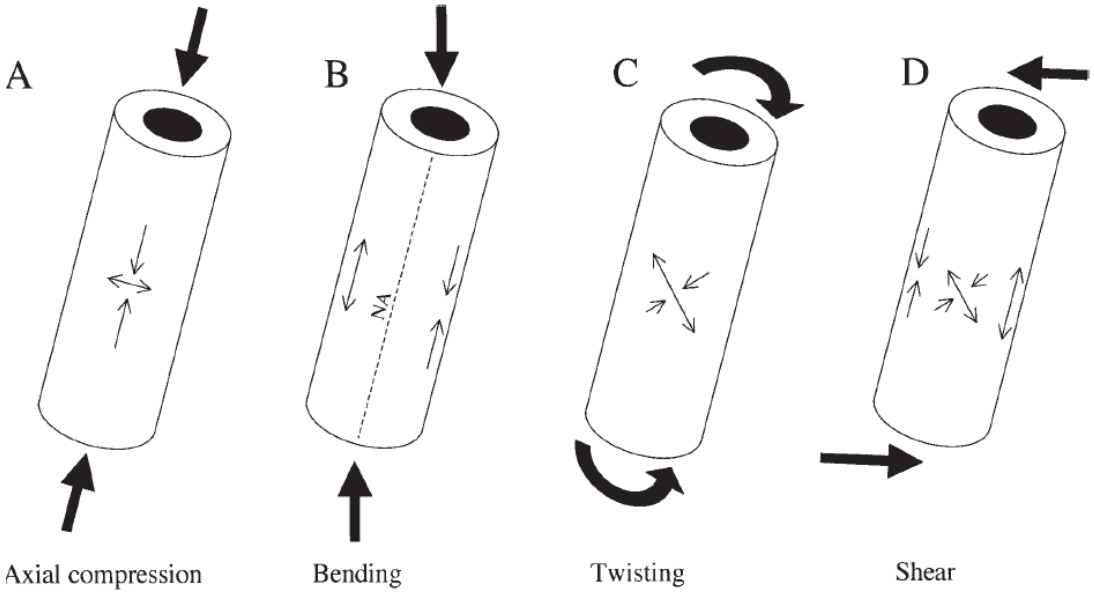

Figure 8. Cross-section view of compressive strain distribution. Thick arrows represent applied loading, thin arrows are subsequent strain in the bone (Pearson and Lieberman, 2004)

Loading stresses on bone generate signals within the BMU's that contribute to bone resorption and deposition (see figure 6). These signals are thought to be generated by changes in either hormone, vitamin, or cytokine levels or the diffusion of metabolites (Frost, 1998; Mullender et al. 1998; Fyhrie and Kimura, 1999). It is thought that bone remodelling is activated when a certain threshold of tissue loading is reached (Figure 9). Below this threshold bone is resorbed, while above this threshold bone is deposited (Frost 1998; Huiskes et al. 2000; Christen et al. 2014). Bone remodelling then continues until the loading stress falls beneath this threshold (Husikes et al. 2000).

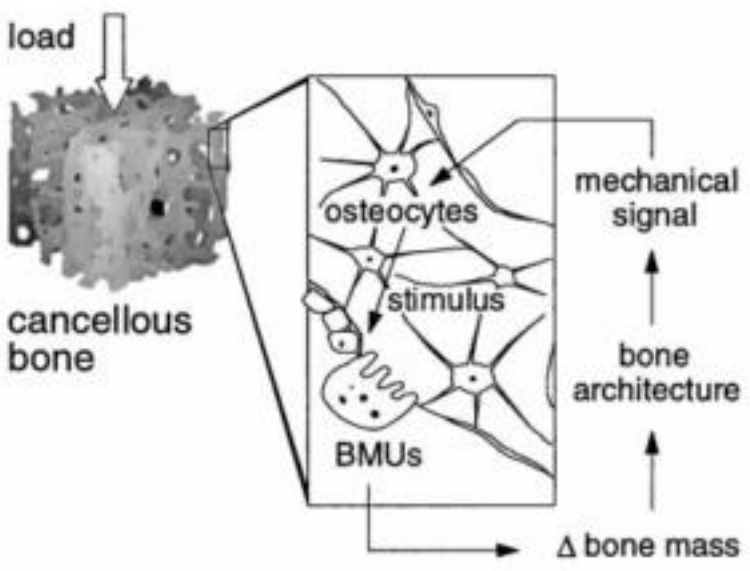

Figure 9. Trabecular bone remodelling response (Mullender et al. 1998)

In humans, the trabecular bone resorption phase takes approximately 33 days and the process of remodeling is slightly different than observed in cortical bone. While cortical bone remodeling involves the BMUs tunneling though bone, in trabecular bone remodeling occurs on top of the existing bone structures (Parfitt, 2003). During the resorption phase, osteoclasts remove bone mineral and create Howship's lacunae. Once enough bone is resorbed, the osteoclasts are deactivated and an intial layer of bone matrix is laid down within the Howship's lacunae. This is often referred to as the reversal phase, and can take up to 9 days in trabecular bone (Ortner, 2003). After the reversal phase, bone formation begins as osteoblasts are activated and transported to the Howship's lacunae, where they deposit collagen and osteocalcin at the resorption site, which will subsequently take approximately 175 days to mineralise. However, it should be noted that bone remodelling also occurs within the activation threshold limits, which suggests that though mechanical loading may be the main influence of bone remodelling, this mechanism is not purely driven by loading stress (Christen et al. 2014).

2.2.3 Developmental Timing of Bone Growth Apes

As detailed as the knowledge of the pre- and post-natal development of specific skeletal elements of modern humans is, just as fragmentary is the same record for bone ontogeny in other primate species. This may be due to the fact that bone remodelling and bone growth in mammalian species works by the same biological and mechanical processes as those observed in modern humans (Christen et al. 2014; Burr and Organ 2017). This would suggest that differences in timing of ossification patterns in primates may be largely due to differences in life history trajectories. Developmental patterns vary greatly across the apes. Adult bodily proportions often are not reached until long after the eruption of the third upper molar and sexual maturity is reached (Harvey and Clutton-Brock, 1985; Noordwijk and van Schaik, 2005). Male chimpanzees do not achieve full adult body proportions until 14-17 years of age, while gorillas not until 16 years of age orangutans are even slower to fully mature, with an average adult body size not being reached until 19-20 years of age (Watts and Pusey, 1993).

Sources on the exact development and timing of epiphyseal fusion of the primate skeleton are scarce. When sources are available, they often only discuss longitudinal growth differences between long bones. A study of bone length proportions in baboons indicates that the humerus increases slowly in length throughout most of the juvenile period, indicating a slow process of ossification in the humerus compared to the femur that may be related to developments in locomotion (Ruff, 2003). However, significant inter-species differences may exist between cercopithecoids and great apes. Velocity of maturation patterns in the ossification of the radius, ulna, and scaphoid of chimpanzees shows a different developmental pattern than observed in modern humans and the baboon humerus (Hamada et al. 2003). In

chimpanzees, an accelerated rate of bone development in the lower arm and scaphoid occurs from early infancy, until approximately 8 years of age. After this period, a deceleration of ossification is then observed from 8 to 12 years of age. The opposite is seen in humans, where maturation and ossification occurs gradually throughout the juvenile period, before accelerating in adulthood (Hamada et al. 2003). In general, the distal radial epiphysis is one of the earliest ossification centres to appear (Markze et al. 1987). Overall, the epiphyses of the upper limb ossify between 6 to 11 years old (Schultz 1940; Bolter and Zihlman 2012).An ontogenetic study of the development of the great ape carpal bones has shown that most carpals complete ossification around the same time as M3 eruption, between 10-12 years of age (Kivell, 2007), and the metacarpals are one of the last bones to fuse in chimpanzees, at 9 – 11 years old (Schultz 1940; Kerley 1966). Very little information is available for the timing of epiphyseal fusion of gorilla long bones. A study by Randall (1944) showed that the metacarpal epiphyses are some of the last to fuse, but did not include any information on a specific age range in which this would occur.

2.2.4 Metacarpal Bone Modelling and Remodelling

This study is focused on the third metacarpal, of which very little developmental data is available for non-human primates. As the general developmental trajectory of this bone in African apes (Kerley 1966; Bolter and Zihlman 2003) has been assumed to be similar to that of modern humans (Scheuer et al. 2000), we presume that bone modelling and remodelling processes in the gorilla third metacarpal will follow a similar pattern to that observed in humans.

In utero, a single primary ossification centre for the metacarpals 2-5 develops *in utero*, which is distally located on the metacarpal corpus (Rolian 2016). After birth and during early ontogeny, cartilage cells are deposited at the growth plate and subsequently ossify, which results in primary trabecular bone being laid down just underneath the growth plate (Scheuer et al. 2000). A secondary ossification centre develops during the first few years after birth, and is located in the epiphysis. In humans the epiphysis is usually identifiable by 10 months of age in females and 2.5 years of age in males (Baker et al. 2005), but their morphology is nondesdript and ovular until approximately 5 years of age, when adult-like morphology develops (Baker et al. 2005). As the bone matures and ossifies, primary trabecular bone is remodeled into secondary trabecular bone under the influence of systemic and mechanical loading. The third metacarpal epiphysis is fully fused in humans between 14-16 years of age (Scheur et al. 2000) and in chimpanzees by nine to 11 years of age (Schultz 1940; Kerley 1966) but has not been formally studied in gorillas.

2.3 Trabecular Bone Studies

Most of the early studies of trabecular properties were done on humans, as trabecular morphology tended to be studied in relation to the field of bioengineering (van Rietbergen et al. 1996; Majumdar et al. 1998; Mullender et al. 1998; Kabel et al. 1999 Ulrich et al. 1999). Early biomechanical analyses of human vertebral bodies have shown that trabeculae are generally oriented in the direction of the most intense load (Mullender et al. 1998; Kabel et al. 1999). This variable, often referred to as degree of anisotropy, combined with bone volume fraction, has been shown to be the two best predictors of bone biomechanical properties. Bone volume fraction could explain over

87 percent of variation in bone strength in the human radius, femur, vertebrae, and tibia. When degree of anisotropy was integrated in the analysis, the reliability of the results increased by another 10 percent (Mullender et al. 1998; Kabel et al. 1999). Though bone volume fraction and degree of anisotropy can be viewed as the main determinants of loading patterns, this does not mean that other trabecular bone parameters may not add additional information to the results. Including other trabecular bone variables in the assessment of the mechanical properties of bone has given more accurate results than when only bone mineral density was investigated (Ulrich et al. 1999; Newitt et al. 2003; Parr et al. 2013). It thus makes sense that bone volume ratio and degree of anisotropy are the most often analysed trabecular variables in both mammalian, primate, and human trabecular studies.

2.3.1 Non-Primate Studies

The best way to study trabecular bone response to changes in mechanical loads is to do *in vivo* studies of animals. Early studies of trabecular response to mechanical loading in animals mainly used strain sensors and x-ray imaging to determine the internal bone structure and were focused more on cortical changes (Lanyon, 1974; Lanyon and Baggott, 1976; Lanyon and Rubin, 1984; Rubin and Lanyon, 1984; 1985). Experiments performed on birds showed that mechanical loading which resulted in peak strains above 0.001 caused new bone formation to occur in the cortical bone of avian long bones (Lanyon and Rubin, 1984;Rubin and Lanyon 1985). Afurther study of avian long bones showed that a response (remodelling/formation) to new strains imposed on bone happened relatively quickly and within four strain cyles (Rubin and Lanyon, 1984), which indicates that in some animals bone morphology may be able

to adapt to different loading regimes quite quickly. A study of the trabecular morphology of sheep calcanei and strain showed a link between trabecular orientation and principal strain direction (Lanyon, 1974), which would indicate that trabecular morphology reflects mechanical loading. However, the same study indicated that similar trabecular orientation could be found in utero, which may suggest that there is also a genetic component influencing trabecular orientation in sheep (Lanyon, 1974).

One such study has been performed on sheep (Barak et al. 2011). During a period of 34 days, three groups of sheep were exercised on treadmills at different angles of elevation for 15 minutes each day. After this period, the distal tibiae of these sheep were sectioned and analysed for trabecular variables. The incline exercised group showed a significant increase in bone volume fraction, trabecular number, trabecular spacing, trabecular thickness and structural model index, when compared to the sheep that walked on level ground. These results suggest that the trabecular microarchitecture remodelled in response to a higher degree of compressive forces at the distal tibia of the inclined walking group (Barak et al. 2011). A second laboratory using mice showed that unloading the mouse femur for extended periods of time resulted in a loss of over 43% in bone volume fraction (Ozcivici and Judex 2014), which corroborates the influence of mechanical stress on trabecular morphology. However, it should be kept in mind that during the above study, animals were put into unnatural joint postures that would not occur during their normal locomotion pattern. This suggests that changes in trabecular structure due to normal changes in locomotion observed during ontogeny may not be as strong as seen in the animal studies.

A more naturalistic *in vivo* study was conducted on inbred mice (Carlson et al. 2008). Two groups of mice were separated and housed in cages specifically designed to either accentuate a form of linear quadrupedalism or turning quadrupedalism as the

main form of locomotion. A third group was kept in normal cages as a control. Though specific types of locomotion were emphasised, the mice did not need to assume any unnatural joint positions. The results of this study did show that not assuming unnatural joint postures caused a weaker correlation between trabecular morphology and mechanical loading patterns, as both test groups had significantly different trabecular bone variables when compared to the control group, but no statistically significant results could be found between the 'turning' and 'linear' quadrupedal mice (Carlson et al. 2008).

The above studies used degree of anisotropy as a measure of trabecular of orientation. Another means to identify loading orientation is by identifying areas of peak trabecular density within the bone. The distal femur of guinea fowl that had been exercised on an inclined treadmill for extended periods of time over a 45-day period showed a higher peak density when compared to the distal femur of guinea fowl exercised for the same time period on a level treadmill. Indicating higher compressive forces occurring at the distal femur for the inclined group (Pontzer et al. 2006).

However, not all trabecular mammalian studies have shown a strong link between mechanical stress and trabecular microarchitecture. Trabecular variables in wild deer and domesticated sheep calcanei were quantified to test if they reflected differences in dorsal compression and plantar tension (Sinclair et al. 2013). Not only was no relationship found between loading stress and trabecular parameters (except trabecular number) in either species, many of the trabecular variables showed the extact opposite architecture in compression or tension between sheep and wild deer (Sinclair et al. 2013). This may indicate that other variables, such as cortical thickness, may influence the degree to which trabeculae respond to mechanical influence in different species. Furthermore, the paradoxical findings in the sheep and wild deer

calcanei indicate that inter-species comparisons of trabecular parameters and the subsequent inferring of behavioural patterns needs to be done with caution. Finally, it should also be noted that variables such as bone volume fraction, trabecular thickness, spacing, and number have been shown to scale negatively when compared to overall body size when trabecular bone parameters were modelled in six terrestrial mammal species of varying size (Christen et al. 2015), which further indicates that other factors besides mechanical loading may have a significant impact on trabecular bone morphology and remodelling. Another factor that may influence trabecular morphology is the frequency and magnitude of the load the specific skeletal element is under. An in vivo study on adult sheep (Rubin et al. 2001;2002) showed that individuals exposed to frequent low-level external loading had an increase in trabecular bone density (34.2%) compared to the control group, while cortical bone did not show a response. This study indicates that trabecular bone is perhaps more responsive to habitual loading patterns than rare high-intensity loading patterns and that unfrequent behaviours may not be well reflected within the trabecular structure (Rubin et al. 2001;2002; Kivell 2016).

2.3.2 Primate Studies

Though studies of non-primate trabecular response to loading may be informative, using direct comparisons of trabecular morphology between primate species may prove more beneficial in reconstructing primate or fossil hominin behaviour. This is especially true when one considers that the gait pattern of primate quadrupedalists and the increased arboreality of primates causes a more complex range of mechanical loading when compared to ungulates (Tanck et al. 2000; Skedros and Baucom 2007; Barak et al. 2011). Most of the studies incorporating trabecular bone analyses have

been done on the lower limb. The trabecular microarchitecture of the femoral head of strepsirrhine primates has been used to separate the leaping primate species from non-leaping species. Non-leaping primates have been shown to have a rather uniform and isotropic trabecular architecture in the femoral head, while leaping species were observed to have a more anisotropic trabecular bone orientation (Ryan and Ketcham, 2002). A subsequent study analysing the fabric directions of the femoral head in the same species showed that trabeculae cluster in a superanterior direction in the femoral head of leaping primates (Ryan and Ketcham, 2005). Trabecular morphology of the vertebral column also successfully teased out differences in positional behaviours of nine strepsirrhine species. The differences in degree of anisotropy in the vertebral body indicated that orthograde primates had a higher degree of anisotropy than pronograde species (Fajardo et al. 2013)

However, a more detailed analysis, which included finite element analysis, of the proximal femur of leaping and quadrupedal strepsirrhines, showed that the trabecular morphology observed in these species could not be wholly explained by differences in loading of the femoral head (Ryan and Rietbergen 2005). Furthermore, the analysis of the femoral neck of several anthropoid primate species indicated that suspensory and quadrupedal species overlapped greatly in their trabecular morphology and could not distinguish between locomotor groups (Fajardo et al. 2007), which indicates that there is inter-specific variation in trabecular response to mechanical loading between different species of primate.

Primate based studies focused on the relationship between mechanical loading patterns and trabecular microarchitecture of the talus have shown mixed *results* (DeSilva and Devlin 2012; Hébert 2012 et al.; Su et al. 2013). A comparison of the trabecular morphology of the talus of several species of small-bodied primates (60 –

500 grams) corroborated earlier studies on human skeletal material that degree of anisotropy is a good predictor of mechanical loading patterns, and thus locomotion group (Hébert et al. 2012). A comparison between talar trabecular architecture in modern humans and great apes also showed a significantly higher degree of anisotropy in modern human tali compared to the extant great apes. Furthermore, differences in trabecular orientation in the anteromedial region of the talar neck could differentiate between human bipedalism and great ape quadrupedal locomotion (Su et al. 2013). In comparison, another study identifying differences in talar trabecular bone microarchitecture in great apes, humans, and fossil hominins had very different results (DeSilva and Devlin 2012). Here, trabecular bone volume fraction and degree of anisotropy was similar in species with different locomotion behaviours, such as gorillas and baboons. Differentiation of locomotion by assessing bone volume fraction and degree of anisotropy of the metatarsal heads of humans and great apes also showed varying results, with anisotropy able to distinguish between humans and great apes, while bone volume fraction did not vary significantly across species (Griffin et al. 2010). An effort to use trabecular morphology at the Achilles tendon insertion site as a means to reconstruct tendon morphologies in extant and extinct primates also proved unsuccessful. The results of this study showed that the trabecular architecture at the Achilles tendon of baboons, chimpanzees, gibbons, and modern humans did not differ significantly along tendon length and muscle stress lines (Kuo et al. 2013).

Recently, more attention has been paid to the trabecular microarchitecture of the upper limb of primates. While a preliminary study of the proximal humerus of several primate species indicated that the degree of anisotropy in the proximal humerus could be used to distinguish between suspensory and quadrupedal primate species (Fajardo and Müller 2001), a comparison of the proximal humerus in five

anthropoid species found no such relationship (Ryan and Walker, 2010). Ryan and Walker (2010) found that humeral bone volume fraction and degree of anisotropy were significantly lower in the humerus than that of the femur across all five primate taxa, but that there were no significant differences in humeral trabecular morphology that could be related to differences in locomotion. A subsequent study by Ryan and Shaw (2012) on the trabecular bone architecture of the humeral and femoral head of eight anthropoid species found that different combinations of trabecular variables (e.g. thickness, separation, degree of anisotropy) were able to distinguish across locomotor groups. Brachiating species were characterised by a relatively isotropic organisation of trabeculae, while terrestrial species show a more densely-packed and highly anisotropic trabecular microstructure. Bipeds (Homo) and quadrumanous climbers (Pongo) had similar humeral trabecular morphologies, which are characterised by low connectivity density, and relatively thin trabeculae (Ryan and Shaw, 2012). A more detailed look at the proximal humerus of orangutans, chimpanzees, and modern humans also showed mixed results (Scherf et al. 2010). While a principal component analysis of trabecular parameters differentiated the three species easily, this separation was only somewhat related to differences locomotion, and could not identify specific differences in loading patterns and joint positions in the hominoid shoulder.

As with the lower limb, there are differences in the degree to which trabecular bone can be used to reconstruct behaviour across skeletal elements. The trabecular structure of the primate wrist bones was not informative when trying to reconstruct behaviour (Schilling et al. 2014). The trabecular parameters of the lunate, scaphoid, and capitate of humans, apes, baboons, and spider monkeys were measured to see if trabecular microarchitecture reflected the individual's locomotion patterns (i.e. bipedal, suspensory, and quadrupedal). Despite clear differences in hand use in

bipedal, suspensory and quadrupedal primate species, trabecular parameters of the lunate, scaphoid and capitate could not distinguish across locomotor groups Schilling *et al.* 2014). Only the bipeds, humans, could be separated from the other groups by a lower value of bone volume fraction, which may reflect the fact that modern humans do not use their hands for locomotion (Schilling et al. 2014) or the systemically low bone volume fraction found throughout the recent human skeleton (Ryan and Shaw 2015; Chirchir et al. 2015). Why the trabecular architecture of primate carpal bones seems restricted in its response to mechanical loading is unclear, though it may be related to the fact that the primate wrist is a densely-packed and extremely complicated joint that plays a vital role in locomotion in non-human primates and manipulation in modern humans, which necessitates genetic predetermination of its trabecular morphology.

It would be expected that metacarpal and phalangeal trabecular architecture would reflect locomotion patterns more strongly than the upper limb or wrist bones, as the digits are directly in contact with the substrate during nonhuman primate locomotion and used in precision grip in modern humans. An assessment of the bone mineral density of the subchondral and trabecular bone of the third metacarpal heads of chimpanzees, orangutans, and humans has shown that areas of low mineral density are related to increased remodelling rates (Zeininger et al 2011). This was exemplified by the low mineral density in the distal region of the metacarpal head of *Pongo*, which undergoes loading during climbing, while the regions mostly loaded during knuckle-walking and vertical climbing were least mineralised in chimpanzees (Zeininger et al. 2011). More detailed analyses of trabecular architecture of the third metacarpal corroborates these findings. Regions of high bone volume are concentrated in areas with high joint reaction forces. This study found high bone volume fraction in the

dorsal region of the metacarpal head in knuckle-walking species, while suspensory taxa, such as *Pongo* and *Hylobates* had a higher bone volume fraction in the palmar regions of the metacarpal head (Tsegai et al. 2013; Matarazzo 2015; Chirchir et al. 2017; Dunmore et al 2019). Similar results were also found using the whole-epiphysis method (Gross et al. 2014) of analysis on the metacarpal heads of all ape species and humans. Here, the bone volume fraction and trabecular distribution across the metacarpal heads was consistent with patterns of hand use during locomotion and highest trabecular volume was found in areas of high peak loading within the hand (Skinner et al. 2015). This trend is further reflected in the proximal and middle phalanges of great apes, gibbons, and macaques. As in the metacarpals, trabecular orientation is one of the primary distinguishing features between locomotor categories in the species under study (Matarazzo, 2015). However, degree of anisotropy in the phalanges is more complex and does not always fall along locomotion categories. For example, the medial phalanges of knuckle-walking species did not show the expected palmar-dorsal orientation in both distal and proximal ends in line with peak loading. Instead, medial phalangeal trabecular orientation in the proximal end was similar to that of gibbons (Matazarro, 2015).

Metacarpal trabecular microarchitecture has been shown to not only be able to identify interspecific variation in hominoids, but also intraspecific variation. When comparing bone volume fraction, trabecular thickness and structural model index of the first, second, and fifth metacarpals of Tai forest and Cameroon chimpanzees, Lazenby et al. (2011) found that these parameters were higher in the Cameroon sample, indicating greater metacarpal robusticity. These differences were interpreted as reflecting a higher degree of knuckle-walking and tool-use practiced by the Cameroon chimpanzees compared to those of the Tai forest. In humans, higher loading

along the ulnar side of the hand has been reflected by a high concentration of bone volume fraction in forager populations, consistent with throwing behaviours, compared to agricultural populations. These results suggest that it may be possible that a difference in the degree of arboreality between mountain gorillas and western lowland gorillas will be reflected in their trabecular bone structure.

Why studies trying to identify locomotor patterns from trabecular morphology in primates have such varying rates of success is unclear. It could be that inter-species differences in phylogenetic constriction, genetic, metabolic, or hormonal influences (Mullender et al. 1998) are muddying the results. However, differences in methodology may also be an attributing factor to the discrepancies observed in the studies mentioned. There currently is no standard methodology to choose regions of interest within the skeletal elements under study. For example, Desilva and Devlin (2012) chose to divide the human and primate talus into four distinct quadrants, while Su et al. (2013) chose to divide the same bone into nine regions of interest. This may also hold true for the analyses of trabecular bone in the upper limb. The use of smaller regions of interest close to the articular surfaces of the humeral and femoral head of 8 anthropoid primate species was able to reflect locomotion patterns (Ryan and Shaw, 2012), where an earlier study using less and larger regions of interest in the same bones found no such relationship (Ryan and Walker, 2010).

A recently developed whole-bone and epiphysis methodology (Pahr and Zysset 2009; Gross et al. 2014) may provide better insight into the validity of using trabecular parameters to reconstruct locomotion patterns, as this methodology analyses the entire bone region and makes choosing regions of interest obsolete. A recent study on the modern human and chimpanzee distal tibia and talus using this methodology has provided some promising results. Tsegai et al. (2017) found that

aside from an overall higher degree of bone volume fraction in *Pan troglodytes* compared to modern humans in both skeletal elements, the distribution of trabeculae in the distal tibia and talus reflected differences in mobility and loading angles in the ankle joint and talonavicular joint of chimpanzees and modern humans. This method was also used recently to identify mechanical loading patterns in modern humans (Stephens et al. 2016) and great apes (Dunmore et al. 2019), as discussed above.

2.3.3 Trabecular Ontogeny Studies

Mechanical stressors incurred during ontogeny play a significant role in the development of bone and can bear influence on the ossification processes from very early in development (Carter 1987; Carter et al. 1990). Primate morphological ontogenetic studies have most often focused on changes to external bone morphology. For example, changes in hand and foot bone proportions in baboons have been shown to be influenced by a shift to quadrupedal locomotion (Raichlen 2005; Druelle et al. 2017). The change in shape of the dorsal scapular fossae of African apes has been linked to the development of knuckle-walking locomotion during ontogeny (Green 2013). Richmond (2006) has shown that the phalangeal curvature can change throughout ontogeny, with more arboreal juveniles showing more curved phalanges then less arboreal adults. Ontogenetic changes in the great ape carpus have been interpreted to show that knuckle-walking evolved independently in *Pan* and *Gorilla*, and differs on a biomechanical level (Dainton and Macho 1999; Kivell and Schmitt 2009). In humans, it has been shown that loading during ontogeny can influence epiphyseal morphology (Carter 1987; Carter et al. 1989), and the development of the femoral bicondylar angle (Tardieu 1999) and that the advent of bipedal walking influences the femoral/humeral strength ratio in cortical bone (Ruff 2003).

Recently, more attention has been given to the ontogeny of the internal structure of bone. As it is hard to conduct ontogenetic studies of trabecular bone on living primates, most studies have been conducted on other mammalian species or on modern human archaeological populations. However, up until now ontogenetic studies of trabecular bone have also given conflicting results. The ontogenetic trajectory of trabecular bone in pigs showcases the influence juvenile behaviours can have on adult morphology. An ontogenetic study of the trabecular bone of the tibiae and vertebrae of pigs aged 6 to 230 weeks showed that trabecular bone adaptation to changes in mechanical loading occur with a developmental lag (Tanck et al. 2001). This study showed that trabecular density increased greatly during the early weeks of life and was one of the first trabecular parameters to respond to loading stress. Changes in trabecular orientation or anisotropy did not occur until later in development.

The ontogenetic pattern of the trabecular architecture of the ulnar medial coronoid process in canines is remarkably similar to that observed in the lower limb of modern humans (Ryan and Ketcham 2006; Raichlen et al. 2015). At birth, a high bone volume fraction and connectivity density is observed in canines, which subsequently drops when the development of independent locomotion occurs, at approximately 8-10 weeks. After this drop bone volume steadily increases once more, which is combined with a thickening of trabeculae (Wolschrijn and Weijs, 2004). A similar ontogenetic trajectory was found in lambs, where trabecular bone density was highest in young individuals and rapidly decreased during development (Nefei et al, 2001)

Similarity in human bone development is also reflected in the ontogenetic trajectory of mice. Age related changes in the tibia of male C56BL/6J mice showed that trabecular ontogeny in this species was incredibly similar to that observed in

modern humans. Over the course of its life (6 months – 2 years), the mouse's tibial trabecular bone volume fracture decreased significantly, as did trabecular number, connectivity density and degree of anisotropy. Meanwhile, trabecular spacing and structural model index increased with age (Halloran et al. 2002). Though this may mean that bone development in laboratory mice may be a good model for human bone development, this cannot be concluded to hold true for other non-human primates until more data on their ontogenetic development is available.

However, not all mammalian analyses show this human-like pattern. Analyses of trabecular bone parameters of stillborn calves and foals has shown that these species have a trabecular bone pattern that anticipated the locomotor and mechanical loading patterns demands that would have occurred in these species after birth (Gorissen et al. 2016). However, these species are precocials, which means that shortly after birth these animals would have already had to move about independently. This is not the case in primate species, where infants are often highly dependent on their mothers for several months to years of their lives. It would thus make sense that trabecular bone morphology in primate species would likely not be predetermined by an anticipatory mechanism, but instead was heavily influenced by the behavioural patterns of immature individuals.

Up until this point, trabecular bone development during the juvenile period of primates has been focused on the development in modern humans, while non-human primates are often overlooked. This is in part due to limited number of non-adult specimens in museum collections, particularly at infant and juvenile stages, and lack of direct data on locomotor behaviour. The adaptive lag observed in the trabecular development of pigs (Tanck et al. 2001) also seems to occur in modern humans, as juvenile behaviours were reflected in adult calcaneal morphology (Pettersson et al.

2010). The adult calcaneus of men who had exercised regularly during their juvenile period, but had since stopped this behaviour in adulthood, showed a higher degree of bone mineral density than the adult calcaneus of men who had never exercised during childhood (Pettersson et al. 2010). This may suggest that juvenile behaviours in humans and non-human primates may influence adult trabecular morphology.

As the main shift of behaviour in the modern human subadult period consists of the advent of unassisted bipedal walking in infants, most ontogenetic studies have focused on the lower limb. Overall, it seems that the trabecular microarchitecture of the proximal femur (Ryan and Krovitz, 2006; Milovanovic et al. 2017), the proximal tibia (Gosman and Ketcham, 2009), and the distal tibia (Raichlen et al. 2015) responds to changing mechanical loads. Bone volume fraction, degree of anisotropy, and trabecular number and connectivity density is higher in perinatal humans than at any other stage of life (Nuzzo et al. 2003; Ryan and Krovitz, 2006; Gosman and Ketcham, 2009; Raichlen et al. 2015; Milovanovic et al. 2017). Between 6 months and the first year of life, a dramatic reduction in bone volume fraction, trabecular number, and connectivity density can be observed in both the femur and the tibia. At the advent of independent bipedal locomotion, around 1.5 – 2 years of age, all these values increase once more in the proximal femur and the distal tibia, though they do not reach the same levels as seen during the perinatal phase. Degree of anisotropy increases at this time, but variation in degree of anisotropy between individuals decreases as infants become more practiced in bipedal walking (Ryan and Krovitz, 2006; Raichlen et al. 2015). Interestingly, the trabecular development of the proximal tibia deviates in its development when compared to the proximal femur and distal tibia. After the initial decrease in trabecular variables seen at approximately 1 year of age, the values of degree of anisotropy, bone volume fraction, and trabecular number rise once more, but

in the proximal tibia this gradual increase continues until 6 to 9 years of age (Gosman and Ketcham, 2009), where this increase plateaued at around 2 years of age.

This difference may be a reflection of interpopulation differences, as the ontogenetic trajectory of the proximal femur and distal tibia were both performed using individuals from the Norris Farms #36 archaeological population from the Illinois River Valley (Ryan and Krovitz 2006; Raichlen et al. 2015), while the study on the proximal tibia used specimens from the SunWatch Village archaeological population from the Late Prehistoric Ohio Valley (Gosman and Ketcham 2006). However, this difference in timing of bone development seems quite large for two populations that had similar subsistence strategies and lived during approximately the same time period. This explanation becomes even more unlikely when it is shown that the ontogenetic pattern of trabeculae in the proximal femur of a more recent medical collection of humans show the exact same pattern of development as seen in the proximal femur and distal tibia of the Norris Farms #36 specimens (Milovavovic et al. 2017). It is more likely that this discrepancy is related to differences in age category choices between these studies. The Norris Farms #36 studies both included individuals between 0-8 years of age, while the SunWatch Village sample included individuals between 0-22 years of age. The broader sample in age categories may not be detailed enough to pick up on very small changes between individuals close in age to one another.

Aside from a study of the ontogenetic development of the ulna in golden retrievers (Wolschrijn and Weijs 2004), very little attention has been paid to how trabecular bone changes in the upper limb during ontogeny, let alone in primates. The humeri of 45 human individuals from Norris Farms #36 were also analysed for trabecular bone development (Perchalski et al. 2017). It seems that the trabecular

pattern of development in the upper limb shows less strong signals related to locomotion and behavioural shifts as is observed in the lower limb. Though once more connectivity density was highest in perinates and decreased significantly during the first year of life, this trend was not observed for bone volume fraction and degree of anisotropy in the humerus (Perchalski et al. 2017). This may be due to the fact that the arm is not weight-bearing for most of the juvenile period of humans.

The ontogenetic trajectory of trabecular bone in the human pelvis further suggests that caution should be taken when assuming the degree of trabecular response to mechanical loading would be similar throughout the human skeleton. Analysis of changes in bone volume fraction, trabecular thickness, spacing, and number in the iliac blades of 28 neonatal infants showed that the trabecular microarchitecture of the illium is largely predetermined (Cunningham and Black 2009). The lack of trabecular response to changes in mechanical loading during ontogeny were further corroborated by Abel and Macho (2011), who used landmark and radiograph data to study the development of cortical bone and trabecular bundles in 73 human iliac blades. Until adolescence most morphological changes occur in the outer bone morphology of the ilium, not the trabeculae (Abel and Macho 2011).

In the past few years there has been some inroads made to identify ontogenetic patterns of trabecular bone morphology in apes (Tsegai et al. 2018a; Ragni 2020). The results of these studies suggest that changes in trabecular morphology may be consistent with ontogenetic changes in locomotor behaviour, and that these changes differ in primates when compared to modern humans. For example, the dip in bone volume fraction during infancy found in humans (Gosman and Ketcham 2006; Ryan and Krovitz 2006; Raichlen et al. 2015) is not seen in the chimpanzee humerus, tibia, or femur (Tsegai et al. 2018a). Instead, bone volume fraction is low at birth and

increases throughout life. A steady increase could also be observed for trabecular thickness. Furthermore, Tsegai et al. (2018a) found a decrease in degree of anisotropy with the humerus and tibia during the first five years of life, while anisotropy remained relatively constant in the femur, suggesting different bones may respond to mechanical loading in different ways throughout ontogeny (Tsegai et al. 2018a).

Only one previous study has analysed ontogenetic changes in trabecular bone structure within the third metacarpal in great apes (Ragni 2020). This study focused on the proximal third metacarpal, or the metacarpal base, and the capitate of gorillas and chimpanzees. Ragni (2020) reported that bone volume fraction decreased throughout ontogeny, while degree of anisotropy remained constant, which suggests a different ontogenetic pattern for apes than that reported by Tsegai et al. (2018a). Furthermore, Ragni (2020) found no significant differences in the ontogenetic changes to trabecular bone between chimpanzee and gorillas despite a higher frequency of arboreal behaviours in the former (Ragni, 2020). However, it should be kept in mind that this study analysed the trabeculae using a volume-of-interest approach in the base of the third metacarpal, a relatively immobile joint compared to the metacarpal head, while Tsegai et al. (2018a) used a whole-bone method (Gross et al. 2014). Given the strong locomotor signals found in the trabecular structure of adult hominoid third metacarpals (Chirchir et al. 2017; Dunmore et al. 2019; Matarazzo, 2015: Tsegai et al. 2013), it may be that the distal metaphysis and epiphysis of the third metacarpal, which represents a more mobile joint than the metacarpal base, would have revealed similar ontogenetic patterns to that seen in the chimpanzee upper limb (Tsegai et al. 2018a). This study will use a whole-bone epiphysis approach to investigate the ontogenetic changes throughout the third metacarpal, including changes at the growth plate and epiphysis (where present).

Past ontogenetic studies have shown that trabecular bone response to changes in mechanical loading during ontogeny may not only be species, but also bone specific. This indicates that it is unwise to assume that the bones in the upper limb and hand of non-human primates will follow similar patterns of trabecular ontogeny as modern humans, nor should it be assumed that all bones within the primate upper limb will share a similar trabecular development pattern. As it has been shown in both suids (Tanck et al. 2001) and humans (Pettersson et al. 2010) that juvenile behaviours can persist in adult trabecular bone morphology long after such behaviours have ceased, it is imperative to understand how changes in mechanical loading during the juvenile period of great apes influences the trabecular bone morphology of the upper limb. Without this knowledge, using adult trabecular morphology of primates to reconstruct behaviour may prove problematic.

3. Materials and Methods

3.1 Study sample

Table 1. Age and species distribution of the study sample.

		No. individuals (M/F/U)		No. per bone section			Resolution (microns)
Age Category	Age	Ggg*	Gbb**	Base	Growth Plate	Head	
Neonate	0 – 6.9 months	0/1/0	1/2/0	4	4	0	0.019 – 0.029
Infant 1	7.0 months – 2.9 years	2/3/0	3/2/0	9	9	1	0.024 – 0.040
Infant 2	3.0 – 5.9 years	3/3/1	3/1/0	12	12	6	0.021 – 0.041
Juvenile	6.0 years – 11.9 years	2/1/1	3/1/1	9	9	7	0.024 – 0.080
Adult	12^{+}	4/4/1	5/4/0	18	18	18	0.020 – 0.080

*Ggg stands for *Gorilla gorilla gorilla* ** Gbb stands for *Gorilla beringei beringei*

The study sample consists of immature and adult third metacarpal specimens from 26 *G. g. gorilla* and 26 *G. b. beringei* individuals (Table 1). Western lowland gorilla specimens are curated at the Powell-Cotton Museum (PC) and the Museum für Naturkunde, Berlin (ZMB). The mountain gorilla sample consists of individuals from the Mountain Gorilla Skeletal Project (MGSP), which contains Virunga mountain gorilla specimens collected from Volcanoes National Park, Rwanda and are curated at the DFGFI'S Karisoke Research Centre in Rwanda. This project was initiated in 2008, and currently includes 160 mountain gorillas from Rwanda and 20 mountain gorillas from Uganda (McFarlin et al. 2009). This study only includes the Rwandan gorillas. The MGSP sample is unique in that not only are these individuals of known sex and age, the individuals observed by Doran (1997) belonged to the same population, which allows us to directly compare known behaviour to trabecular morphology. Individuals from all sources were individuals that were wild-caught and specimens did not show any signs of pathology. Trabecular bone morphology was analysed in the base, the

distal metaphysis (i.e. growth plate), and the epiphysis of the third metacarpal. In early ontogeny the epiphysis is unfused and highly cartilaginous, and was therefore not present for every individual in the sample.

3.1.1 Age Categories

All individuals within the mountain gorilla category are of known age. Age of the western lowland gorillas was estimated using dental eruption times and assigned to a specific age category following Smith et al. (1994) and Kivell (2010). Five age categories were defined based on locomotor transitions reported by Doran (1997) (Figure 1).

Neonate (0 – 6.9 months):

This category is defined by the first 6 months of life. This period is categorised by little to no independent locomotion. Individuals are mainly carried by the mother and the main hand positions involve clinging to mother.

Infant 1 (7.0 months – 2.9 years):

Individuals aged 7 months to two yearsmonths. During this period independent locomotion commences, but the overall activity pattern is characterised by a high degree of arboreal and suspensory behaviours (climbing, jumping, swinging etc). Terrestrial knuckle-walking is practised during this time, but is often combined with terrestrial palmigrade locomotion. At this time locomotion is forelimb dominated (Doran 1997; Ruff et al. 2013).

Infant 2 (3.0 to 5.9 years):

During this period infants are still dependent on their mother, but are shifting to terrestrial knuckle-walking as their dominant form of locomotion. Suspensory and

arboreal behaviours decrease, but their frequency is still much higher than observed in adult gorillas.

Juvenile (6.0 – 11.9 years):

Suspensory, arboreal and play behaviours decrease even further, though is still slightly higher than observed in adults. During this period loading becomes hind-limb dominant and knuckle-walking becomes the main and most frequently used form of locomotion. During this time fusion of the epiphysis commences, but is often not complete.

Adult (12+ years):

At this time fusion of the epiphysis is complete, though a remnant epiphyseal line may still be visible in the internal bone structure. Terrestrial knuckle-walking has become the main form of locomotion and the rate of suspensory behaviours is adult-like.

Since detailed ontogenetic behavioural data is only available for mountain gorillas (Doran, 1997), we assume that similar transitions in locomotor behaviour occur during western lowland gorillas development, but likely with an increased frequency in arboreality, particularly later in ontogeny (Remis, 1995). Infant individuals of both species have been described as highly arboreal (Ruff et al 2013, Fleagle 2013). As the locomotor transition from highly arboreal to mainly terrestrial is more pronounced in mountain gorillas than western lowland gorillas, the former is used to define the age categories.

3.2 Scan Acquisition

Micro-computed tomography scans (micro-CT) were collected using NIKON XTH225 ST scanners housed at the Cambridge Biotomography Centre, Department of Zoology, University of Cambridge (UK) and at the Shared Materials Instrumentation Facility at Duke University (USA), and using the BIR ACTIS 225/300, Diondo D3, and SkyScan1173 scanners housed at the Department of Human Evolution, Max Planck Institute for Evolutionary Anthropology (Germany). Scan parameters were 100-160 kV and 70-190µA, using a brass or copper filter of 0.25 – 0.50 mm. Voxel resolution was influenced by individual specimen size, and ranged from 19 – 45 microns. Three specimens (one 8 years of age, two adults) scanned at 80 microns, and six specimens (all adults) at 50 - 60 microns were included and, although their resolution was much lower, trabecular parameter values and BV/TV patterns were similar to that of the rest of the sample. All scans were reconstructed as 16-bit and 8-bit TIFF image stacks.

Scans included all bones of the hand and the third metacarpal was cropped from the image stacks using AVIZO 6.3 (Visualisation Sciences Group, SAS). Subsequently, all specimens were reoriented into standardised positions. In cases where the epiphysis had not yet fused to the distal metaphysis, the two skeletal structures were separated manually in Avizo 6.3 and saved as separate TIFF image stacks.

For individuals where fusion of the epiphysis had commenced and the epiphysis and growth plate were no longer clearly separated by a layer of cartilage, a cutting script was used to divide the bone up into four sections: base, shaft, metaphysis, epiphysis. These areas were identified visually on the scans in AVIZO 6.3 and the slice numbers at the edges of these regions recorded to include in a cutting script that

would be run through medtool (see the medtool section for further explanation). The edge of base was identified as the area where the shaft became more concave palmarly and above the articulations for the other metacarpals and carpals (see figure 7). The shaft was identified as the area between the upper edge of the base and the lower edge of the metaphysis and was not analysed. The metaphysis' upper border was the growth plate. The proximal border of the metaphysis was defined in this study by the start of dorsal-palmar widening of the shaft, and the extrusion of the palmar transverse muscle attachment enthesis (see figure 10). The epiphysis was defined as the metacarpal head. Where fusion was extensive or complete, the proximal edge of the epiphysis was the remnant epiphyseal line, or a straight horizontal border just above the dorsal ridge if the epiphyseal line had been obliterated.

Figure 10. Showing the cutting lines on the third metacarpal pf a gorilla.

3.3 Segmentation

All scans were segmented using the MIA-clustering segmentation method (Dunmore et al. 2018). Previous segmentation methods, such as RCA, worked by creating a segmentation threshold based on a grey value chosen by the authors. The mia-clustering method does not rely on chosen grey scale values and is thus slightly more objective.

Medical image analysis (mia) clustering was developed for linux and can be run on other operating systems through the docker desktop tool. As we used a windows machine for analysis, all mia segmentation was run through docker via text-based input. The mia-segmentation method uses both global and local clustering approaches to sort voxels of an image, in this case a grey scale microCT scan, into groups based on colour. The global clustering assigns a probability to each voxel that they would be black, grey or white (i.e. empty space or bone). This method does not get to fine detail, such as variations in white/grey due to thickness of bone or small trabeculae. These details can be taken into account by running a local clustering method as well (figure 11).

The local clustering asks for a grid size to be defined by the author. The grid size defines the size of a small cube that will laid over the scan, allowing smaller areas of analysis. The grid size was determined by opening the original TIFF-stack scans in Avizo 6.3. In Avizo, the measurement tool was used to identify the size of a trabecula in millimetres. The grid size was then chosen to be slightly larger than this measurement by steps of 5, so if the trabecula was 7 millimetres, a grid size of 10 was chosen, 13 millimetres a grid size of 15 et cetera.

Once grid size had been established, the mia-segmentation used this information to divide the volume or scan into overlapping cubes that reflected the chosen grid size. The class probabilities obtained through the global clustering were then used to define the probability vector for class membership for each cube. If the probability of the voxels in the cube falls below the threshold for that class, then this cube is discounted for local clustering. This allows for the identification of empty space vs. bone. The probabilities obtained for voxels in overlapping grids are merged (figure 11). Subsequently, the program analyses for which class these voxels have the highest membership probability and are assigned to this class. This process eventually produces a complete segmented image in nifti format.

Separate segmentation sequences were run for each specimen with the following grid sizes: 5, 10, 15, 20, and 25. The segmented nifti images were then loaded into Avizo and compared to the original TIFF-stack to ascertain which segmentation contained the most detail. Most of the scans of individuals under 2 years of age had a grid size between 10 and 15, while the older individuals averaged a grid size of 20 – 25. Once a segmentation was chosen for each specimen, this file was saved as a binarized raw image and was ready for medtool analysis.

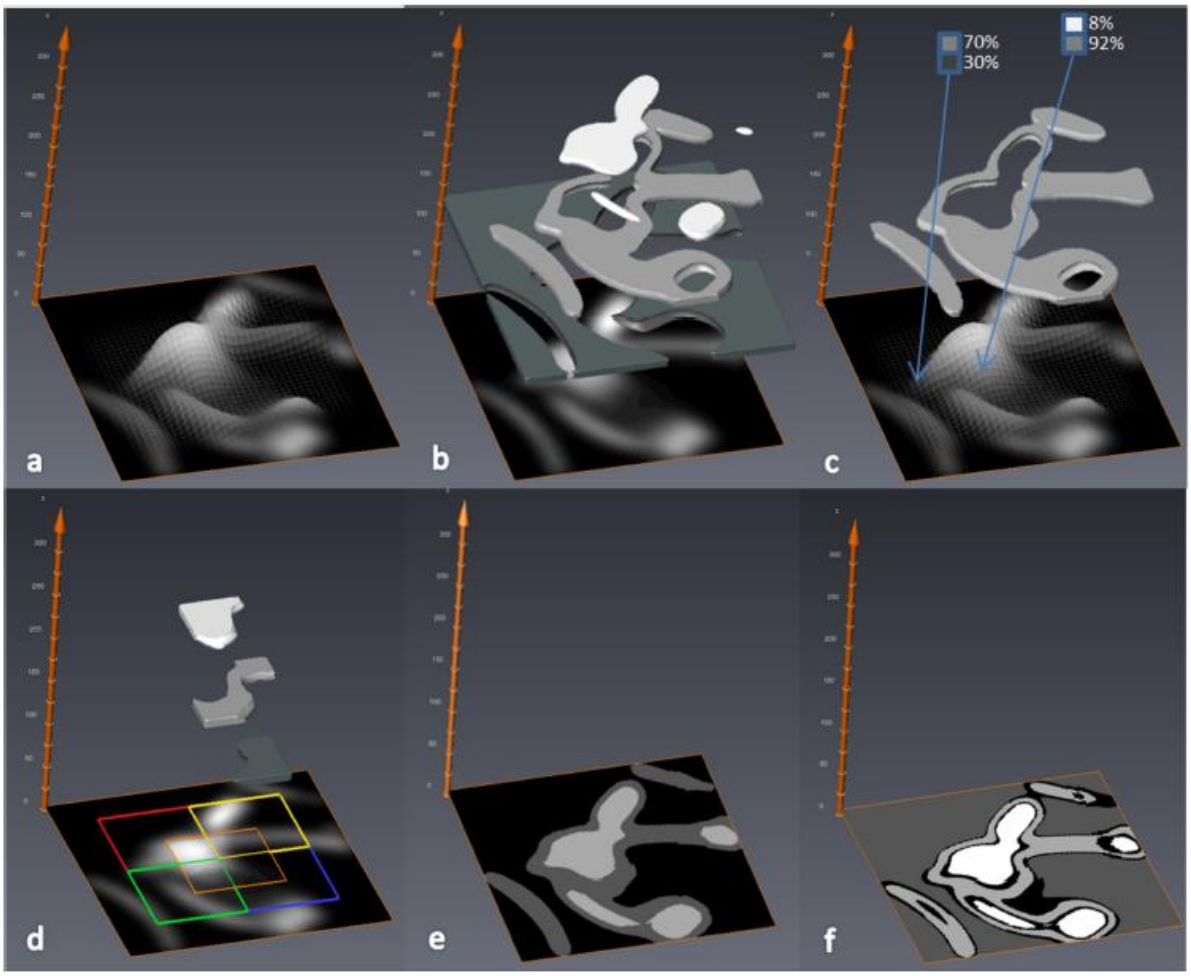

Figure 11. Step-wise segmentation of an image using mia-segmentation clustering. As seen in Dunmore et al. (2018).

3.4 Medtool 4.4

The segmented 3D images were analysed further using medtool 4.4 (http://www.dr-pahr.at/medtool). Medtool is a processing program that allows for the processing and quantitative analysis of CT scans, and the creation of colourmaps and simulation models, using python scripts. This study used scripts from the whole-bone epiphysis method (Gross et al. 2014; Pahr and Zysset 2009) to analyse its data. The following paragraphs briefly summarise the most relevant processes occurring during the medtool analysis. Figure 12 shows some of these steps as well.

Initialisation: During this step the segmented raw files are loaded and rewritten as mhd files for further use in medtool. During this time, a clean version of the segmented scan is also created. When the scan was binarised in Avizo, voxels were given a value of 1 or 0, with 1 being bone. The clean filter applied during initialisation identifies any voxels assigned a value of 1 that are not connected to any other voxels and deletes them. This allows the removal of floating voxels outside the bone structure that most likely represented noise in the scan.

Morphological filters: A close mask was created next. This step uses a sphere with a predetermined radius (kernel size, defined by user) to move across the cortical shell of the scan and fills in any porosities. An outer mask is then created from the close, which represents the cortical shell. The inner mask is created by using the sphere to identify the first voxel representing bone, and then the voxel representing empty space. The close is then subtracted from this space to create the inner mask. Subsequently, the inner mask is subtracted from the outer mask to create the thickness mask, which calculates the thickness of cortical bone. Finally, this thickness mask is subtracted from the close to identify the trabecular mask, which does not include the cortical shell.

Thickness evaluation: under normal circumstances, the thickness evaluation uses a BoneJ plugin from ImageJ (Doube et al. 2010), which outputs a text file with the mean trabecular thickness, standard deviation and max deviation. The mean trabecular thickness value is then used to adjust kernel sizes if these do not match up to expected trabecular thickness values assumed before analysis. This is done by multiplying the trabecular thickness in pixels by resolution. In previous adult metacarpal studies of gorilla using this method, kernel size was always 2-2-4 or 3-3-6. This study used these same kernel sizes from the onset. However, an issue arose with the correction system

described above when analysing the under 2 years old specimens. It was found that the thickness evaluation consistently suggested that kernel size should be much greater (i.e.4-4-8 and 5-5-10), but when these new kernel sizes were used the masks consistently incorporated most of the cortical bone into the trabecular mask, especially in the metaphyseal area, which would be problematic for analysis. Tanck et al. (2006) have shown that it is very difficult to distinguish between the metaphysis and trabecular bone in six week old pigs, and that this may be due to trabeculae merging into the cortex around the growth plate. Visual examination of the scans of the infant gorilla metacarpal showed that it was difficult to make a visual distinction between cortical bone and trabecular bone near the growth plate. The plugin used most likely could not properly identify the trabecular bone, which caused the much higher mean thickness results. Several iterations using different kernel sizes were made to identify the best size determinant. In the end, this study found that using 2-2-4 kernel size created the best segmentation mask that were true to reality. For three scans, we manually removed the cortical shell in Avizo 6.3 and saved the trabecular bone 'mask' and ran that through medtool 4.4. It was found that result of trabecular variables were very similar using the 2-2-4 kernel size masks that ignored the thickness evaluation and the manual trabecular masks. As manually removing the cortical bone in scans is very time consuming, it was decided that in this case the 2-2-4 kernal size scans for individuals under 2 would run without thickness evaluation.

Create mask overlays: This step uses the inner mask and thickness mask to define the cortical bone, trabecular bone, and empty air within the scan. A mask is created that assigns for values to voxels in the scan: 0 = outside, 1 = air, 2 = cortical, and 3 = trabecular. This study analysed the bone as a whole and separated into anatomical sections (base, metaphysis, epiphysis). In order to analyse sections of bone separately,

a cutting script was used to cut the maskseg into separate sections. This was done by giving the program the slice numbers from each scan where cuts were to be made. These 'cut' masks were then run through further analysis in the same manner as the whole masksegs.

Create CGAL meshes: using the inner and outer masks, a mesh is created in which the trabecular bone volume fraction and degree of anisotropy can then be plotted.

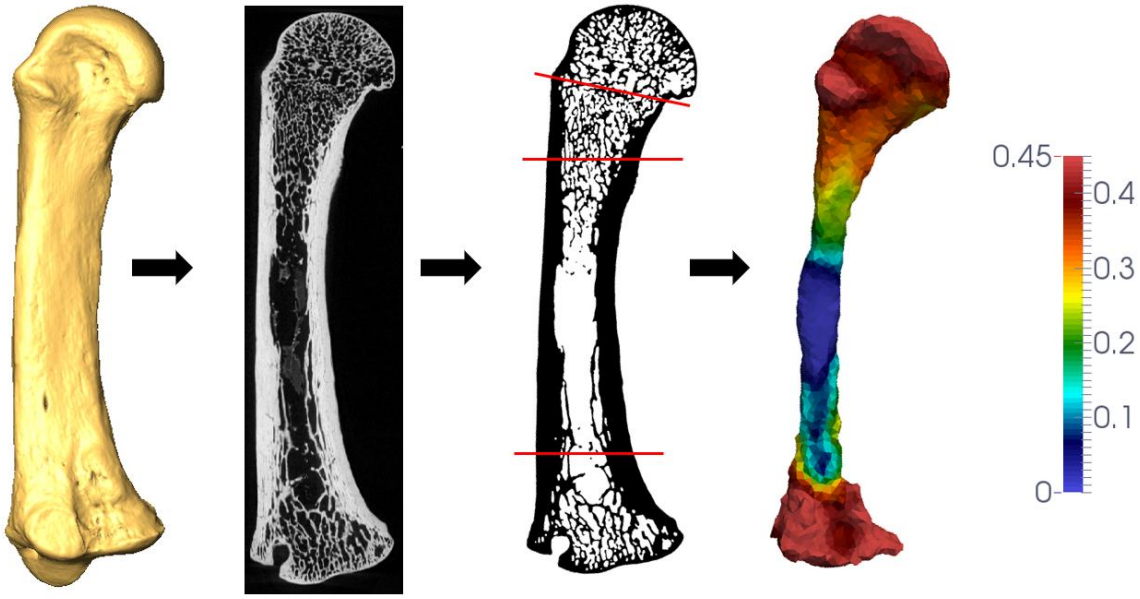

Figure 12. Example of process of whole-epiphysis method. From left to right: MC3 surface model, midsection showing trabecular structure, segmented midsection showing locations of cutting points (red lines), 3D mesh model coloured by BV/TV as per scale.

3.5 Quantification of trabecular variables

Five trabecular bone parameters were quantified from the inner mask generated using the in-house script for medtool 4.4 (www.dr-pahr.at): BV/TV, DA, trabecular thickness (Tb.Th), trabecular number (Tb.N), and trabecular separation (Tb.Sp). A more detailed description og what these variables represent can be found in table 2. This script calculates these parameters as follows: BV/TV was calculated by dividing the total number of bone voxels by the total number of voxels; DA was measured using

the mean intercept length [1 – (smallest eigenvalue/largest eigenvalue)] and bounded between 0 (isotropic) and 1 (anisotropic); The sphere fitting method by Hildebrand and Rüegsegger (1997) was used to calculate Tb.Th and Tb.Sp. Finally, Tb.N was calculated 1/(Tb.Th+Tb.Sp). Colour maps of BV/TV distribution were created according to the Gross et al. (2014) protocol, using CGAL (www.cgal.org) and Paraview (www.paraview.org).

Table 2. Overview of Trabecular Variables

Variable	Description
BV/TV	Bone volume to total volume ratio. Ratio of the volume of trabecular bone to cortical bone within a region of interest.
Tb.Th	Trabecular thickness. Mean thickness of the trabeculae, measured in mm. Usually calculated by fitting spheres into the space between trabeculae within a region of interest and measuring their diameter.
Tb.N	Trabecular number per mm. Calculated by taking the distance between trabecular struts.
Tb.Sp	Trabecular spacing. The mean width per mm of space between trabecular structs within a region of interest.
DA	Degree of anisotropy. Describes the orientation of trabeculae within region of interest. Isotropic structures, referred to by values between 0 and 1, show symmetry of orientation in all directions. Anisotropic structures, referred to by values >1, show preferred orientation in one or several directions.

3.6 Statistical analysis

The small sample size of this study required us to use non-parametric methods to test for significant differences in trabecular variables. In both cases, the Shapiro-Wilk test showed a non-normal distribution of variables, requiring non-parametric testing. Two

main analyses were perfomed; one with the *Gorilla beringei* and *Gorilla gorilla* species pooled, which tested for overall ontogenetic changes as a whole, and one where these species were separated, to test for ontogenetic differences between subspecies. Kruskal-Wallis tests were employed to test for differences in trabecular variables between age groups, followed by post-hoc Nemenyi tests. The ratio of trabecular variables between the proximal metaphysis, epiphysis, and base of the third metacarpal was also calculated to test for significant changes in trabecular morphology in these specific regions during ontogeny using Kruskal-Wallis tests. Statistical comparisons could only be made between homologous regions. As the neonate category lacked epiphyses, comparisons between other age categories and this age group were only performed for the metaphyses and metacarpal bases, This was also the case for older individuals which lacked an epiphysis (see Table 1 for distribution of those individuals). A p-value of <0.05 was considered significant. All statistical tests were conducted in R v3.6.3 (R Core Team, 2016) and visualised using the ggplot2 package (Wickham, 2009).

4 Results

This section discusses the results from this study. First, a qualitative description of ontogenetic changes in the pooled species sample will be reported for bone volume fraction (BV/TV). Results from quantitative and statistical analysis of bone volume fraction, degree of anisotropy (DA) , trabecular thickness (Tb.Th), trabecular number (Tb.N), and trabecular spacing (Tb.Sp) will follow for pooled species and separated species samples.

4.1 Qualitative trabecular patterns of BV/TV during ontogeny

The overall distribution of bone volume fraction, whichwill be referred to as BV/TV from here onwards w, of the gorilla third metacarpal was quantified using medtool 4.4. (www.dr-pahr.at/medtool) and mapped onto a specimen specific bone mesh using CGAL (www.cgal.org). This resulted in individual colour maps that showed the distribution of BV/TV for each individual in the sample. As visual comparison of colour maps of similarly aged individuals of *Gorilla beringei* and *Gorilla gorilla*, and quantitative analyses showed little difference in BV/TV between species (see section 4.2.1.3), this qualitative description of ontogenetic changes in the trabecular bone structure of the third metacarpal describes changes for the *Gorilla* species as a whole. Figure 13 shows cross-sections of segmented microCT data and colour maps of the distribution of BV/TV in a subset of the study sample. The figure shows BV/TV scaled to 0.0 – 0.45 for each specimen (centre) to allow comparison of BV/TV values across age categories, as well as BV/TV scaled to the range of each individual specimen (right), which shows a more detailed picture of distribution of BV/TV for each individual specimen. The 0.0 – 0.45 BV/TV maps will be referred to as BV/TV scaled in the following section, the individual BV/TV ranges will be referred to as individual BV/TV values.

Neonate (0 – 6 months of age):

When comparing both the individual BV/TV and scaled BV/TV maps, overall BV/TV is higher at birth (though not as high as adult values) and decreases by 6 months of age. Bone volume fraction is variable at the metacarpal base in the neonate category, but relatively high palmar and dorsally across all age categories when looking at individual BV/TV. Scaled BV/TV maps show high BV/TV inferiorly in the base at birth and a large decrease by 6 months of age.

Individual BV/TV is high at the metaphysis and growth plate across the age category, with the largest BV/TV concentration occurring palmarly, and distally. Scaled BV/TV shows similar high concentrations palmo-distally at birth, but identifies the same large decrease in overall bone volume concentration by 6 months of age observed in the metacarpal base.

The epiphysis could not be analysed for the neonate category, as due to the cartilaginous nature of the structure none had been preserved in the museum collections used in this study.

Infant 1 (7 months – 2 years of age):

Both the scaled and individual BV/TV maps show that by 10 months of age, overall bone volume fraction within the third metacarpal has increased to represent similar values as those observed at birth. The metacarpal base has a high BV/TV concentration along its inferior edge, where it articulates with the capitate, and the highest BV/TV concentrations distally and palmarly across the age range when looking at individual BV/TV. Scaled BV/TV indicates an increase in BV/TV at the base by 2.5 years of age, with concentration mainly focused palmarly and distally.

Individual BV/TV maps show that BV/TV concentrations are highest at the growth plate across the age category, and that the distribution of BV/TV across this structure is fairly homogenous. However, when comparing the scaled BV/TV maps of individuals from this age category, it shows that the younger individuals (<1 years old) have lower BV/TV at the growth plate, and that the highest concentration is located palmarly here, than observed in individuals aged over 1 years old. By 2.5 years of age, BV/TV has increased in the growth plate and this high concentration is now extending towards the more proximal border of the metaphysis.

Only one specimen in this age category had an epiphysis. This individual was 11 months old. Scaled BV/TV maps show that BV/TV is low in the epiphysis in this age category compared to older individuals and that bone distribution is fairly homogenous overall, with a very slight increase in bone volume fraction disto-dorsally (see figure 12). The individual BV/TV scale shows that overall BV/TV distribution across the epiphysis is similar to that seen in the infant 2 category, with high BV/TV disto-dorsally and very low BV/TV proxo-palmarly.

Infant 2 (3 – 5 years of age):

Overall BV/TV, both scaled and individual, values remain similar across this age category and are within the same range as those observed in the 2+ years specimens of the infant 1 category. While these values are also observed in some of the adult specimens, the distribution of BV/TV across the metacarpus differs. As individual BV/TV values for specimens in this age range were very close to the scaled BV/TV values, the colour maps are nearly identical (figure 13). Scaled BV/TV is high across the metacarpal base at 3 years old, with the two highest concentrations located palmarly and dorsally. This overall high BV/TV across the base decreases by 5 years

of age, when BV/TV is relatively low and only two small concentrations of high BV/TV remain. The first high BV/TV concentration is still located proximo-palmarly at the base, while the second high concentration has moved from a proximo-dorsal concentration at 3 years of age, to a dorsal concentration a few millimetres above the capitate articulation

Both individual and scaled BV/TV is highest at the growth plate, and decreases slightly near the proximal edge of the metaphysis. No palmar or dorsal concentration can be observed at this time.

Compared to the infant 1 category, the scaled BV/TV in the epiphysis shows an increase in bone volume fraction across the bone, with BV/TV concentrations being highest distally and dorsally and lowest palmarly. Scaled and individual BV/TV show an increase in BV/TV at the most distal point of the epiphysis by 4 years of age, while distally BV/TV decreases slightly when examining the individual BV/TV maps.

Juvenile (6 – 11 years of age):

During the juvenile stage, an increase in overall BV/TV can be observed when looking at individual BV/TV maps. Both scaled and individual BV/TV is high in the metacarpal base across the age category and this high concentration is no longer reserved to two small points, as observed in the previous category. Instead BV/TV is still highest dorsally and palmarly, but the inferior edge of the base that articulates with the capitate also shows a higher degree of BV/TV.

At 6 years of age, scaled and individual BV/TV is high at the growth plate, but incursion of high BV/TV into the proximal metaphysis has decreased. While BV/TV remains highest across the entire edge of the growth plate, two high BV/TV concentrations can be identified dorsally and palmarly in the metaphysis. By 11 years

of age, a decrease in BV/TV begins at the growth plate, medially of the dorsal high concentration, which remains (figure 13).

The overall BV/TV concentration (scaled and individual) in the epiphysis rises during this age category, but still does not resemble the adult distribution pattern. At 6 years of age, a large increase of overall bone volume can be observed in the epiphysis compared to the infant 2 group when looking at scaled BV/TV. Bone volume fraction is highest distally, but remains high throughout the entire epiphysis. Individual BV/TV shows a medium concentration of BV/TV dorso-distally as well, but this has disappeared by 8 years of age, By 11 years of age, a decrease in scaled BV/TV can be observed in the centre of the epiphysis, while BV/TV concentrations remain high distally and proximally along the epiphyseal plate. As fusion commences around 10-11 years, the palmar and distal BV/TV concentrations underneath the growth plate and within the epiphysis remain high until full fusion has occurred and the epiphyseal line has been resorbed.

Adult (12+ years of age):

By 12+ years fusion has occurred in all individuals and the epiphysis is no longer a separate structure. Scaled and individual BV/TV in the base shows an adult-like pattern, with high BV/TV, but variation between individuals. A decrease in BV/TV can be seen at the dorsal side of the base in some older individuals (see figure 13), but not others. The highest concentrations remain palmarly and dorsally.

Once fusion has occurred, the metaphysis shows a significant decrease in BV/TV concentration across its structure, though a very small concentration of higher BV/TV can be observed palmarly. However, in many of the individuals between 12 and 20 years of age in this study, a remnant epiphyseal line kept the BV/TV

concentration (scaled and individual) from representing an adult-like pattern. In these individuals, BV/TV remained high across the growth plate, and especially dorsally.

In the epiphysis of individuals with a remnant epiphyseal line. Scaled and individual BV/TV shows a high concentration distoulnarly and distodorsally (as seen in other adults (Dunmore et al. 2019), but this concentration extends further into the centre of the epiphyseal body than in adults without a remnant epiphyseal line. A higher concentration of BV/TV can also be observed in the proximal edge of the epiphysis, where it fused to the metaphysis. In individuals aged 30 and over, no such remnant was observed. Here scaled and individual BV/TV showed an adult like pattern of BV/TV distribution, with the highest concentration occurring distoulnarly and distodorsally and low BV/TV proximally and palmarly.

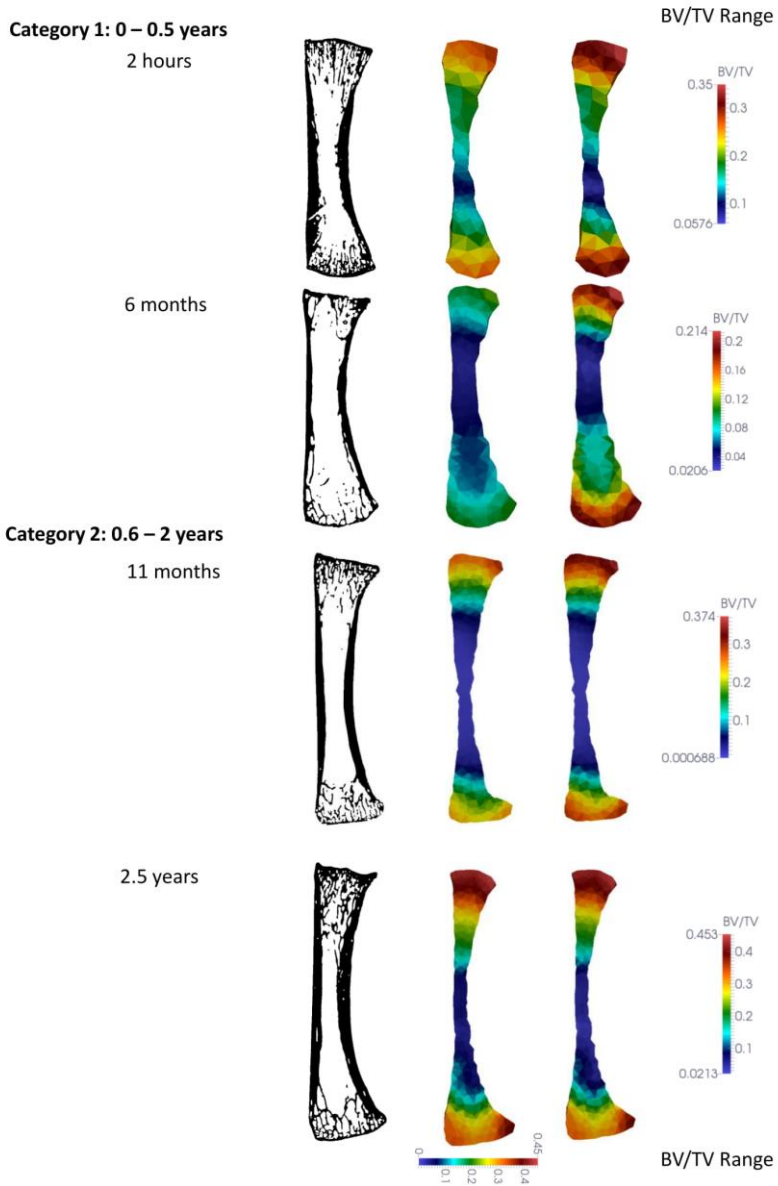
Category 1: 0 – 0.5 years
2 hours
6 months
Category 2: 0.6 – 2 years
11 months
2.5 years
BV/TV Range
BV/TV
0.35
0.3
0.2
0.1
0.0576
0.214
0.16
0.12
0.08
0.04
0.0206
0.374
0.000688
0.453
0.0213
0
0.45
Category 3: 3 – 5 years
3.5 years
5 years
Category 4: 6 – 11 years
6.8 years
11 years
0.406
0.054
0.441
0.0172
0.506
0.5
0.000572
0.568
0.00865
Distal
Dorsal
Palmar
Proximal

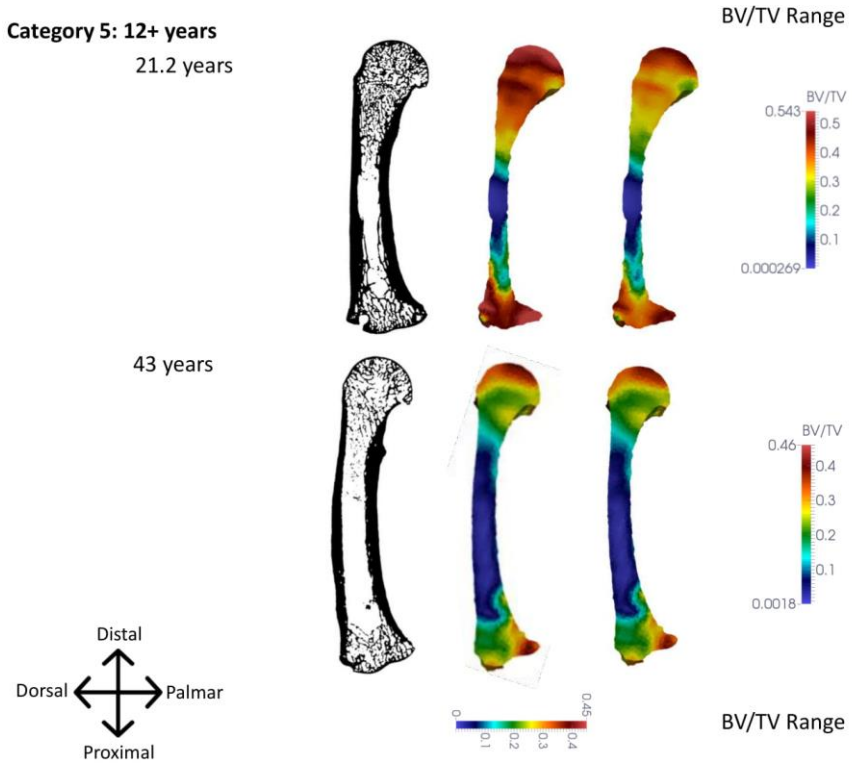

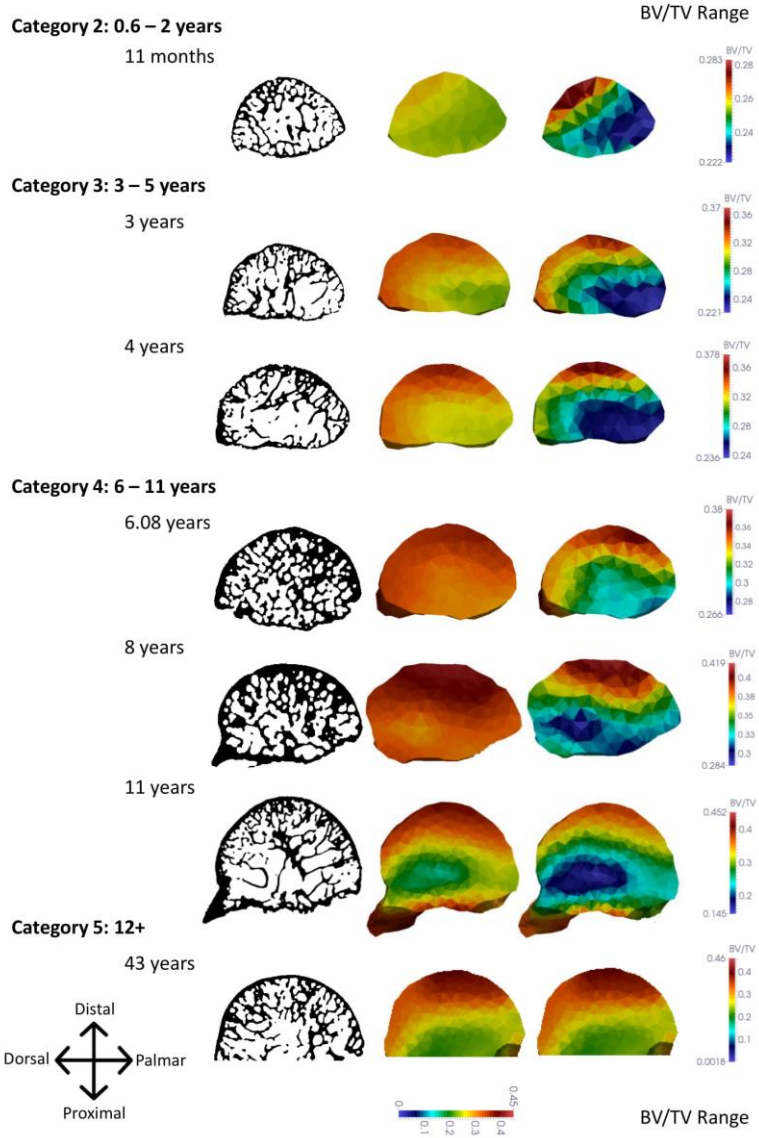

Figure 13. Ontogenetic changes in BV/TV of the gorilla third metacarpal corpus and epiphysis. Shown in the midcoronal plane, segmented trabecular and cortical bone (left), trabecular structure scaled from 0.0 – 0.45 BV/TV (center) and scaled to the range of each specimen (right)

4.2 Quantitative trabecular patterns during ontogeny

Due to the small sample size of some of the age categories, and the non-normal distribution data, all statistical analyses reported below were the result of non-parametric tests. Kruskal-Wallis tests were used to test for differences between age categories with species pooled, as well as to test for differences in trabecular parameters within the same age categories for the different species of gorilla (*Gorilla beringei* and *Gorilla gorilla*). Due to the small sample size of the neonate age category, this category was merged with the infant 1 age category and potential species differences in the epiphyses were not tested due to the absence of an epiphysis for many individuals in the infant1/2categories. Post-hoc Nemenyi tests were completed to see which groups had significantly different trabecular variables. A p-value of <0.05 was considered significant. Tests were run to test for difference in trabecular variables in three areas of the third metacarpal: the base, the metaphysis, and the epiphysis (where present). The results of the post-hoc Nemenyi tests are summarized in tables 3 -5. Kruskal-Wallis and post-hoc Nemenyi tests were also run to test for differences in trabecular ratios between the areas of bone for each age category, to test for significant differences in trabecular response within the skeletal element by age. The rest can be found in the appendix. All statistical tests were conducted in R v3.6.3 (R Core Team, 2016) and visualised using the ggplot2 package (Wickham, 2009). In all boxplots, Gbb refers to *Gorilla beringei*, and Ggg refers to *Gorilla gorilla.*

Table 3. Post-hoc Nemenyi results for pooled species by age group of the base.

Variable	Neonate	Infant 1	Infant 2	Adolescent
BV/TV				
Infant 1	0.9938			
Infant 2	0.2612	0.2350		
Juvenile	**0.0154**	**0.0050**	0.4811	
Adult	**0.0017**	**0.0001**	0.1037	0.9895
Tb.Th				
Infant 1	0.8740			
Infant 2	0.4017	0.8603		
Juvenile	**0.0012**	**0.0024**	**0.0290**	
Adult	**0.0001**	**0.0024**	**0.0009**	0.9944
Tb.N				
Infant 1	0.7361			
Infant 2	0.1832	0.7531		
Juvenile	0.0631	0.3711	0.9492	
Adult	**0.0028**	**0.0172**	0.2821	0.8529
Tb.Sp				
Infant 1	0.6897			
Infant 2	0.1832	0.8102		
Juvenile	0.1687	0.7618	0.9998	
Adult	**0.0037**	**0.0331**	0.3424	0.5568
DA				
Infant 1	0.6394			
Infant 2	0.6399	1.0000		
Juvenile	**0.0083**	0.1005	0.0537	
Adult	0.0686	0.5627	0.4146	0.6674

***Significant results in bold (p<0.05)**

Table 4. Post-hoc Nemenyi results species pooled of the growth plate.

Variable	Neonate	Infant 1	Infant 2	Juvenile
BV/TV				
Infant 1	0.5899			
Infant 2	**0.0357**	0.4083		
Juvenile	0.0518	0.4961	1.0000	
Adult	0.7117	0.9928	0.0834	0.1510
Tb.Th				
Infant 1	0.7233			
Infant 2	0.5344	0.99773		
Juvenile	**0.0050**	**0.03916**	0.05551	
Adult	**5e-050.0001**	**0.00014**	**0.00012**	0.81360
Tb.N				
Infant 1	1.0000			
Infant 2	0.9091	0.7650		
Juvenile	0.9589	0.9182	0.2313	
Adult	0.0657	**0.0041**	**1.6e-06**	0.0817
Tb.Sp				
Infant 1	0.6897			

Infant 2	0.1832	0.8102		
Juvenile	0.1687	0.7618	0.9998	
Adult	**0.0037**	**0.0331**	0.3424	0.5568
DA				
Infant 1	0.5083			
Infant 2	0.1725	0.9450		
Juvenile	0.4157	0.9997	0.9821	
Adult	**0.0088**	0.2080	0.5978	0.3104

***Significant results in bold (p<0.05)**

Table 5. Post-hoc Nemenyi results species pooled of the epiphysis.

Variable	Infant 1	Infant 2	Juvenile
BV/TV			
Infant 1			
Infant 2	0.9527		
Juvenile	0.9326	0.9993	
Adult	0.8958	**0.0314**	**0.0120**
Tb.Th			
Infant 1			
Infant 2	0.9858		
Juvenile	0.3571	0.0635	
Adult	0.1612	**0.0011**	0.8281
Tb.N			
Infant 1			
Infant 2	0.9765		
Juvenile	0.3492	0.0815	
Adult	0.1711	**0.0025**	0.8750
Tb.Sp			
Infant 1			
Infant 2	0.9642		
Juvenile	0.3976	0.1580	
Adult	0.2395	**0.0148**	0.9438
DA			
Infant 1			
Infant 2	0.9995		
Juvenile	0.9977	0.9992	
Adult	0.6995	0.1537	0.1681

***Significant results in bold (p<0.05)**

4.2.1 Bone Volume Fraction (BV/TV)

4.2.1.1 Species Pooled

An increase of BV/TV from birth to adulthood can be seen in the base, growth plate, and epiphysis. A decrease can be seen in adulthood for the metaphysis and the epiphysis (figure 14). Kruskal-Wallis tests identified significant differences in BV/TV across all regions of bone for all age categories. Post-hoc Nemenyi tests further identified the age categories that had significant differences (tables 3 – 5). In the base significant differences in BV/TV could be observed between the neonate and juvenile category ($p = 0.0154$), the infant 1 and juvenile category ($p = 0.005$), the neonate and adult category ($p = 0.0017$), and the infant 1 and adult category ($p = 0.001$). For the growth plate, only the BV/TV between the neonate and infant 2 category was significant ($p = 0.0357$). The bone volume fraction differences in the epiphysis were significant for the infant 2 and adult category ($p = 0.0314$) and the juvenile and adult category ($p = 0.0120$). Showing that the main difference in BV/TV in the base, growth plate, and epiphysis is between individuals aged younger than 5 years old and those older than 5 years old and in the epiphysis also between individuals with fused and unfused epiphyses.

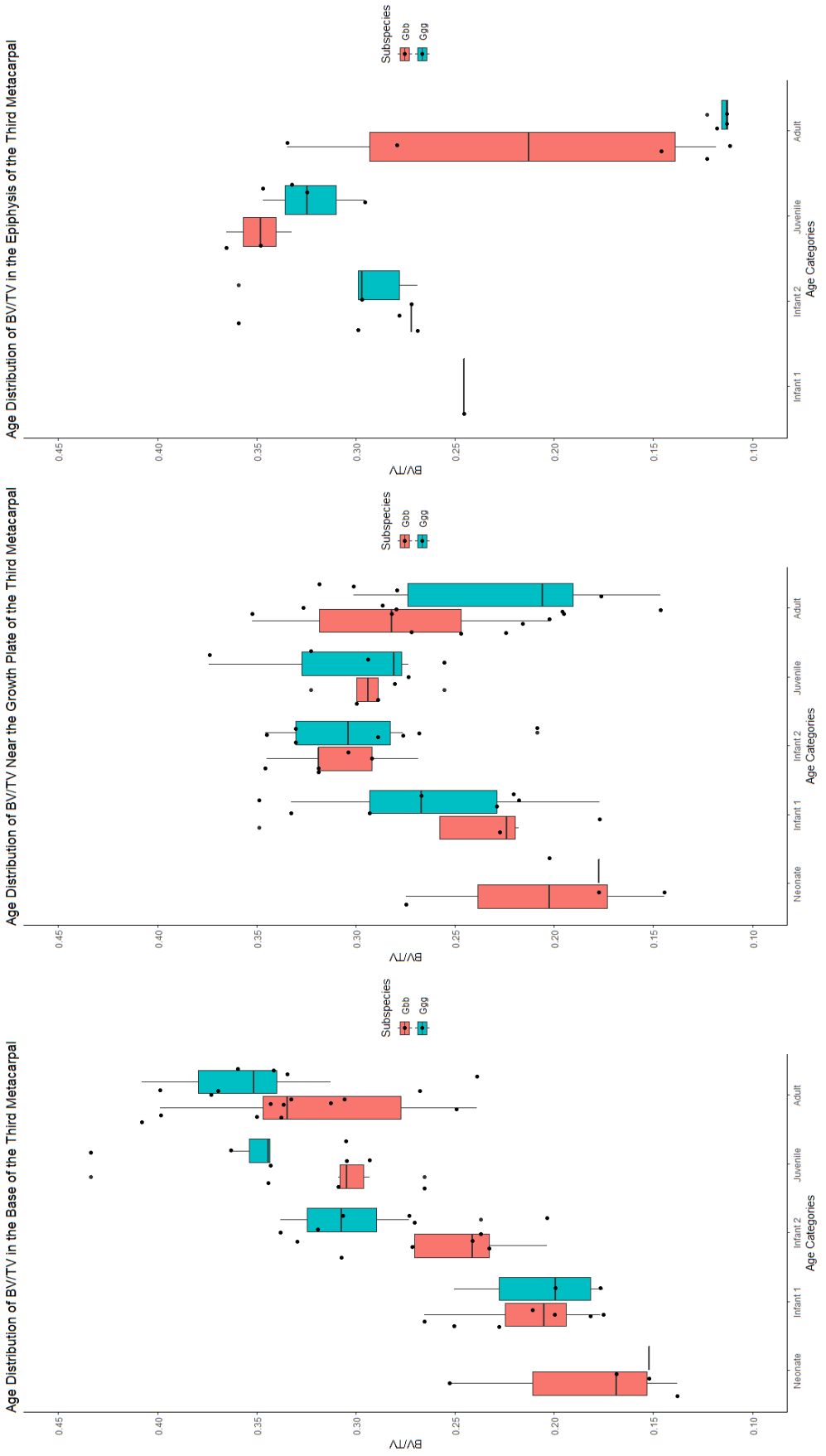

Figure 14. Boxplots showing the distribution of BV/TV across age categories and species.

4.2.1.2 Species Pooled Ratios

BV/TV ratios remain similar in all bone sections until adulthood, when there is higher BV/TV in the base and growth plate compared to the epiphysis. BV/TV ratio between the base and growth plate increases slightly from infant 2 onwards (figure 15), and differences in this ratio were significant between the neonate and adult ($p = 0.0171$), the infant 1 and adult ($p = 0.0001$), and the infant 2 and adult categories ($p = 0.0004$). When comparing the ratio of BV/TV in the base to that of the epiphysis, a small increase in the difference in BV/TV values of these bone sections could be identified around the juvenile stage and a larger increase in adulthood (figure 16). However, Ratio differences between the base and epiphysis were only significant for the infant 2 and adult ($p = 0.0180$) and the juvenile and adult ($p = 0.04979$) categories. A similar difference in the ratio of growth plate and epiphysis BV/TV was found (figure 17), but no significant differences were detected between age groups.

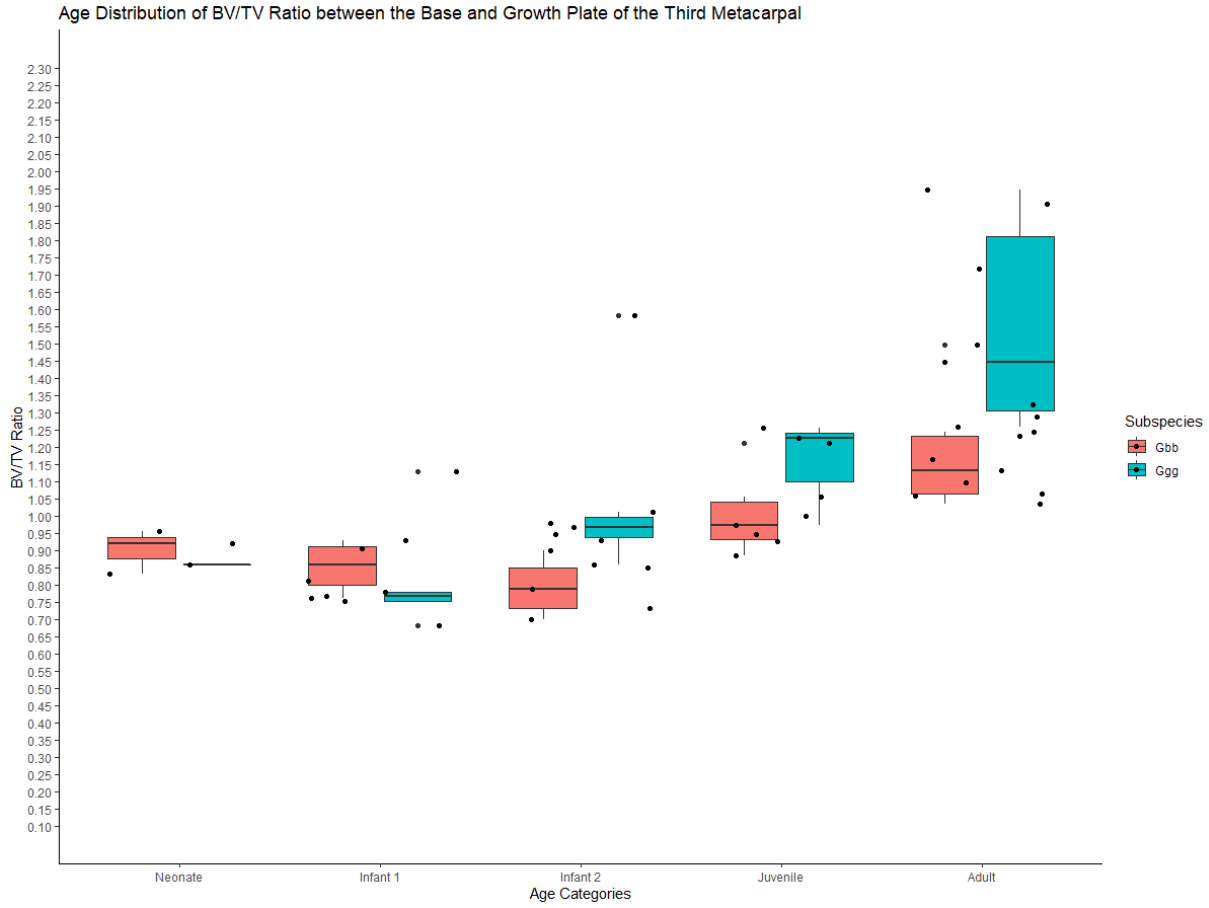

Figure 15. Boxplot of ratio of base and growth plate BV/TV across age groups and species.

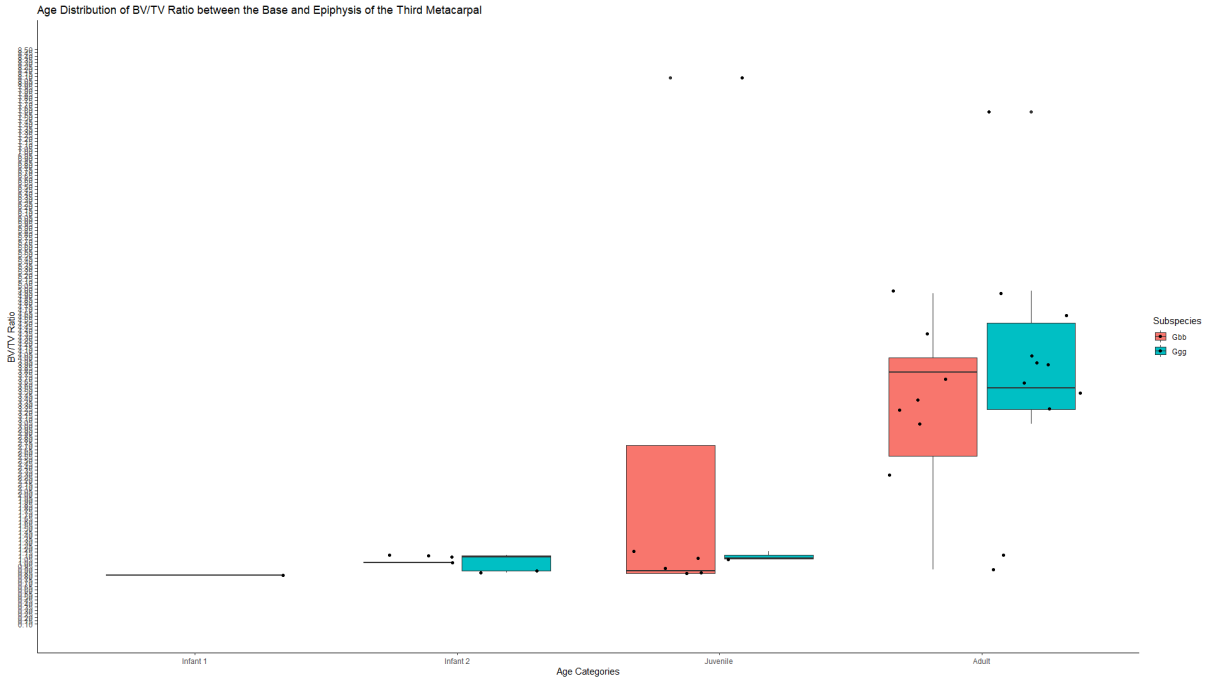

Figure 16. Boxplot of ratio of base and epiphysis BV/TV across age groups and species.

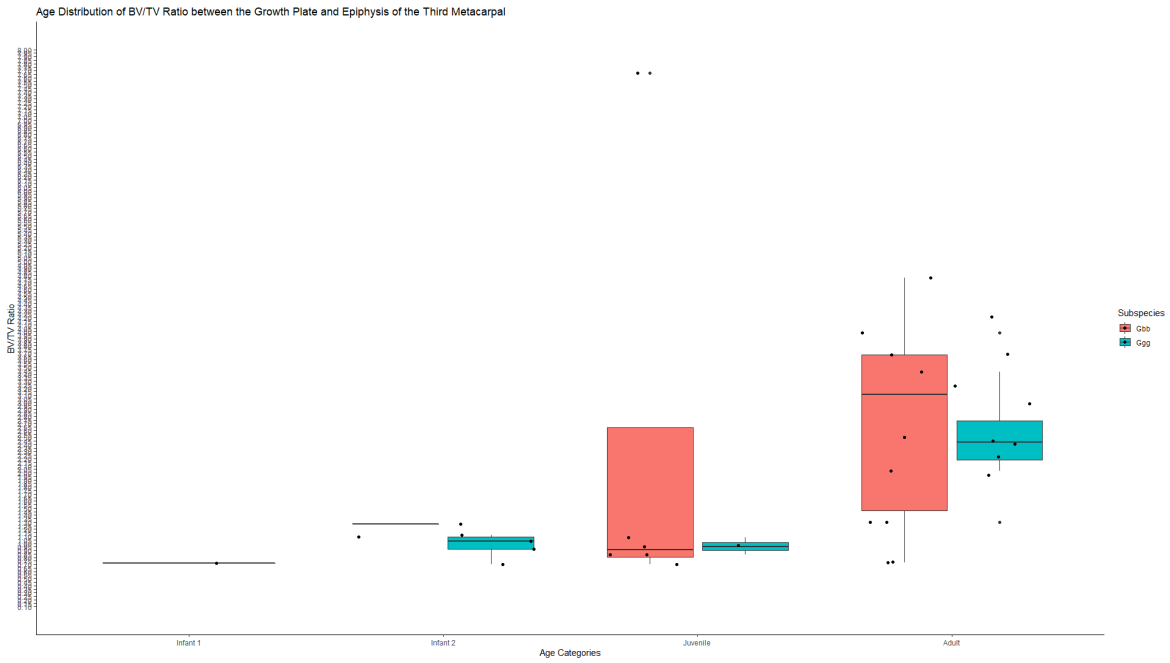

Figure 17. Boxplot of ratio of growth plate and epiphysis BV/TV across age groups and species.

4.2.1.3 Interspecies Analysis

Overall, *Gorilla beringei* has slightly lower BV/TV values for each age category, except in the epiphysis, where *Gorilla gorilla* has lower BV/TV in the juvenile and adult category. It also seems as if *Gorilla beringei* has more variation in BV/TV values within each age category. However, significant differences in BV/TV are only observed for the base in the infant 2 age category (p=0.019).

4.2.2 Degree of Anisotropy (DA)

4.2.2.1 Species Pooled

Degree of anisotropy ranges from 0 (isotropic) to 1 (anisotropic). Overall, DA remains relatively stable across all age ranges and shows a mixture of anisotropy and isotropy (i.e. values between 0.30 and 0.55). A very small decrease in DA can be observed from birth to adulthood in the base and growth plate, and an increase can be seen in the epiphysis (figure 18). Significant differences in the DA of the base were only detected between the neonate and juvenile categories ($p = 0.0083$), while the neonate and adult categories only had significant difference in the metaphysis ($p = 0.0088$). No significant differences could be detected for the epiphysis.

4.2.2.2 Species Pooled Ratios

DA ratios between the base and growth plate remains relatively constant through early development and then shows a slight decrease in anisotropy in adulthood, indicating that the distal metaphysis (i.e. the region that used to be the growth plate) in adulthood is more anisotropic than the base of the third metacarpal in gorillas (figure 19). The difference in DA between the base and growth plate ratio is significant only between the juvenile and adult category (0.0358) A decrease in degree of anisotropy can also be detected between the base and the epiphysis between the juvenile and adult categories (figure 20), but this is not significant. Here, only the difference in DA between the infant 2 and adult categories is significant ($p = 0.0415$). The bone in the epiphysis seems some anisotropic than that of the growth plate for the infant 1 and infant 2 categories compared to the juvenile and adult categories (figure 21), however only the difference between the juvenile and adult categories shows a significant difference ($p = 0.0121$)

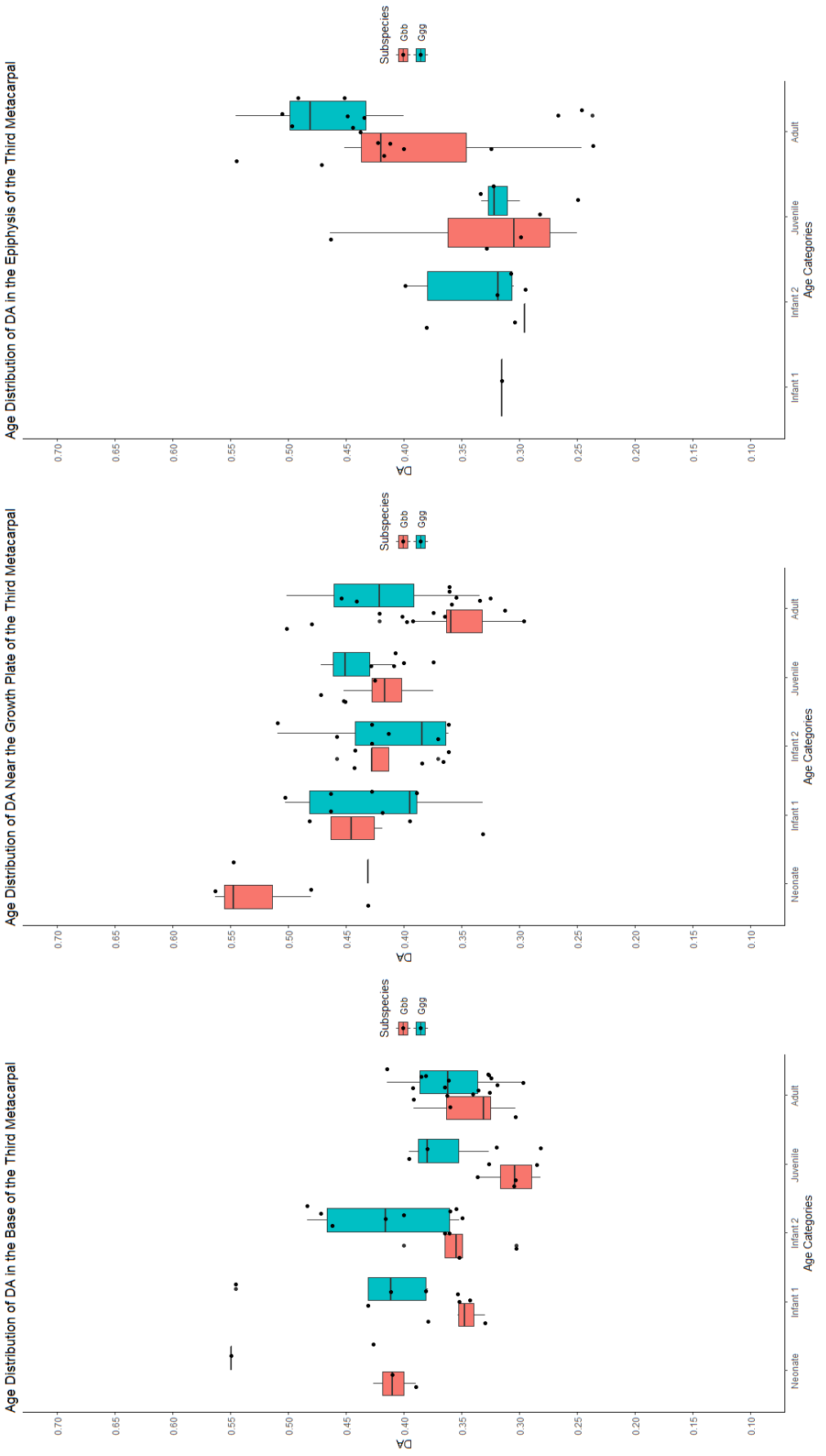

Figure 18. Boxplots showing the distribution of DA across age categories and species.

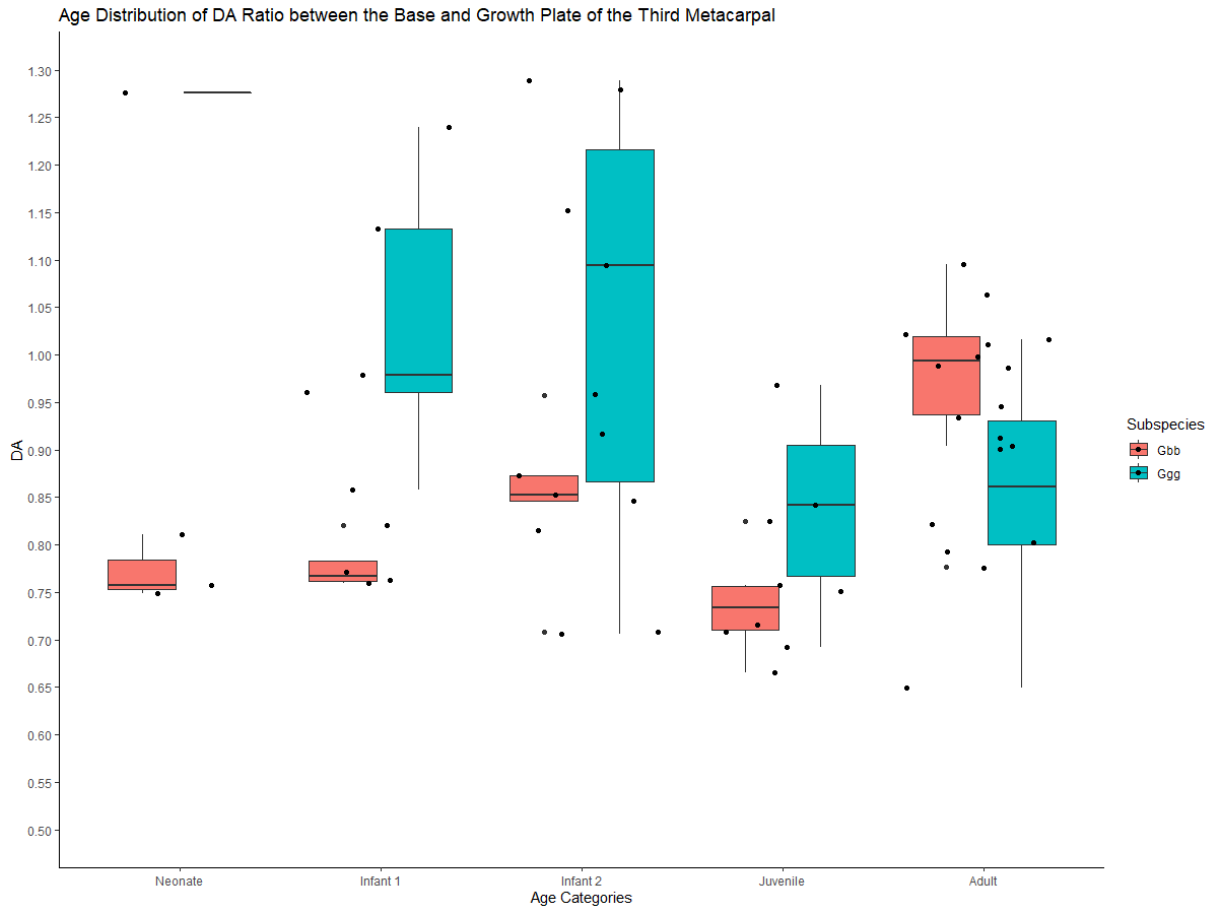

Figure 19. Boxplot of ratio of base and growth plate DA across age groups and species.

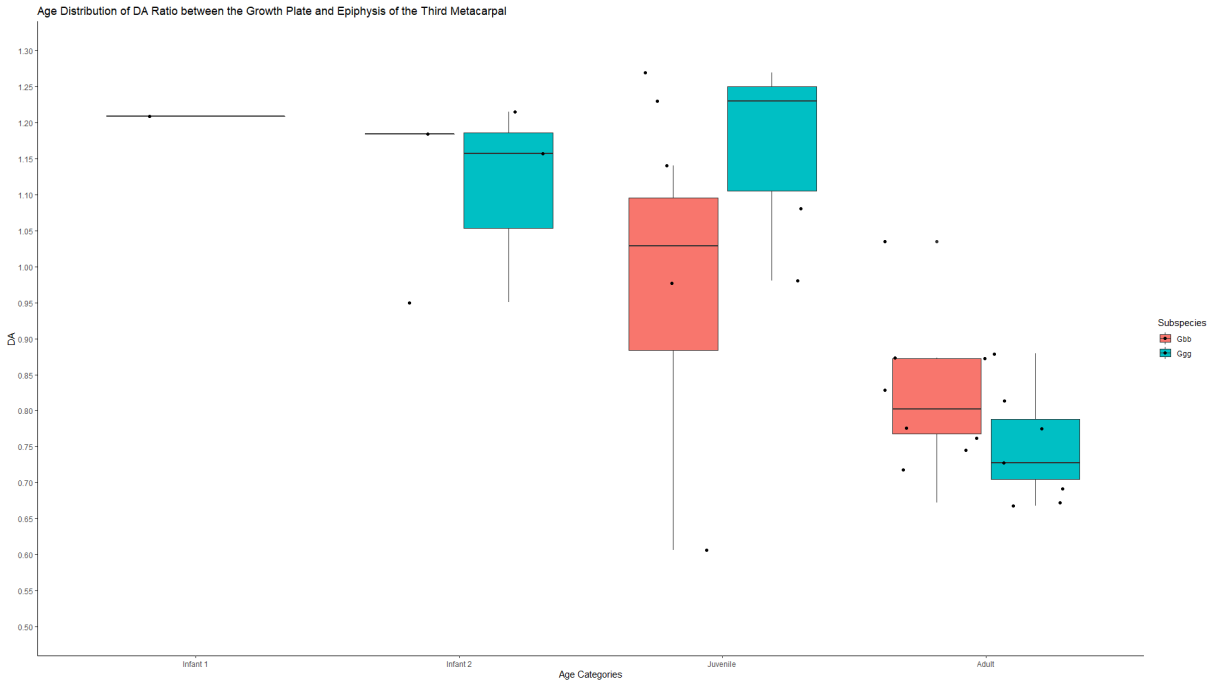

Figure 20. Boxplot of ratio of base and epiphysis DA across age groups and species.

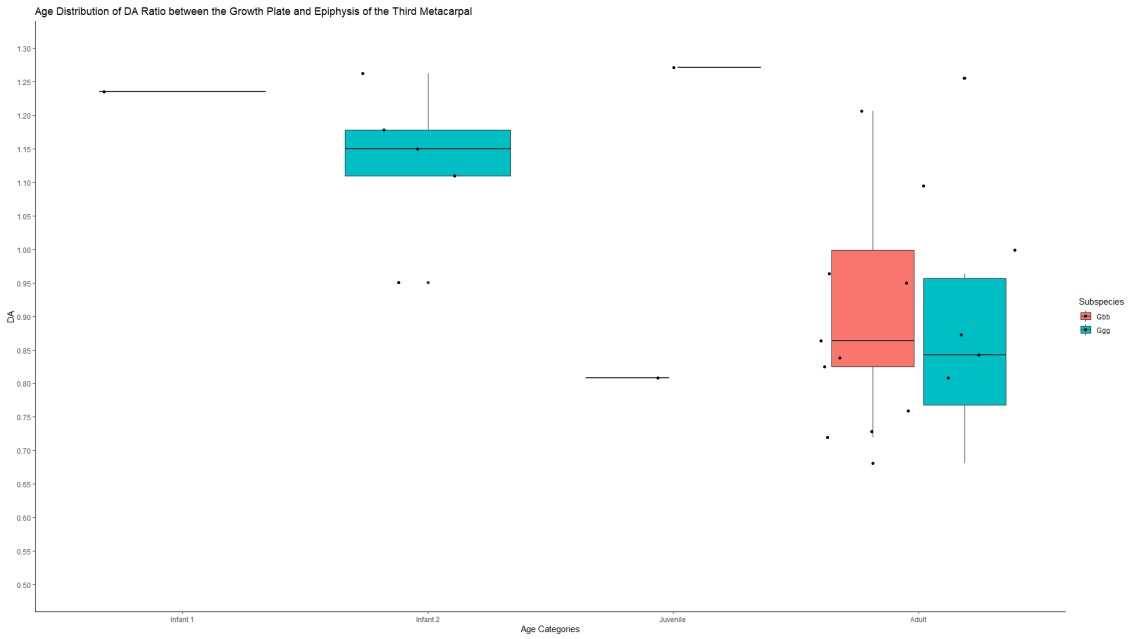

Figure 21. Boxplot of ratio of growth plate and epiphysis DA across age groups and species.

4.2.2.3 Interspecies Analysis

DA follows the same pattern of change in both species as observed when species were pooled, but greater variability in each age category is now found in *G. gorilla* (figure 19). Here, significant differences in DA are found in the metacarpal base in the pooled neonate/infant 1 category ($p = 0.046$) and juvenile category ($p = 0.039$), while DA differs significantly in the growth plate in adulthood ($p = 0.010$).

4.2.3 Trabecular Thickness (Tb.Th)

4.2.3.1 Species Pooled

Trabecular thickness is low at birth and increases throughout ontogeny in the base, growth plate, and epiphysis. Variation in Tb.Th seems to increase in the juvenile and adult age categories when compared to the neonate, infant 1, and infant 2 categories, especially in the metacarpal base (figure 22). Increases in Tb.Th in the base and metaphysis were significant for all categories except the neonate-infant 1, neonate-infant 2, and infant 1-infant 2 categories (table 3 and 4).This suggests a significant increase in trabecular thickness after 5 years of age, perhaps due to increase in body size. Trabecular thickness in the epiphysis was only significant between infant 2 and adult age groups ($p = 0.0011$).

4.2.3.2 Species Pooled Ratios

Trabecular thickness ratios between the base and the epiphysis and the metaphysis and the epiphysis remain relatively constant throughout ontogeny and no significant differences could be found (figures 24 and 25). The ratio of Tb.Th between the base and the growth plate does show an increase in trabecular thickness, especially once the juvenile period is reached (figure 23). However, only a significant difference was found between the juvenile and adult categories ($p = 0.0358$).

4.2.3.3 Interspecies Analysis

When looking at figure 22, little species difference can be observed between *Gorilla gorilla* and *Gorilla beringei*. Over all three areas, base, metaphysis, and epiphysis, the *Gorilla beringei* seems to show slightly more variation in trabecular thickness within each age category than observed in *Gorilla gorilla*, and the latter species tends to have slightly lower thickness scores as well in each bone section. However, none of these differences were statistically significant.

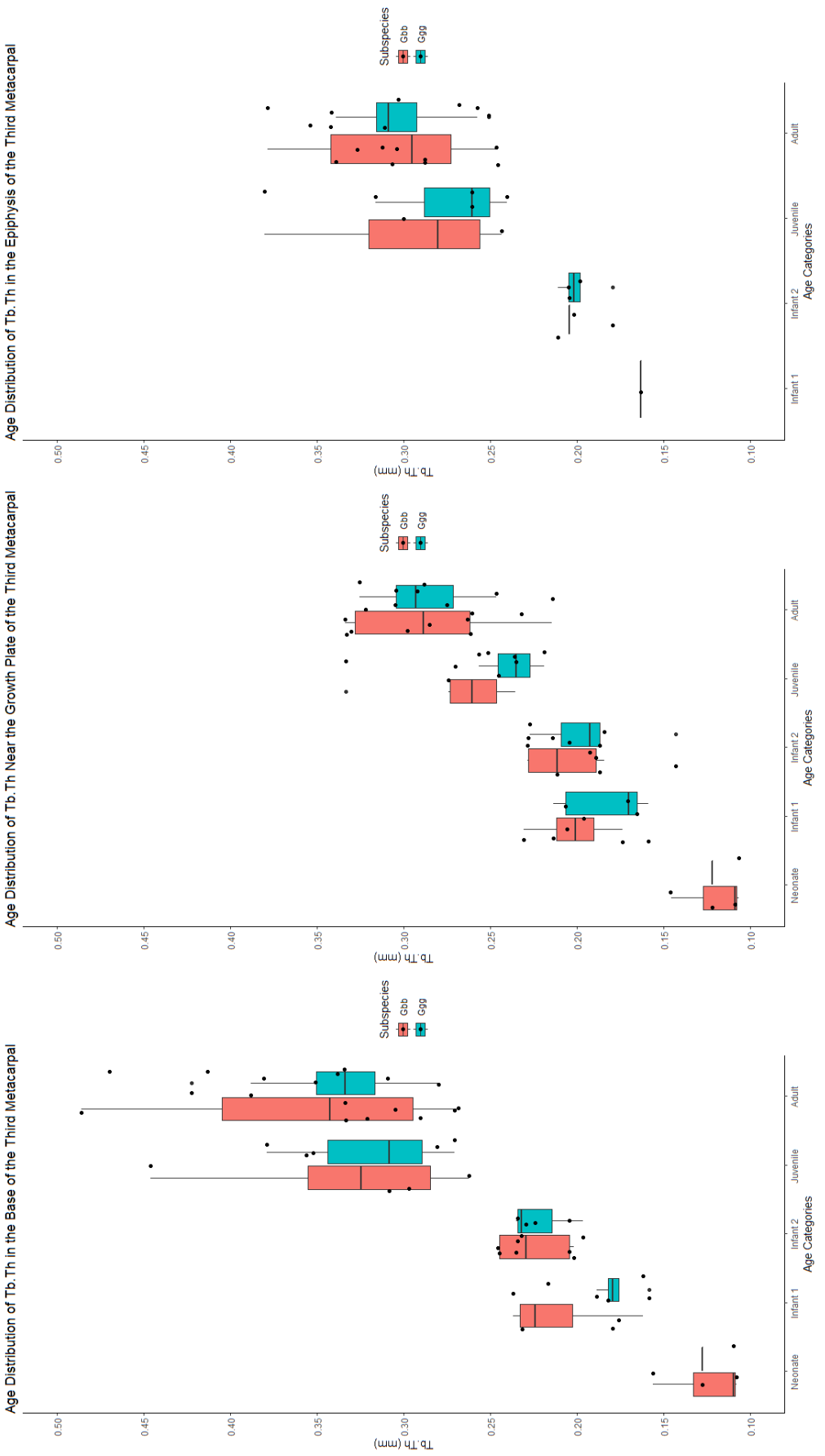

Figure 22. Boxplots showing the distribution of Tb.Th across age categories and species.

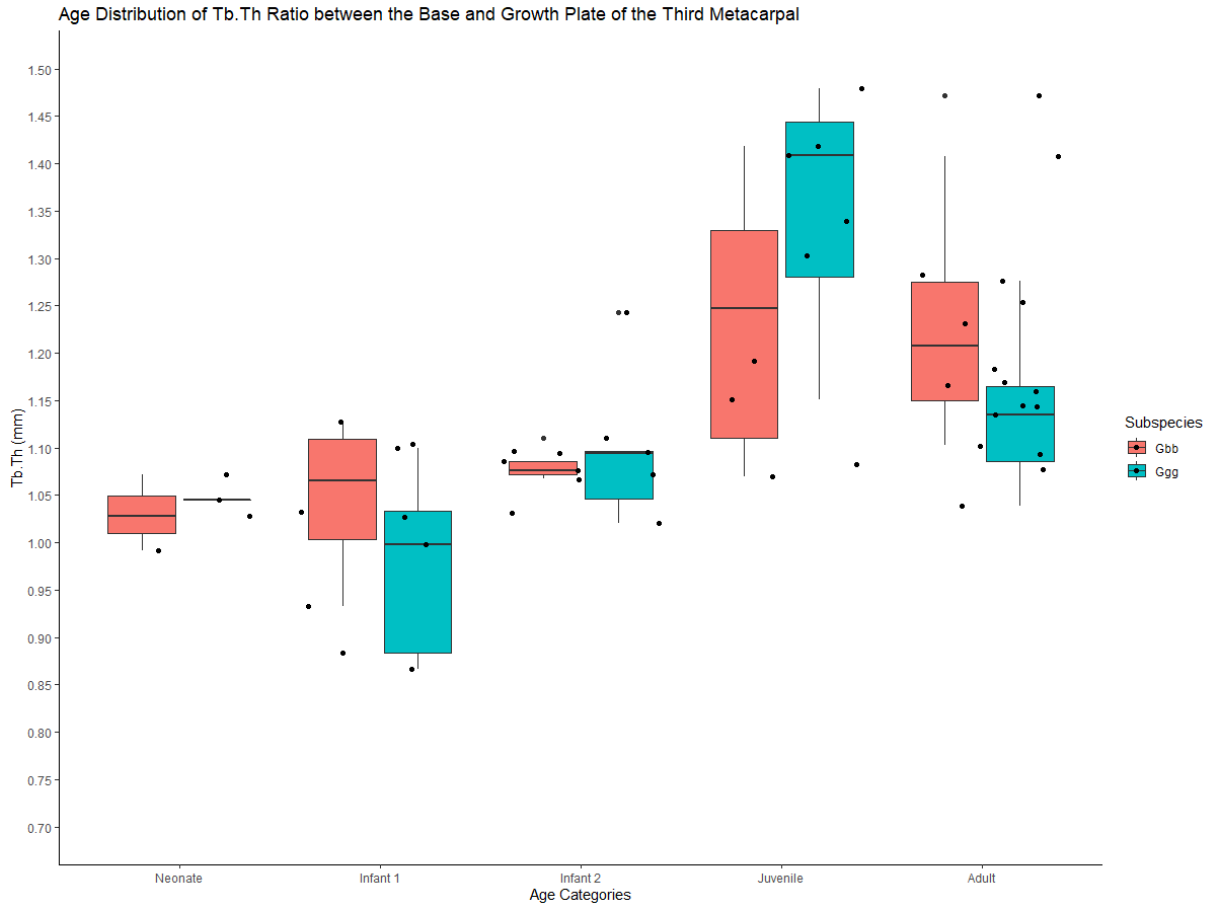

Figure 23. Boxplot of ratio of base and growth plate Tb.Th across age groups and species.

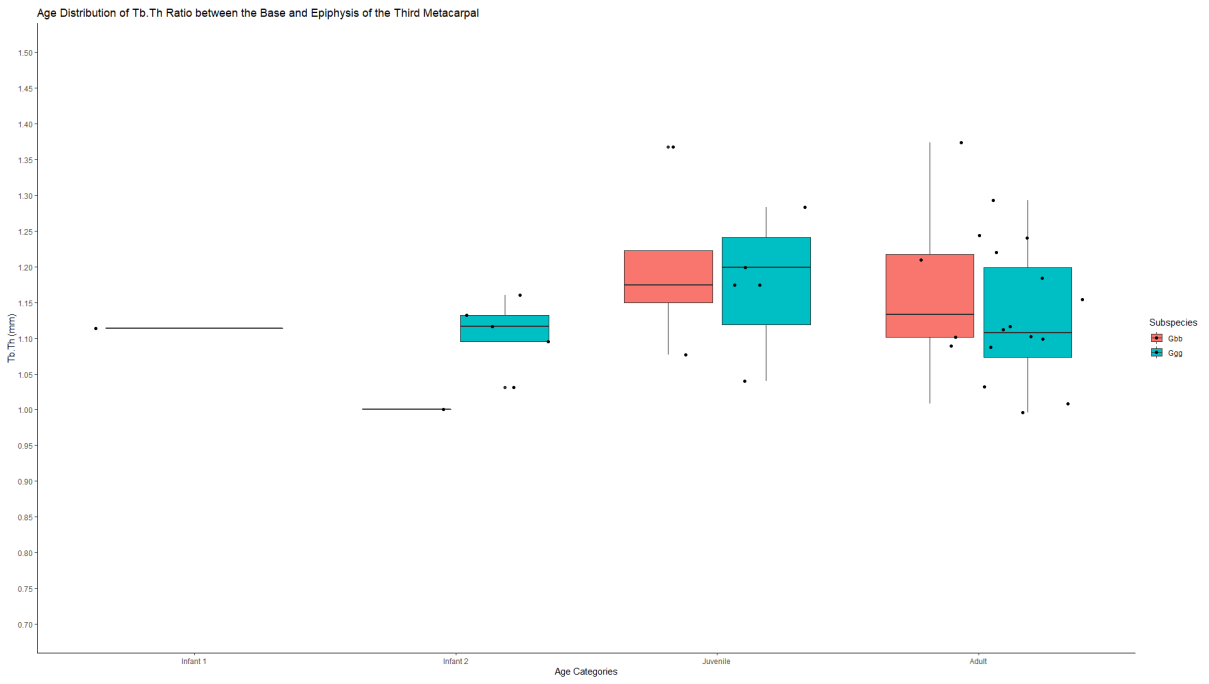

Figure 24. Boxplot of ratio of base and epiphysis Tb.Th across age groups and species.

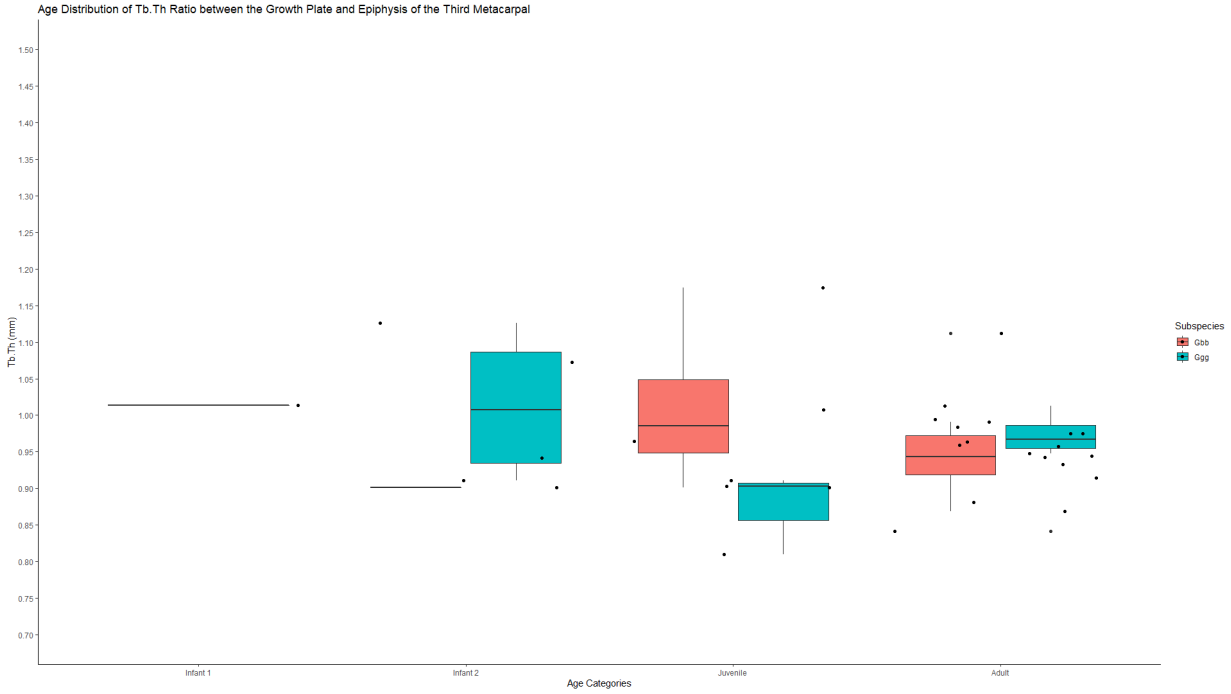

Figure 25. Boxplot of ratio of growth plate and epiphysis Tb.Th across age groups and species.

4.2.4 Trabecular Number (Tb.N)

4.2.4.1 Species Pooled

Trabecular number is higher at birth and decreases throughout ontogeny in the base, metaphysis, and epiphysis. Variation in trabecular number is high per age category. In the base and the growth plate, the most notable decrease in trabecular number occurred between the juvenile and adult age categories (figure 26), and is larger in the metaphysis, perhaps as a representation of bone resorption at the epiphyseal line. However, differences in Tb.N were only significant between neonates and adults ($p = 0.0028$) and infant 1 and adults ($p = 0.0172$) in the base, and infant 1 and adults ($p = 0.0041$) and infant 2 and adults ($p = 0.0001$) In the epiphysis a decrease in trabecular number is most visible between infant 2 and the juvenile category, but significance was only reached for difference in Tb.N between infant 2 and adult categories ($p = 0.0148$).

4.2.4.2 Species Pooled Ratios

The ratio of trabecular number between the base and the growth plate is larger at birth, decreases until approximately 5 years of age, and then starts increasing again (figure 27). Which suggests that there are more trabeculae present at the base early in life and later in life, when compared to the growth plate, which is somewhat reflected in figure 12 and the statistical results. Tb.N ratio difference between the base and growth plate were statistically significant for neonate and infant 2 ($p = 0.0011$) and infant 2 and adult ($p = 0.0210$). No statistically significant differences were found in trabecular number ratios between the base and the epiphysis, as values remained almost constant across age categories (figure 28). Trabecular number ratio between the epiphysis and growth plate is lower at 11 months of age and increases until 5 years of age (infant 2),

before slowly decreasing during the juvenile and adult categories (figure 29). Trabecular number ratio was significantly lower in the infant 1 category compared to infant 2 ($p = 0.0422$), but one only had one specimen. The difference in trabecular number ratio between the growth plate and epiphysis was also significant between infant 2 and adults ($p = 0.0020$).

4.2.4.3 Interspecies Analysis

Overall, both species follow the same pattern of higher trabecular number at birth and a decrease throughout development. Both species seem to have a lot of variation in number per category for each bone section. Interestingly, *Gorilla gorilla* has slightly higher Tb.N in the base than *Gorilla beringei* across age categories, while the opposite is true in the growth plate and epiphysis. No statistically significant differences were detected.

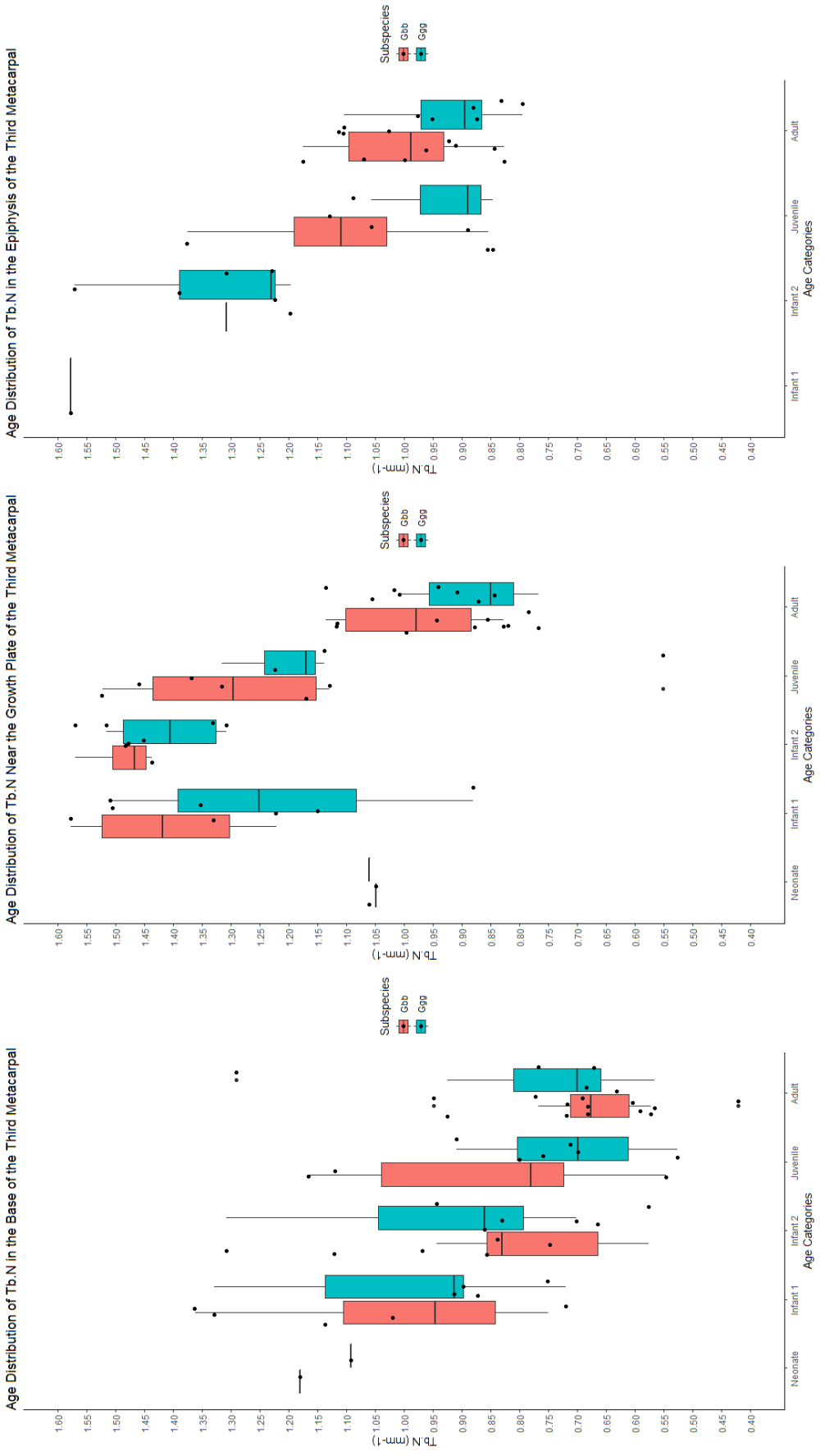

Figure 26. Boxplots showing the distribution of Tb.N across age categories and species.

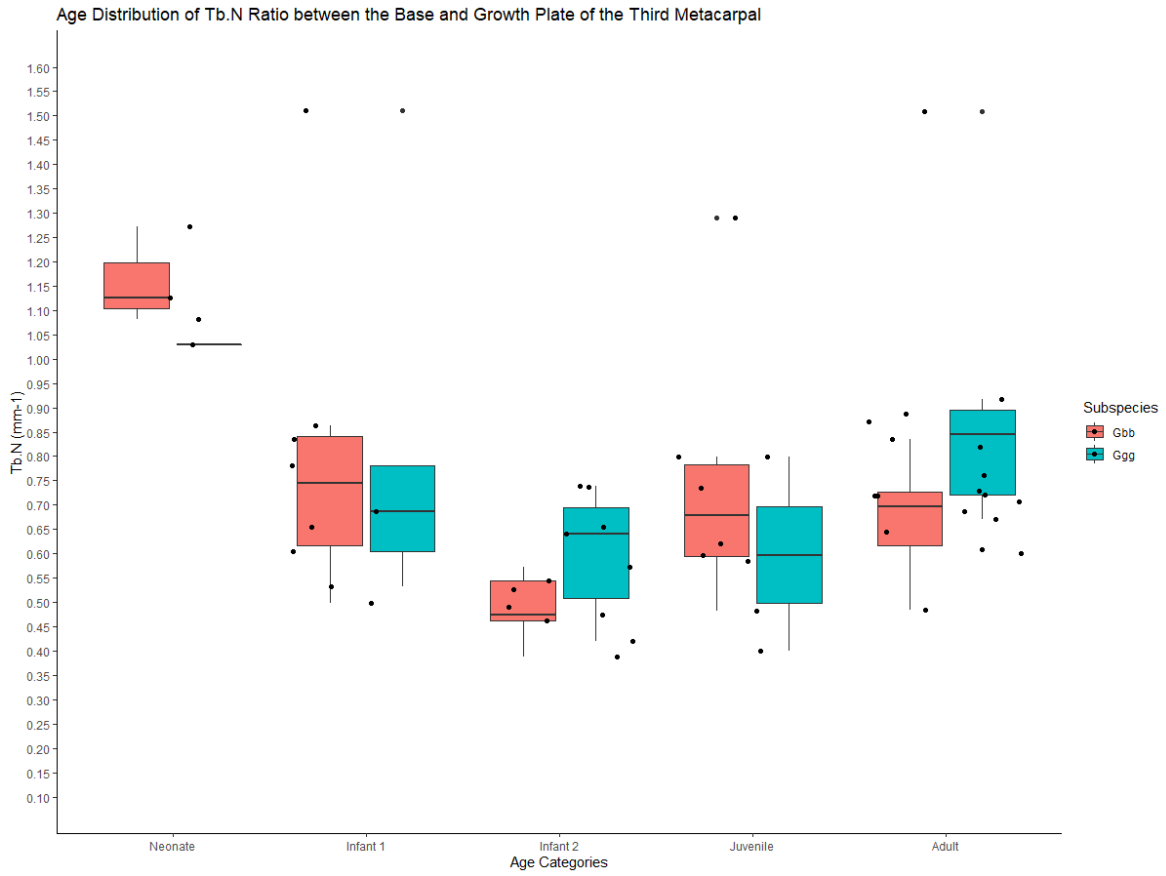

Figure 27. Boxplot of ratio of base and growth plate Tb.N across age groups and species.

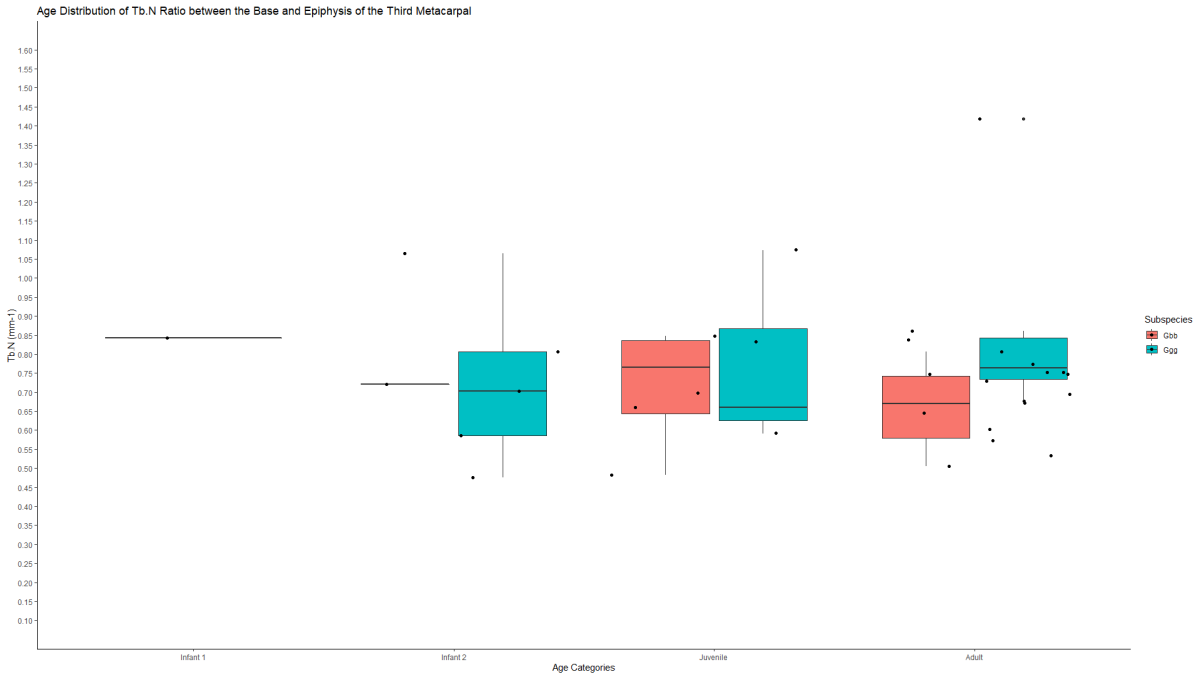

Figure 28. Boxplot of ratio of base and epiphysis Tb.N across age groups and species.

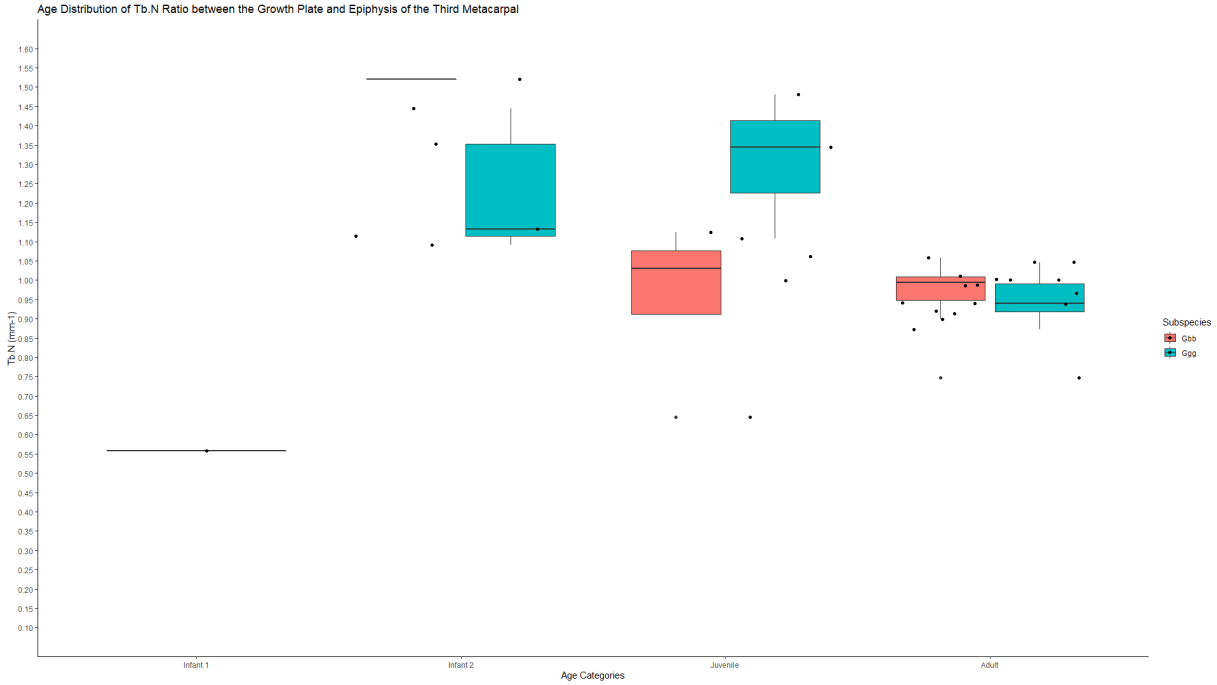

Figure 29. Boxplot of ratio of growth plate and epiphysis Tb.N across age groups and species.

4.2.5 Trabecular Spacing (Tb.Sp)

4.2.5.1 Species Pooled

Trabecular spacing was lower during the neonate period and increased throughout ontogeny for the metaphysis and base, and from infant 1 until adulthood in the epiphysis (figure 30). In the base, the largest increase can be seen between the neonate and infant 1 categories, and the infant 1 and 2 categories. However, statistical significance was only achieved between the neonate and adult categories ($p = 0.0037$) and the infant 1 and adult categories ($p = 0.0331$). In the metaphysis, a slight decrease can be observed in trabecular spacing from infant 1 to infant 2, before increasing once more, but once again only Tb.Sp between neonates and adults ($p = 0.037$) and infant 1 and adults ($p = 0.0331$) was found. In the epiphysis the trabecular number increases throughout ontogeny, but only the difference in trabecular spacing between infant 2 and adults was significant ($p = 0.0148$).

4.2.5.2 Species Pooled Ratios

Trabecular spacing ratios between the base and epiphysis and the epiphysis and the metaphysis remain relatively constant throughout ontogeny (figure 31 and 32). This is reflected in a lack of statistical significance in these values per age group. The trabecular spacing ratio between the base and the metaphysis shows an inverse pattern (figure 31) of that observed in the trabecular number base-metaphysis ratio (figure 27). Tb.Sp ratio is lowest in neonates and increases until infant 2, or 5 years of age, when a decrease can be observed throughout the juvenile and adult period. As trabecular spacing and number are interconnected, this mirroring makes sense. Significant differences in the ratio of trabecular spacing between the base and the growth plate were found between the neonate and infant 2 ($p = 0.00048$) and the infant 1 and adult ($p = 0.00932$) categories.

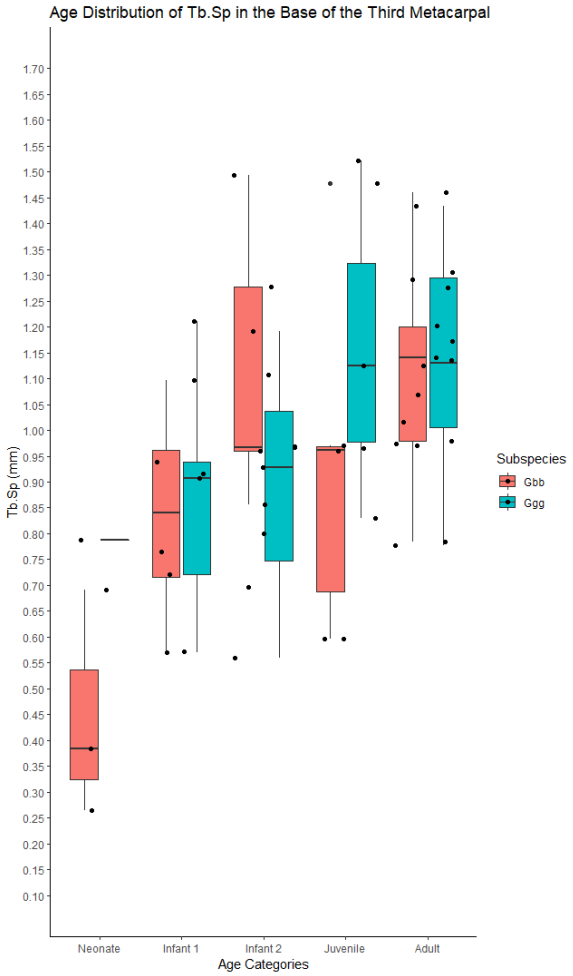
Age Distribution of Tb.Sp in the Base of the Third Metacarpal
Tb.Sp (mm)
Age Categories
Neonate
Infant 1
Infant 2
Juvenile
Adult
Subspecies
Gbb
Ggg

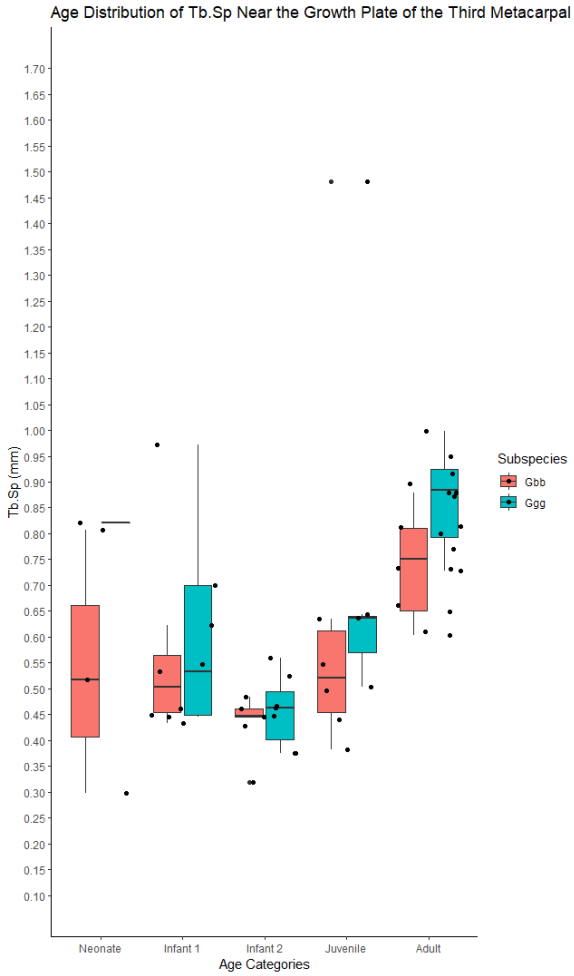
Age Distribution of Tb.Sp Near the Growth Plate of the Third Metacarpal
Tb.Sp (mm)
Age Categories
Neonate
Infant 1
Infant 2
Juvenile
Adult
Subspecies
Gbb
Ggg

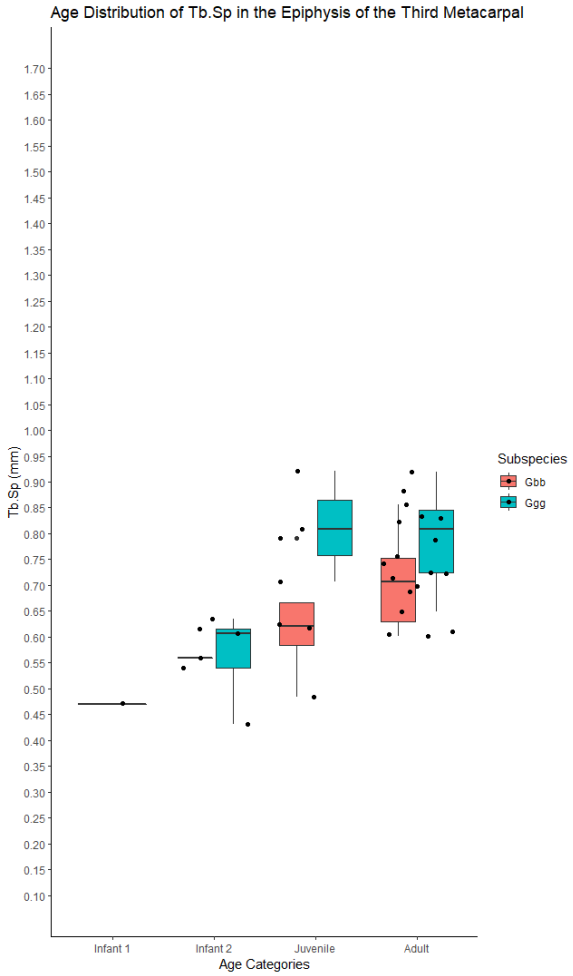
Age Distribution of Tb.Sp in the Epiphysis of the Third Metacarpal
Tb.Sp (mm)
Age Categories
Infant 1
Infant 2
Juvenile
Adult
Subspecies
Gbb
Ggg

Figure 30. Boxplots showing the distribution of Tb.Sp across age categories and species.

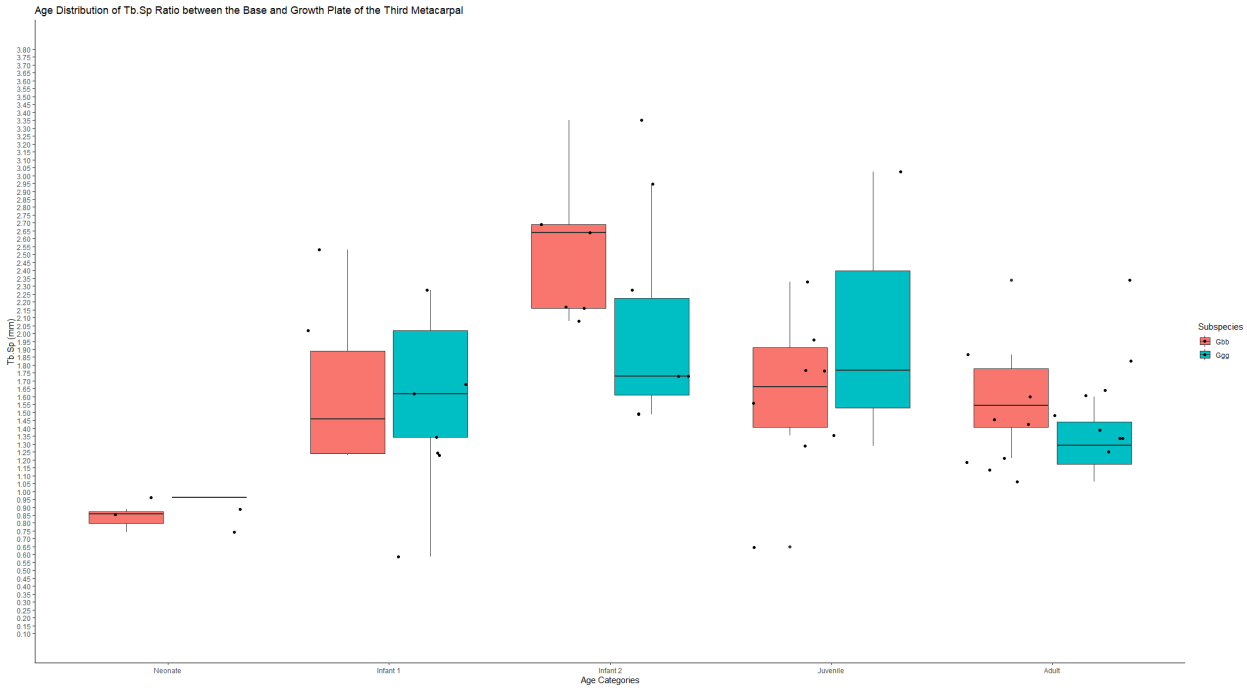

Figure 31. Boxplot of ratio of base and growth plate Tb.Sp across age groups and species.

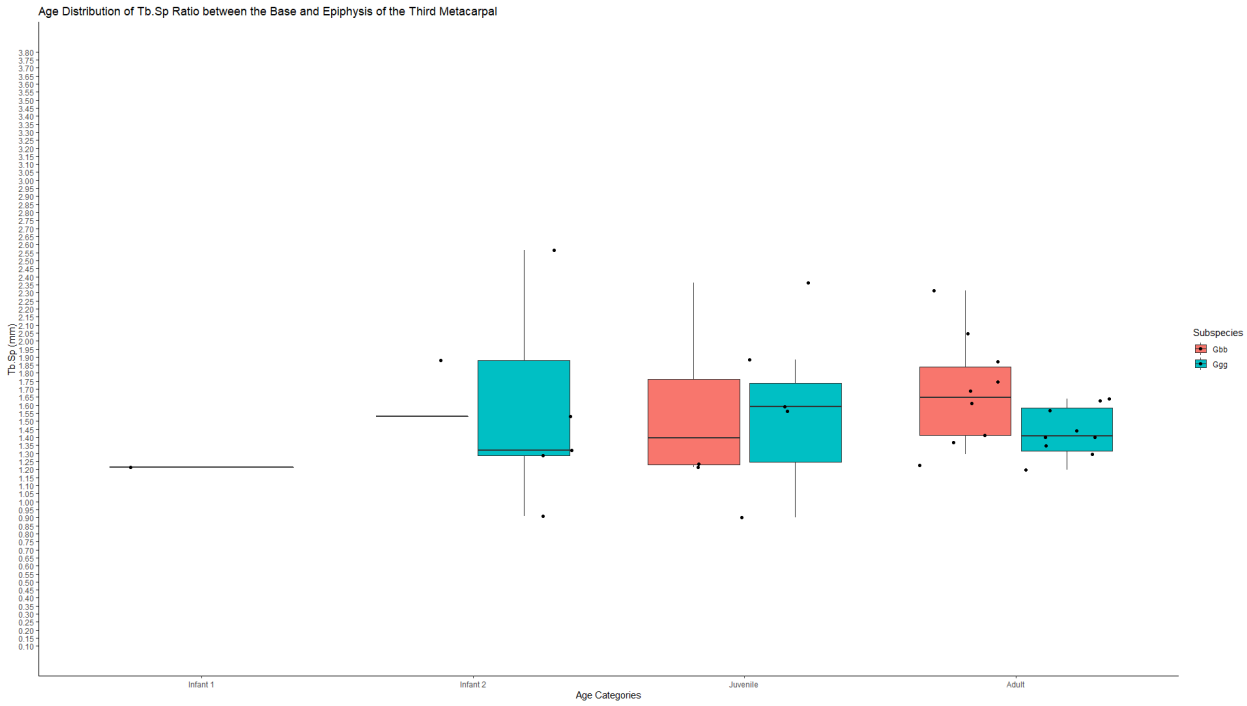

Figure 32. Boxplot of ratio of base and epiphysis Tb.Sp across age groups and species.

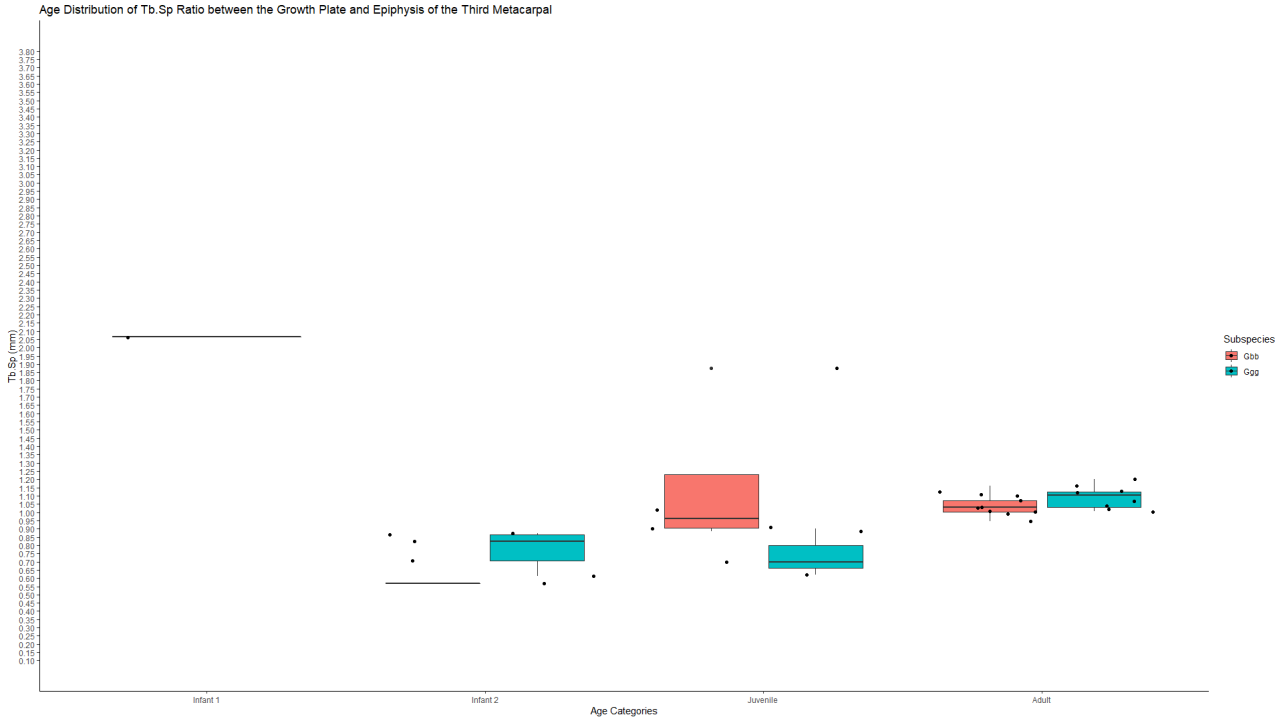

Figure 33. Boxplot of ratio of growth plate and epiphysis Tb.Sp across age groups and species.

4.2.5.3 Interspecies Analysis

Once again, no significant differences between species were found for each age category. However, we do see some interesting trends that are worth mentioning. In the base of the third metacarpal, trabecular spacing is higher for *Gorilla beringei* than *Gorilla gorilla* in age categories infant 1 and infant 2, before this reverses from the juvenile period onwards (figure 30). This same trend cannot be observed in the metaphysis and epiphysis, where trabecular spacing is always higher in *Gorilla gorilla*.

5 Discussion

This study aimed to provide greater insight into trabecular changes in the gorilla third metacarpal throughout ontogeny and its potential correlation to shifts in locomotor patterns with age. Understanding how immature activity patterns influence adult trabecular bone provides further insight into the functional interpretations we can draw from adult great ape trabecular morphology and more robust reconstructions of behaviour in fossil hominins.

5.1 *Gorilla* ontogenetic changes

We found that gorilla trabecular bone structure in the neonate category was categorised by thin, closely spaced trabeculae, with low BV/TV compared to older age groups. As age progressed, BV/TV and Tb.Th increased in all bone sections, while Tb.Sp remained relatively constant throughout ontogeny. Trabecular number decreased throughout ontogeny in the distal metaphysis and epiphysis, while remaining relatively constant in the base. As the base of the metacarpal does not have a secondary growth centre, this difference between the growth plate and base of metacarpal in Tb.N most likely reflects higher rates of (re)modelling creating new trabecular struts at the growth plate and epiphyses. In contrast, in the base, the increase in Tb.Th, but relatively constant Tb.N, may suggest a different bone functional response to stress in which extra bone is deposited on already existing trabecular struts. One explanation could be that overall morphology (orientation and number) of trabeculae is more genetically constrained in order to maintain bone integrity while changes in mechanical loading, increases in body mass, and growth at the metaphysis are still occurring. In sheep calcanei (Lanyon 1974), and the human os coxae

(Cunningham and Black 2009) trabecular structure has been found to be largely predetermined. Significant differences between age categories for most trabecular variables were mainly found to be between the neonate/infant 1 categories and the juvenile/adult categories. As the juvenile age category is marked by the full adoption of knuckle-walking and more adult-like activity patterns (Figure 1), it may be that these trabecular changes reflect this locomotor shift.

When comparing our results to other ontogenetic studies of non-human ape (Ragni, 2020, Tsegai et al. 2018; Zeiniger 2013) and human (Milovanovic et al. 2017; Perchalski et al. 2017; Ryan and Krovitz, 2006; Gosman and Ketcham, 2009; Raichlen et al. 2015) trabecular bone, we find both similarities and differences in the ontogenetic pattern of trabecular bone in the gorilla third metacarpal. In humans, BV/TV and Tb.N in the proximal femur (Ryan and Krovitz, 2006; Milovanovic et al. 2017), the proximal tibia (Gosman and Ketcham, 2009), and the distal tibia (Raichlen et al. 2015) are higher in perinatal humans than at any other stage of life (Nuzzo et al. 2003). Between 6 months and the first year of life, a dramatic reduction in BV/TV, Tb.N, and connectivity density were observed in both the femur and the tibia (Ryan and Krovitz, 2006; Gosman and Ketcham, 2009; Raichlen et al. 2015). At the advent of independent bipedal locomotion, around 1.5 – 2 years of age, all of these trabecular parameters increased once more in the proximal femur and the distal tibia, though they do not reach the same levels as seen during the perinatal phase (Ryan and Krovitz, 2006; Gosman and Ketcham, 2009; Raichlen et al. 2015). This decrease in BV/TV and Tb.N in early childhood is most likely related to the advent of bipedal locomotion in humans, as this decrease is not observed in the human humerus (Perchalski et al. 2017). The human upper limb shows the same high perinatal BV/TV and Tb.N and low Tb.Sp, but does not show the dramatic decrease at approximately 6 months – 1

year. Instead BV/TV and Tb.N increase gradually throughout ontogeny (Perchalski et al 2017). This same trend of high BV/TV at birth, with a decrease as locomotion commences, was found in the limb bones of canines (Wolschrijn and Weijs, 2004). However, in contrast, equines showed high BV/TV at birth but no decrease in BV/TV as locomotion commences (Gorissen et al 2018). This difference may be an artefact of differences in the rate of changes in bone volume related to total volume (i.e. BV vs TV). A reduction in BV/TV could be due to a faster increase of total volume compared to bone volume, or a reduction in bone volume and a very slow increase in total volume. This could mean that a similar reduction in BV/TV in two separate species could be due to a difference in the rate of growth compared to the rate of bone resorption and deposition. It should also be kept in mind that body size differences between these species may be causing unexpected results. The level of trabecular thickness seems to be the main contributor to BV/TV in large mammals, while in small mammals this is mainly regulated by trabecular number (Barak et al 2013a).

As great apes use both their fore- and hind limbs for locomotion, it might be reasonable to predict that ontogeny of trabecular bone morphology would be similar to that of other quadrupedal mammals and to the human lower limb in particular. However, it has been shown that this is not the case. In the great ape calcaneus (Zeiniger, 2013), the chimpanzee humerus, femur, and tibia (Tsegai et al. 2018a), and the gorilla third metacarpal base (Ragni 2020), BV/TV and Tb.Th was lowest at birth and increased throughout ontogeny, without a decrease occurring at 6 months of age or any other juvenile period. Our results showed a similar pattern to that of the chimpanzee forelimb (Tsegai et al. 2018a). Overall, we observed that BV/TV and Tb.Th were low at birth and increased throughout ontogeny. However, the youngest individual in our sample (2 hours old) had low BV/TV when compared to older age

categories, but had higher BV/TV than Infant 1 specimens aged 2 weeks and older. There may be several reasons for this documented ontogenetic variation in trabecular morphology across species. The high density of trabecular bone in humans compared to other mammals may be due to genetic regulation (Acquaah et al 2015), and this may also be the case for other primate species. Although there is movement of the fetus *in utero*, it is possible that it is not until after birth that biomechanical loading will have an influence on trabecular bone structure. Furthermore, it may be more effective to remodel a dense trabecular structure by removing bone in response to mechanical loading than it is to create new struts in a sparsely populated trabecular structure (Tanck et al 2001; Tsegai et al. 2018a). The high density of trabecular bone in early life may also me related to calcium metabolism. Lower levels of calcium have been linked to loss of trabecular bone in rats (Seto et al. 1999) and humans (Gallagher et al. 1982), while high rates are linked to greater bone density. The high trabecular number at birth may be a mechanism to allow for greater storage of calcium, which can subsequently be used for bone growth and remodelling (Schwartz et al. 1998). Variation in life history likely also plays an important role in which precocial species need to load their limbs immediately after birth. Thus, the consistently high BV/TV found in precocial species, may be a result of shift in timing, in which the BV/TV decrease actually happens *in utero* and the trabecular structure is subsequently predetermined to anticipate the mechanical loading that will occur after birth (Gorissen et al. 2016; Gorissen et al. 2018; Tsegai et al 2018). This latter explanation, however, is unlikely to explain the decrease in BV/TV observed in the gorilla metacarpal between individuals that were 2 hours and 2 weeks of age, as during this time the infants are wholly dependent on their mothers and carried most of the time (Doran, 1997). The high BV/TV in the 2 hour-old individual may simply be

pathological (given its early death). More individuals of similar age are necessary to ascertain if this is an aberration in the data or a developmental pattern in *Gorilla*.

The results of our study found some differences in the ontogeny of trabecular morphology compared with that of Ragni's (2020) trabecular study of the third metacarpal base. We found that BV/TV increased throughout ontogeny, as has been reported in other mammalian ontogenetic studies (Tanck et al. 2000; Wolschrijn and Weijs, 2004; Ryan and Krovitz, 2006; Gosman and Ketcham, 2009; Raichlen et al. 2015; Tsegai et al. 2018a), while a decrease in BV/TV was observed by Ragni (2020). This discrepancy may be due to methodological differences. Ragni (2020) used a volume-of-interest approach and thus only quantified a subset of trabeculae within in the metacarpal base, while we analysed the entire trabecular structure within the proximal metacarpal. It may be that BV/TV decreases in the centre of the metacarpal base, while it increases in other areas of the base (as seen in Figure 5.)

Degree of anisotropy is often used to infer changes in direction of joint loading throughout life (Ryan and Ketcham, 2002; Barak et al. 2011; Kivell, 2016). In the gorilla third metacarpal, DA showed an intermediate (i.e. a mix of isotropic and anisotropic trabeculae) value, and was relatively constant throughout ontogeny in the base, distal metaphysis, and epiphysis. This result was also found by Ragni (2020) and was expected for the region of the growth plate before fusion occurred as the deposition of primary trabeculae during bone growth would be uniform until remodeled into secondary trabeculae under the influence of mechanical loading (Scheuer et al. 2000). However, it was expected that DA in the base and epiphysis would become more anisotropic throughout life as suspensory and play behaviours decreased (Doran, 1997) after 5 years of age and more habitual loading during knuckle-walking increased. In contrast to our results, a reduction in DA reflecting a

more isotropic structure consistent with more variable joint loads, was observed in the infant chimpanzee humerus and tibia before increasing again at the juvenile stage (>5 years of age) stage (Tsegai et al. 2018a). This pattern was also found in the humerus and lower limb of modern humans, where DA decreases when independent locomotion commences (6 months – 1 year) and increase as bipedality becomes habitual (Gosman and Ketcham 2009; Perchalski et al. 2017; Raichlen et al. 2015; Ryan and Krovitz, 2006). The relatively constant DA across all regions of the gorilla metacarpal throughout ontogeny that we found may reflect differences in locomotion, and variation in hand postures (Neufuss et al. 2017; Thompson et al. 2018) that result in an 'intermediate DA' pattern. Another explanation for these results may be methodological. Our method analyses the whole structure and not a VOI located near an articulation, it may be that there are differences in DA subchondrally, but that these are being averaged out by opposite DA values found elsewhere in the bone.

5.2 Interspecific comparisons

Our hypothesis that there would be significant differences between species in the trabecular structure due to changes in activity patterns after 5 years of age was not supported. Although we did find significant differences between *G.gorilla* and *G.beringei* in DA in the base among juveniles and in the distal metaphysis among adults that may be indicative of slightly different loading patterns, these did not occur in the other bone regions as would be expected. While adult western lowland gorillas have been reported to be more arboreal than mountain gorillas (Doran, 1997; Remis, 1995; Remis, 1998), their overall locomotor patterns remain similar. Both practice terrestrial knuckle-walking as their main form of locomotion, interspersed with vertical climbing and other arboreal behaviours. These species differences in locomotion have been shown to be reflected in the overall morphology of the talus

(Knigge et al. 2015), and the cortical geometry of the fore- and hindlimb (Ruff et al. 2013). The lack of difference observed between species in this study may indicate that trabecular bone responds to different types and directions of mechanical loading (together with metacarpal cortical bone), but is not sensitive enough to reflect slight differences in frequency of these behaviours.

Another explanation may be that differences in cortical bone development throughout ontogeny may be occurring instead. Ruff et al. (2013) showed that the cross-sectional geometry of mountain gorilla fore- and hind limbs reflected changes in their locomotion patterns during ontogeny. The forelimb/hindlimb strength ratio of mountain gorilla individuals under the age of two years was similar to that of adult western lowland gorillas, consistent with a higher rate of arboreal behaviour in the immature mountain gorillas compared to their adult counterparts and the higher rate of arboreal behaviour in adult western lowland gorillas compared to mountain gorillas (Ruff et al., 2013). However, a similar study has not yet been done for gorilla metapodials.

It may be that some of the similarities in the trabecular morphology of the metacarpal in the two gorilla species under study are due to phylogenetic convergence. Geometric morphometric analysis of the catarrhine talus showed that not all aspects of a skeletal element reflect phylogeny (Turley and Frost 2013). Turley and Frost (2013) found that the proximal facet of the talus morphology was closely linked to locomotor behaviours, while the distal facet shape reflected phylogeny in catarrhines, However, a subsequent study of the shape difference of the distal talar facet in western lowland gorillas and mountain gorillas (Knigge et a. 2015) found that shape differences were related to ecological rather than phylogenetic differences. A lack of phylogenetic signal between gorilla subspecies was also found in the humerus.

Analysis of the external morphology of the humerus (Holliday and Friedl 2013), specifically the articular surface size, humeral torsion, and length, has shown that there is a phylogenetic signal for all African apes. However, this study showed that western lowland gorillas were more like chimpanzees than mountain gorillas in their humeral morphology, suggesting a lack of phylogenetic convergence between gorilla species (Holliday and Friedl 2013). This suggests that it is more likely that the lack of interspecific difference in trabecular morphology found here is due to similarity in behaviour instead of phylogeny.

5.3 Trabecular bone distribution

In addition to measuring changes in trabecular variables in the base, distal metaphysis, and epiphysis of the gorilla third metacarpal, this study also analysed the distribution of trabecular bone across the whole bone to identify areas of increased bone volume, which in adults have previously been shown to be reflective of locomotion. A high concentration in BV/TV in the dorsal and palmar aspects of the metacarpal head have been linked to knuckle-walking (extended metacarpophalangeal joint) and arboreal grapsing (flexed metacarpophalangeal joint) in chimpanzees and gorillas, respectively (Chirchir et al. 2017; Dunmore et al. 2019; Matarazzo, 2015: Tsegai et al. 2013). A higher concentration of palmar BV/TV has been linked to the flexed metacarpophalangeal joint postures used during suspensory behaviours in orangutans (Chirchir et al. 2017; Dunmore et al. 2019; Matarazzo, 2015; Tsegai et al.2013) and manipulation in humans (Chirchir et al. 2017; Skinner et al. 2015; Stephens et al. 2018; Tsegai et al. 2013). We found the same adult gorilla distribution of BV/TV in the metacarpal head, but that this pattern was not present at birth and did not appear until become fully adult-like until well after sexual maturity has been reached (Figures 5-6). During the first 6 months of life, BV/TV was fairly homogenously distributed

compared to older individuals, but showed higher BV/TV concentrations underneath the growth plate and in the dorsal and palmar aspects of the base. No data was available for the epiphysis for this age category. As independent locomotion is minimal at this age, it is more likely that the higher concentrations of BV/TV, especially at the growth plate, are due to general changes in morphology due to growth (Rolian, 2006; Scheur et al. 2000) and not due to biomechanical changes related to behaviour.

From 6 months – 5 years of age (Infant 1 to Infant 2), BV/TV becomes more concentrated at the growth plate and the metacarpal base, with the highest BV/TV values found palmarly in both regions. As palmigrade and suspensory behaviours are still frequent during this time (Doran, 1997), it may be that these higher palmar concentrations in the metacarpal reflect greater use of flexed metacarpophalangeal joint postures (Matarazzo, 2013; Susman, 1979; Tuttle, 1969). During this time BV/TV remains low in the epiphysis, and the highest concentrations occur distally, which may be reflective of both the beginning of knuckle-walking (hyperextended metacarpophalangeal joint) but also frequent arboreal grasping (flexed metacarpophalangeal joint).

The same overall pattern of BV/TV distribution in the metacarpal corpus described for 6 months to 5 years of age was also found between 5-11 years of age, although there was an increase in BV/TV at the palmar and dorsal aspects of the base, as well a decrease in BV/TV at the centre of the growth plate. The BV/TV increase in the base is most likely a result of a thickening of the trabeculae, which may also reflect increased body size. The decrease of BV/TV in the centre of the growth plate, combined with an increase in the dorsal and palmar BV/TV concentrations, most likely reflect the beginning of epiphyseal fusion. As trabeculae at the centre of the epiphyseal line are resorbed, more load needs to be distributed through the trabeculae in the dorsal

and palmar sections. Interestingly, before fusion occurs in the younger individuals (5 – 8 years), BV/TV was higher and more homogenously distributed across the epiphysis than at any other time in ontogeny. This BV/TV increase may help compensate for increased loads related to locomotion and body size to the metacarpal corpus while the cartilaginous layer of the epiphyseal plate is ossifying (Scheur et al. 2000). It is not until after full fusion of the epiphysis (12+ years) that the adult-like BV/TV distribution pattern emerged, in which BV/TV concentrations were highest distodorsally on the metacarpal head and palmarly in the base. This pattern is consistent with the habitual hand postures of knuckle-walking, as previously discussed (Chirchir et al. 2017; Dunmore et al. 2019; Matarazzo, 2015: Tsegai et al. 2013).

Although the trabecular distribution pattern described above was found in all adult individuals, we also noted that the epiphyseal line remained in several individuals until approximately 30 years. These individuals retained a higher concentration of BV/TV where the growth plate used to be, and have an overall higher BV/TV in their metacarpal heads than in individuals where the epiphyseal plate has been completely remodelled (Figure 6, category 5). This finding suggests that bone growth is not complete when the individual is considered sexually mature. The retention of high BV/TV, particularly within the palmar region of the metacarpal head was found in both mountain and lowland gorillas with remnant epiphyseal plates. This BV/TV distribution may indicate an adaptive lag in the bone's response to adult-like locomotion patterns. Such an adaptive lag has been observed in the trabecular development of suids, where peak bone density was reached many weeks before DA reached its adult-like configuration (Tanck *et al.* 2001). Evidence of adult trabecular morphology reflecting juvenile behaviour can also be found in modern humans calcaneal morphology (Pettersson et al. 2010). The adult calcaneus of men who had

exercised regularly during their juvenile period, but had since stopped this behaviour in adulthood, showed a higher degree of bone mineral density than the adult calcaneus of men who had never exercised during childhood (Pettersson et al. 2010). This may suggest that juvenile behaviours in humans and great apes may influence adult trabecular morphology.

5.4 Systemic Factors

It should also be kept in mind that some of the discrepancies found in our data may be due to other systemic factors, such as gene or hormone control or differences in the microbiome. Previous studies have found that bone growth processes may be genetically controlled to a much greater degree than previously thought. Lovejoy et al. (2003) argued that bone morphology in mammals is mainly determined by positional information, not specifically mechanical loading, and that the processes of ossification at the growth plates appear to be regulated mainly by selector genes, such as Hox genes. Furthermore, a study that varied the severity and frequency of mechanical stimuli in mice with genetically determined varied bone mineral density propensities showed that bone formation rates were related to already present bone mineral density at birth, with high-density mice showing no response in bone formation rates due to mechanical stimuli (Judex et al. 2002). A similar result was found in the cortical bone of these mice (Robling and Turner 2002). This would suggest that at least for some species, the sensitivity of trabecular bone to mechanical loading patterns may vary, and that this sensitivity may be genetically controlled. While a mechanical signal can be demonstrated in our study, the influence of predetermination of certain growth patterns must be taken into account as a possible explanation and a degree of genetic predetermination in the trabecular structure of the

gorilla third metacarpal may account for the lack of difference in trabecular morphology between the two species despite their differing locomotor patterns.

Hormones are another factor that may have a significant effect on trabecular bone morphology. A study looking at sex differences in modern humans (Eckstein et al. 2007) showed that there were significant differences in trabecular bone morphology that were most likely related to differences in testosterone/oestrogen hormones between sexes. However, these differences were only found at specific skeletal sites (i.e. distal radius, femoral neck) and not others, suggesting that trabecular bone response to hormone input varies across the skeleton. Different hormones may also have a different effect on bone morphology. A study looking at the influence of testosterone and growth hormone on cortical and trabecular bone in rats (Prakasam et al. 1999) showed that, while variations in the levels of these hormones showed a significant effect in the bone mineral density of the cortical bone, no such effect could be seen in the metaphysis or its trabecular structure. This may indicate that the process of bone growth at the epiphysis and metaphysis is controlled by other factors, such as the mechanical loading patterns looked at in this study. Another study that combined mechanical loading with pituitary growth hormone release in rats (Kim et al. 2003) showed that an increased bone formation rate was only achieved when both stimuli (hormone and mechanical) were applied, and that bone formation decreased to that of the control groups when only one of the stimuli was applied. This further suggests that while hormones may be influencing bone formation, mechanical loading also provides a significant effect on bone growth patterns.

5.5 Relevance to Fossil Record

Previous descriptions of the external bone structure of juvenile fossil hominins indicate that overall bone morphology reflects locomotion in species such as Australopithecus afarensis (Alemseged et al. 2006; Green and Alemseged, 2012), Australopithecus sediba (Berger et al. 2010; Cameron et al. 2013), Homo habilis (Leakey et al. 1964), Homo naledi (Bolter and Cameron, 2020; Bolter et al. 2020), Homo erectus (Brown et al. 1985), Dmanisi (Lordkipanidze et al. 2007), Homo antecessor (Bermúdez de Castro et al. 1997), and Homo neanderthalensis (Rosas et al. 2017), but trabecular variables in juvenile fossil hominins have not been studied extensively. So far, most of the studies that have included the above mentioned juvenile fossil material have been concerned with cranial and dental analyses (Anton and Leigh 2003; Kuykendall 2003). Dental eruption sequences of modern humans and primates are often used as a comparative basis for reconstructing life history events in fossil hominins (Bolter et al. 2004; Bolter and Zihlman 2012). The timing of eruption of the first molar is often used as an indicator for the end of infancy in humans and extant apes and fossil remains are often compared to these species to identify when they would have had this same life history event (Smith, 1989;1991;1995, Smith et al. 1994). However, recent work has shown that ecological differences could influence ontogenetic timings (Bolter et al. 2004; Bolter and Zihlman 2012). A comparison of captive and wild chimpanzees showed that wild chimpanzees have slower life histories than their captive counterparts, with wild chimpanzees taking almost 3 years longer to mature and the emergence of the first permanent molar happening later than in 90 percent of the captive individuals (Bolter et al. 2004; Bolter and Zihlman 2012). This finding has influenced the age estimation of KNM-WT15000, the juvenile *Homo erectus* individual, who is now estimated to be younger. This, combined with this

overall estimation of body mass and stature, would indicate that early *Homo* achieved adult body proportions earlier in life, which would suggest a more ape-like life history (Dean and Lucas 2009).

This finding of a more ape-like growth pattern for most fossil hominin species has also been corroborated by studies of juvenile external morphology. A comparative analysis of the juvenile and adult pelvis of apes and humans and the pelvic fragments of several *Australopithecus* (STS 14, AL-288, MLD7) showed a closer relation in pelvic growth to apes than humans (Berge 1998; 2002). A further study (Green and Alemseged 2012) of the morphology of the scapula of the DIK-1-1 infant compared this to ontogenetic changes in humans and apes and concluded that the Dikika scapular spine orientation was more similar to that of juvenile apes. The only ontogenetic studies to date that have indicated a more human-like growth and development pattern have been those conducted on juvenile *Neanderthalensis* (Rosas et al 2017; Chevalier et al 2021), which would suggest that modern human life history patterns are a fairly recent development in our evolutionary history.

This study provides new data on trabecular bone response to mechanical loading in juvenile gorilla, which in the future may be used as a comparative framework in the behavioural reconstruction of (juvenile) fossil hominins via trabecular bone parameters. The transition from suspensory to mainly terrestrial locomotion observed in this study indicates that similar locomotion transitions may also be reflected in fossil hominin trabecular architecture and may shed light on whether species such as Australopithecus afarensis were still semi-arboreal or obligate bipeds (Ward, 2002).

Furthermore, the possible adaptive lag observed between the trabecular structure and adult-like external skeletal morphology and adult behaviours in the

gorilla sample should also be of the most interest. The adaptive lag in this study not only indicates we should be cautious when interpreting behaviour from trabecular bone in adult fossil hominin species, as we may be observing signals of juvenile behaviour if such a lag exists in these species as well, but that we may not understand skeletal bone development in apes as well as we think we do. A further understanding of the interaction between trabecular and cortical bone is necessary to see whether this lag may also influence cortical bone. If this is the case, it could influence age estimates, as young adult external morphology may be reflecting juvenile behaviours. This could influence the results of the ontogenetic studies discussed above (e.g. Berge 1998; 2002; Green and Alemseged 2012) as ontogenetic external morphology data of great apes was used as a comparative sample. The delay in full internal fusion of the third metacarpal epiphysis observed in this study also indicated that skeletal maturity and dental maturity do not match up, and thus we should be careful in inferring and comparing life history patterns from differing fossil species when dental and/or skeletal data is not available for each respectively.

5.6 Limitations

While this study has provided novel data on the ontogenetic response of trabecular bone in the epiphysis and metaphysis and the results of this study are promising, as they show that a possible adaptive lag between mechanical loading patterns and internal bone structure in primates, this study was not without its limitations. This study has assumed that more frequently performed behaviours, such as knuckle-walking and climbing, would be better reflected by the trabecular morphology of the third metacarpal than infrequent behaviours (Rubin et al. 2002). As there was no behavioural data available for the specimens included in this study, we have assumed that ontogenetic behaviours and forms of locomotion changed in the same manner as

described by Doran (1997). It must also be remembered that systemic and environmental factors might also be of some influence on the trabecular bone structure.

Unfortunately, the sample size of this study also prevented some additional analyses that may have given different results. When comparing trabecular ontogeny between species, our study could not pick up any results that reflected the differences in behaviour between the two species. Studies have shown that adult western lowland gorillas are more arboreal (Remis 1998) than their mountain gorilla counterparts (Doran 1997). Differences have also been detected in life history patterns between the two species, with mountain gorillas weaning their infants approximately a year earlier than western lowland gorillas (Breuer et al. 2008; Stoinski et al 2013). These differences were not reflected in our results, but the sample size for our infant category was 1 and 3 for western lowland and mountain gorillas, respectively. A future study involving more younger specimens may be able to note these differences in the internal bone structure.

Another factor that was not taken into account was differences body size. As this is an ontogenetic study, it should be obvious that there would be massive size differences between age categories as well as between sexes, as *gorilla* is a highly sexual dimorphic species (Shea, 1985; Taylor, 1997). Unfortunately, body size data was not available for this sample. This study decided not to adjust the data according average body mass due to previous studies indicating that BV/TV, which is one of the main predictors of mechanical loading, was not correlated to body mass changes (Doube et al. 2011; Ryan and Shaw, 2013). Previous studies on mammalia (Doube et al 2011;Barak et al, 2013a; Christen et al 2015) have shown that BV/TV itself is not dependent on body size, while variables such as Tb.Th, Tb.N, and Tb.Sp showed

negative allometry. A study of 34 primate species with a range of body sizes (Ryan and Shaw 2013) showed that trabecular number, connectivity density, and degree of anisotropy all scaled inversely with size. However, it should be noted that other variables, such as Tb.Th and Tb.N, which influence BV/TV have been shown to de size dependent (Doube et al 2011; Barak et al. 2013a). Smaller mammals were shown to have high BV/TV due to an increase in Tb.N, while larger mammals had high BV/TV due to high Tb.Th. Though it should be noted that Ryan and Shaw (2013) found the opposite was true in primates. Bone volume fraction also showed no correlation to body size in an intraspecific human study of the calcaneus (Saers et al. 2019).As BV/TV has been shown to be negligibly influenced by animal size (Doube et al 2011), body mass differences would not have had a significant influence on our results. However, it should be kept in mind that body mass differences may be influencing how BV/TV is reached.

The small sample size also prevented this study from making a distinction between sexes. This may be problematic, as gorilla is highly sexually dimorphic and differences in behaviour have been observed between sexes. Studies on the epiphyseal fusion of macaques and gorillas (Randall 1944; Cheverud 1981) have indicated that epiphyseal fusion follows the same pattern in males and females, the timing of fusion differs, with females consistently having earlier fusion than males. This could influence the distribution of load through the epiphyses between sexes, as the cartilaginous layer at the growth plate is present for longer in males. A study on scapular ontogeny in mountain gorillas also showed that sexual dimorphism and size differences influence bone growth (Taylor 1995). Male scapulae were shown to grow faster and for a longer duration than those of females. This is most likely related to bigger body size for males, as the same study showed that sexual differences in

locomotor behaviours could not explain this difference in ontogenetic growth (Taylor 1995). However, as females have been shown to remain slightly more arboreal than males throughout life (Remis 1995; Taylor 1995; Doran 1997), it may be that when a larger sample size is used, differences in locomotion after 5 years of age, when knuckle-walking becomes predominant, may be reflected in trabecular structure. Strangely, females have also been shown to have larger body size then males until approximately 4 years of age (Shea 1981; Leigh and Shea 1996) and faster growth curves than males until 6 years of age, when this trend reverses (Leigh and Shea 1996), which may also influence the results.

5.7 Future Studies

Future studies should focus on three main aspects; an increase in sample size for gorilla, a comparison with different skeletal elements within species, and an inclusion of other primate species for comparison. Firstly, the small sample size for each age group made it difficult to ascertain for certain whether small differences in behaviour between species were present in the trabecular bone. Furthermore, the small sample size made it impossible to statistically test for sex and body size differences. Future studies should increase the sample size and focus on individuals with epiphyses. This will allow for testing of sex and body size differences and give a more detailed view of changes occurring in the epiphysis.

While the overall trend of low BV/TV at birth and an increase of this throughout the rest of ontogeny was observed in this study, we also have some preliminary evidence that in gorilla BV/TV is higher at birth and decreases during the first few months of life before increasing again. This trend was not observed in chimpanzees (Tsegai et al. 2018a) or the base of the gorilla third metacarpal (Ragni 2020), but was observed in humans (Ryan and Krovitz, 2006; Gosman and Ketcham,

2009; Raichlen et al. 2015; Saers et al. 2020) and thought to be related to the advent of bipedal movement. Here, we could not find a link between this trend and infant gorilla behaviour. The inclusion of other skeletal elements from the same species (and perhaps the same individuals) could show us if this is a systemic pattern, a pathology, or perhaps an unknown response to some biomechanical input.

Further inquiries should also try to get a comparative sample of other species, specifically of the other great apes and modern humans. This will allow us to test for how interspecific differences in locomotion are reflected in the trabecular structure of each species, and if each species' trabecular bone responds to mechanical loading to the same degree. We have already collected data on the third metacarpal of chimpanzees and plan to compare not only the trabecular ontogeny, but also cortical ontogeny of these two knuckle-walking species to one another. This will hopefully shed light on whether there are differences in how bone responds to similar mechanical loads in different species.

Study should also be done into the biomechanics of the growth plate and its effect on load distribution throughout the growing metacarpus. In 2014, Nguyen et al. published a finite element model of the third proximal phalanx. Finite element modelling is not done frequently, as it requires a lot of computing power and known data on bone densities, cartilage densities, bending stresses and the magnitude and directionality of other forces to be created, Currently, we do not know everything to be able to accurately model the growth plate in apes. Combining data from kinematic studies on live apes with bone variables may get us close, though. Creating a finite element model of the epiphysis and growth plate of the third metacarpal could inform us of how immature bone responds to mechanical loads during life and give us novel data on growth plate biomechanics in not only apes, but humans also.

6 Conclusion

This paper has shown that overall distribution of BV/TV in the third metacarpal of gorillas during ontogeny reflects shifts in locomotion, but has not demonstrated a link between a specific locomotor strategy and trabecular bone properties. Prior to 5 years of age, gorillas practice a combination of terrestrial palmigrady, knuckle-walking, vertical climbing, clinging, and other suspensory and arboreal behaviours that require the third metacarpal to be used in a flexed position more frequently. These behaviours were reflected in the trabecular bone, which showed a palmar BV/TV concentration in younger specimens, consistent with a flexed hand. Once terrestrial knuckle-walking became more dominant after 5 years of age, the BV/TV concentration moved dorsally on the epiphysis, consistent with more hyperextended hand postures. Overall, BV/TV, Tb.N, and Tb.Th were low at birth and increased throughout ontogeny, as seen in the upper limb of chimpanzees (Tsegai et al. 2018a). However, this study had access to a pair of very young (2 hours and 2 weeks old) specimens, which showed an initial higher concentration in BV/TV than specimens aged a few months. This drop was not related to any behavioural shifts, as seen in humans (Ryan and Krovitz, 2006; Gosman and Ketcham, 2009; Raichlen et al. 2015; Saers et al. 2020). Thus, while the results for changes in trabecular variables in the third metacarpal are similar to those found in the chimpanzee upper limb (Tsegai et al. 2018a) and third metacarpal base (Ragni, 2020), the pattern of higher BV/TV at birth may indicate that not all skeletal elements in great apes follow the same pattern of response to loading throughout ontogeny. Furthermore, an adaptive lag was discovered between adult locomotion and the fusion/resorption of trabeculae at the epiphysis, which suggests that More data should be collected on peri-natal trabecular bone morphology to identify to what degree early trabecular bone is genetically predetermined or influenced by biomechanical loads.

7 Bibliography

Abel, R. and Macho, G.A., (2011). Ontogenetic changes in the internal and external morphology of the ilium in modern humans. *Journal of Anatomy*, *218*(3), 324-335.

Aiello, L., and Dean, C. (1990). *An introduction to human evolutionary anatomy*. Academic Press.

Alemseged, Z., Spoor, F., Kimbel, W. H., Bobe, R., Geraads, D., Reed, D., and Wynn, J. G. (2006). A juvenile early hominin skeleton from Dikika, Ethiopia. *Nature*, *443*(7109), 296-301.

Almécija, S., Smaers, J. B., and Jungers, W. L. (2015). The evolution of human and ape hand proportions. *Nature communications*, 6(1), 1-11.

Antón, S. C., and Leigh, S. R. (2003). Growth and life history in Homo erectus. *Cambridge Studies in Biological and Evolutionary Anthropology*, 219-245.

Acquaah, F., Robson Brown, K. A., Ahmed, F., Jeffery, N., and Abel, R. L. (2015). Early trabecular development in human vertebrae: overproduction, constructive regression, and refinement. *Frontiers in endocrinology*, *6*, 67.

Baker, B. J., Dupras, T. L., and Tocheri, M. W. (2005). *The osteology of infants and children* (Vol. 12). Texas A&M University Press.

Barak, M.M., Lieberman, D.E. and Hublin, J.J., (2011). A Wolff in sheep's clothing: trabecular bone adaptation in response to changes in joint loading orientation. *Bone*, *49*(6), 1141-1151.

Barak, M. M., Lieberman, D. E., and Hublin, J. J. (2013a). Of mice, rats and men: trabecular bone architecture in mammals scales to body mass with negative allometry. *Journal of structural biology*, *183*(2), 123-131.

Barak, M. M., Lieberman, D. E., Raichlen, D., Pontzer, H., Warrener, A. G., and Hublin, J. J. (2013b). Trabecular evidence for a human-like gait in Australopithecus africanus. *PloS one*, 8(11), e77687.

Berge, C. (1998). Heterochronic processes in human evolution: an ontogenetic analysis of the hominid pelvis. *American Journal of Physical Anthropology*, *105*(4), 441-459.

Berger, L.R., De Ruiter, D.J., Churchill, S.E., Schmid, P., Carlson, K.J., Dirks, P.H. and Kibii, J.M., (2010). Australopithecus sediba: a new species of Homo-like australopith from South Africa. *Science*, *328*(5975),195-204.

Behringer, V., Deschner, T., Deimel, C., Stevens, J. M., and Hohmann, G. (2014). Age-related changes in urinary testosterone levels suggest differences in puberty onset and divergent life history strategies in bonobos and chimpanzees. *Hormones and behavior*, *66*(3), 525-533.

Bermúdez de Castro, J., Arsuaga, J.L., Carbonell, E., Rosas, A., Martınez, I. and Mosquera, M., (1997). A hominid from the Lower Pleistocene of Atapuerca, Spain: possible ancestor to Neandertals and modern humans. *Science*, *276*(5317),1392-1395.

Bertram, J. E., and Swartz, S. M. (1991). The 'law of bone transformation': a case of crying Wolff?. *Biological Reviews*, 66(3), 245-273.

Best, A., Holt, B., Troy, K. L., and Hamill, J. (2017). Trabecular bone in the calcaneus of runners. *PLoS ONE, 12(*12), e0190553.

Bevill, G., Eswaran, S. K., Gupta, A., Papadopoulos, P., and Keaveny, T. M. (2006). Influence of bone volume fraction and architecture on computed large-deformation failure mechanisms in human trabecular bone. *Bone*, 39(6), 1218-1225.

Biewener, A.A., Fazzalari, N.L., Konieczynski, D.D. and Baudinette, R.V., (1996). Adaptive changes in trabecular architecture in relation to functional strain patterns and disuse. *Bone*, *19*(1), 1-8.

Bolter, D.R. and Cameron, N., (2020). Utilizing auxology to understand ontogeny of extinct hominins: A case study on Homo naledi. *American Journal of Physical Anthropology*, *173*(2), 368-380.

Bolter, D. R., Elliott, M. C., Hawks, J., and Berger, L. R. (2020). Immature remains and the first partial skeleton of a juvenile Homo naledi, a late Middle Pleistocene hominin from South Africa. *Plos one*, *15*(4), e0230440.

Bolter, D. R., and Zihlman, A. L. (2003). Morphometric analysis of growth and development in wild-collected vervet monkeys (Cercopithecus aethiops), with

implications for growth patterns in Old World monkeys, apes and humans. *Journal of Zoology*, 260(1), 99-110.

Bolter, D. R., and Zihlman, A. L. (2012). Skeletal development in Pan paniscus with comparisons to Pan troglodytes. *American journal of physical anthropology*, *147*(4), 629-636.

Breuer, T., Hockemba, M. B. N., Olejniczak, C., Parnell, R. J., and Stokes, E. J. (2009). Physical maturation, life-history classes and age estimates of free-ranging western gorillas—Insights from Mbeli Bai, Republic of Congo. *American Journal of Primatology*, *71*(2), 106-119.

Brown, F., Harris, J., Leakey, R. and Walker, A., (1985). Early Homo erectus skeleton from west lake Turkana, Kenya. *Nature*, *316*(6031), 788-792.

Burr, D. B., and Organ, J. M. (2017). Postcranial skeletal development and its evolutionary implications. In: Percival, C.J. and Richtsmeier, J.T., (Eds). *Building bones: Bone formation and development in anthropology*, Cambridge University Press. Pp. 148 – 179.

Byers, S., Moore, A. J., Byard, R. W., and Fazzalari, N. L. (2000). Quantitative histomorphometric analysis of the human growth plate from birth to adolescence. *Bone*, *27*(4), 495-501.

Cameron, N., Bogin, B., Bolter, D., and Berger, L. R. (2017). The postcranial skeletal maturation of A ustralopithecus sediba. *American journal of physical anthropology*, *163*(3), 633-640.

Carlson, K. J., Sumner, D. R., Morbeck, M. E., Nishida, T., Yamanaka, A., and Boesch, C. (2008). Role of nonbehavioral factors in adjusting long bone diaphyseal structure in free-ranging Pan troglodytes. *International journal of primatology*, *29*(6), 1401-1420.

Carter, D. R. (1987). Mechanical loading history and skeletal biology. *Journal of biomechanics*, 20(11-12), 1095-1109.

Carter, D. R., and Beaupré, G. S. (2007). *Skeletal function and form: mechanobiology of skeletal development, aging, and regeneration*. Cambridge university press.

Carter, D. R., Orr, T. E., and Fyhrie, D. P. (1989). Relationships between loading history and femoral cancellous bone architecture. *Journal of biomechanics*, 22(3), 231-244.

Carter, D. R., Wong, M., and Orr, T. E. (1991). Musculoskeletal ontogeny, phylogeny, and functional adaptation. *Journal of biomechanics*, 24, 3-16.

Charles, J. F., Ermann, J., and Aliprantis, A. O. (2015). The intestinal microbiome and skeletal fitness: Connecting bugs and bones. *Clinical Immunology*, *159*(2), 163-169.

Chevalier, T., Colard, T., Colombo, A., Golovanova, L., Doronichev, V., and Hublin, J. J. (2021). Early ontogeny of humeral trabecular bone in Neandertals and recent modern humans. *Journal of Human Evolution*, *154*, 102968.

Cheverud, J. M. (1981). Epiphyseal union and dental eruption in Macaca mulatta. *American Journal of Physical Anthropology*, *56*(2), 157-167.

Chirchir, H. (2019). Trabecular bone fraction variation in modern humans, fossil hominins and other primates. *The Anatomical Record*, 302(2), 288-305.

Chirchir, H., Kivell, T. L., Ruff, C. B., Hublin, J. J., Carlson, K. J., Zipfel, B., and Richmond, B. G. (2015). Recent origin of low trabecular bone density in modern humans. *Proceedings of the National Academy of Sciences*, *112*(2), 366-371.

Chirchir, H., Zeininger, A., Nakatsukasa, M., Ketcham, R.A. and Richmond, B.G., (2017). Does trabecular bone structure within the metacarpal heads of primates vary with hand posture?. *Comptes Rendus Palevol*, *16*(5-6), 533-544.

Christen, P., Ito, K., Ellouz, R., Boutroy, S., Sornay-Rendu, E., Chapurlat, R. D., and Van Rietbergen, B. (2014). Bone remodelling in humans is load-driven but not lazy. *Nature communications*, 5(1), 1-5.

Christen, P., Ito, K., and van Rietbergen, B. (2015). A potential mechanism for allometric trabecular bone scaling in terrestrial mammals. *Journal of anatomy*, 226(3), 236-243.

Churchill, S. E., Holliday, T. W., Carlson, K. J., Jashashvili, T., Macias, M. E., Mathews, S., Sparling, T.L., Schmid, P., de Ruiter, D.J., and Berger, L. R. (2013). The upper limb of Australopithecus sediba. *Science*, 340(6129).

Cowin, S.C., (2002). Mechanosensation and fluid transport in living bone. *Journal of Musculoskeletal and Neuronal Interactions*, *2*(3), 256-260.

Crompton, R. H., Sellers, W. I., and Thorpe, S. K. (2010). Arboreality, terrestriality and bipedalism. *Philosophical Transactions of the Royal Society B: Biological Sciences*, 365(1556), 3301-3314.

Cunningham, C. A., and Black, S. M. (2009). Anticipating bipedalism: trabecular organization in the newborn ilium. *Journal of Anatomy*, 214(6), 817-829.

Currey, J.D. (2002). *Bones: Structure and Mechanics.* Princeton University Press.

Dainton, M., and Macho, G. A. (1999). Did knuckle walking evolve twice? *Journal of Human Evolution*, 36(2), 171-194.

Deckers, K. (2017). Rods and Plates: An Ontogenetic Framework for Trabecular Bone Development and Gait Mechanics in the Human Talus of a 19th Century Dutch Population. *MSc Thesis*, Leiden University.

Dean, M. C., and Lucas, V. S. (2009). Dental and skeletal growth in early fossil hominins. *Annals of human biology*, *36*(5), 545-561.

DeSilva, J. M., and Devlin, M. J. (2012). A comparative study of the trabecular bony architecture of the talus in humans, non-human primates, and Australopithecus. *Journal of Human Evolution*, *63*(3), 536-551.

Domínguez-Rodrigo, M., Pickering, T. R., and Bunn, H. T. (2012). Experimental study of cut marks made with rocks unmodified by human flaking and its bearing on claims of~ 3.4-million-year-old butchery evidence from Dikika, Ethiopia. *Journal of Archaeological Science*, 39(2), 205-214.

Dominguez-Rodrigo, M., Pickering, T.R., Baquedano, E., Mabulla, A., Mark, D.F., Musiba, C., Bunn, H.T., Uribelarrea, D., Smith, V., Diez-Martin, F. and Pérez-González, A., (2013). First partial skeleton of a 1.34-million-year-old Paranthropus boisei from Bed II, Olduvai Gorge, Tanzania. *PLoS One*, *8*(12).

Doran, D. M. (1997). Ontogeny of locomotion in mountain gorillas and chimpanzees. *Journal of Human Evolution*, 32(4), 323-344.

Doran, D.M. and McNeilage, A., 1998. Gorilla ecology and behavior. *Evolutionary Anthropology: Issues, News, and Reviews: Issues, News, and Reviews*, *6*(4), 120-131.

Doran, D.M., McNeilage, A., Greer, D., Bocian, C., Mehlman, P. and Shah, N., 2002. Western lowland gorilla diet and resource availability: New evidence, cross-site comparisons, and reflections on indirect sampling methods. *American Journal of Primatology: Official Journal of the American Society of Primatologists*, *58*(3), 91-116.

Doube, M., Kłosowski, M. M., Arganda-Carreras, I., Cordelières, F. P., Dougherty, R. P., Jackson, J. S., Schmid, B., Hutchinson, J.R., and Shefelbine, S. J. (2010). BoneJ: free and extensible bone image analysis in ImageJ. *Bone*, *47*(6), 1076-1079.

Doube, M., Kłosowski, M. M., Wiktorowicz-Conroy, A. M., Hutchinson, J. R., and Shefelbine, S. J. (2011). Trabecular bone scales allometrically in mammals and birds. *Proceedings of the Royal Society B: Biological Sciences*, *278*(1721), 3067-3073.

Druelle, F., Aerts, P., d'Août, K., Moulin, V., and Berillon, G. (2017). Segmental morphometrics of the olive baboon (Papio anubis): a longitudinal study from birth to adulthood. *Journal of anatomy*, 230(6), 805-819.

Dunmore, C. J., Kivell, T. L., Bardo, A., and Skinner, M. M. (2019). Metacarpal trabecular bone varies with distinct hand-positions used in hominid locomotion. *Journal of anatomy*, 235(1), 45-66.

Dunmore, C. J., Skinner, M. M., Bardo, A., Berger, L. R., Hublin, J. J., Pahr, D. H., Rosas, A., Stephens, N.B., and Kivell, T. L. (2020). The position of Australopithecus sediba within fossil hominin hand use diversity. *Nature Ecology and Evolution*, *4*(7), 911-918.

Dunmore, C. J., Wollny, G., and Skinner, M. M. (2018). MIA-Clustering: a novel method for segmentation of paleontological material. *PeerJ*, *6*, e4374.

Eckstein, F., Matsuura, M., Kuhn, V., Priemel, M., Müller, R., Link, T. M., and Lochmüller, E. M. (2007). Sex differences of human trabecular bone microstructure in aging are site-dependent. *Journal of Bone and Mineral Research*, 22(6), 817-824.

Fajardo, R. J., Desilva, J. M., Manoharan, R. K., Schmitz, J. E., Maclatchy, L. M., and Bouxsein, M. L. (2013). Lumbar vertebral body bone microstructural scaling in small to medium-sized strepsirhines. *The Anatomical Record*, *296*(2), 210-226.

Fajardo, R. J., and Müller, R. (2001). Three-dimensional analysis of nonhuman primate trabecular architecture using micro-computed tomography. *American Journal of Physical Anthropology*, *115*(4), 327-336.

Fajardo, R. J., Müller, R., Ketcham, R. A., and Colbert, M. (2007). Nonhuman anthropoid primate femoral neck trabecular architecture and its relationship to locomotor mode. *The Anatomical Record: Advances in Integrative Anatomy and Evolutionary Biology: Advances in Integrative Anatomy and Evolutionary Biology*, *290*(4), 422-436.

Ferretti, M., Cavani, F., Roli, L., Checchi, M., Magarò, M.S., Bertacchini, J. and Palumbo, C., 2019. Interaction among calcium diet content, pth (1-34) treatment and balance of bone homeostasis in rat model: The trabecular bone as keystone. *International journal of molecular sciences*, *20*(3), 753.

Fleagle, J.G., 2013. *Primate adaptation and evolution*. Academic press.

Fletcher, A. W. (2001). Development of infant independence from the mother in wild mountain gorillas. In Robbins, M.M., Sicotte, P., and Stewart, K.J. *Mountain gorillas: Three decades of research at Karisoke*. Cambridge University Press, pp

Frost, H. M. (1998). Changing concepts in skeletal physiology: Wolff's Law, the Mechanostat, and the “Utah Paradigm”. *American Journal of Human Biology: The Official Journal of the Human Biology Association*, 10(5), 599-605.

Fyhrie, D. P., and Kimura, J. H. (1999). Cancellous bone biomechanics. *Journal of biomechanics*, *32*(11), 1139-1148.

Gallagher, J.C., Jerpbak, C.M., Jee, W.S., Johnson, K.A., DeLuca, H.F. and Riggs, B.L., 1982. 1, 25-Dihydroxyvitamin D3: short-and long-term effects on bone and calcium metabolism in patients with postmenopausal osteoporosis. *Proceedings of the National Academy of Sciences*, *79*(10), 3325-3329.

Gasser J.A., Kneissel M. (2017) Bone Physiology and Biology. In: Smith S., Varela A., Samadfam R. (eds) *Bone Toxicology*. Molecular and Integrative Toxicology. Springer International, pp. 27 – 94.

Gorissen, B. M., Wolschrijn, C. F., van Vilsteren, A. A., van Rietbergen, B., and van Weeren, P. R. (2016). Trabecular bone of precocials at birth; Are they prepared to run for the wolf (f)?. *Journal of morphology*, *277*(7), 948-956.

Gorissen, B.M., Wolschrijn, C.F., van Rietbergen, B., Rieppo, L., Saarakkala, S. and van Weeren, P.R., (2018). Trabecular and subchondral bone development of the talus and distal tibia from foal to adult in the warmblood horse. *Anatomia, histologia, embryologia*, *47*(3), 206-215.

Gosman, J. H., and Ketcham, R. A. (2009). Patterns in ontogeny of human trabecular bone from SunWatch Village in the Prehistoric Ohio Valley: General features of microarchitectural change. *American Journal of Physical Anthropology*, 138(3), 318-332.

Green, D. J. (2013). Ontogeny of the hominoid scapula: The influence of locomotion on morphology. *American journal of physical anthropology*, *152*(2), 239-260.

Green, D. J., and Alemseged, Z. (2012). Australopithecus afarensis scapular ontogeny, function, and the role of climbing in human evolution. *Science*, 338(6106), 514-517.

Green, D. J., Gordon, A. D., and Richmond, B. G. (2007). Limb-size proportions in Australopithecus afarensis and Australopithecus africanus. *Journal of Human Evolution*, 52(2), 187-200.

Griffin, N. L., D'Août, K., Ryan, T. M., Richmond, B. G., Ketcham, R. A., and Postnov, A. (2010). Comparative forefoot trabecular bone architecture in extant hominids. *Journal of human evolution*, *59*(2), 202-213.

Gross, T., Kivell, T. L., Skinner, M. M., Nguyen, N. H., and Pahr, D. H. (2014). A CT-image-based framework for the holistic analysis of cortical and trabecular bone morphology. *Palaeontologia Electronica*, *17*(3), 13.

Haile-Selassie, Y., Latimer, B. M., Alene, M., Deino, A. L., Gibert, L., Melillo, S. M., Saylor, B.Z., Scott, G.R., and Lovejoy, C. O. (2010). An early Australopithecus

afarensis postcranium from Woranso-mille, Ethiopia. *Proceedings of the National Academy of Sciences*, 107(27), 12121-12126.

Haile-Selassie, Y., Saylor, B.Z., Deino, A., Levin, N.E., Alene, M. and Latimer, B.M., (2012). A new hominin foot from Ethiopia shows multiple Pliocene bipedal adaptations. *Nature*, *483*(7391), 565-569.

Halloran, B. P., Ferguson, V. L., Simske, S. J., Burghardt, A., Venton, L. L., and Majumdar, S. (2002). Changes in bone structure and mass with advancing age in the male C57BL/6J mouse. *Journal of bone and mineral research*, *17*(6), 1044-1050.

Hamada, Y., Chatani, K., Udono, T., Kikuchi, Y., and Gunji, H. (2003). A longitudinal study on hand and wrist skeletal maturation in chimpanzees (Pan troglodytes), with emphasis on growth in linear dimensions. *Primates*, 44(3), 259-271.

Harmand, S., Lewis, J. E., Feibel, C. S., Lepre, C. J., Prat, S., Lenoble, A., Boes, X., Quinn, R.L., Brenet, M., Arroyo, A., Taylor, N., Clement, S., Daver, G., Brugal, J., Leakey, L., Mortlock, R.A., Wright, J.D., Lokorodi, S., Kirwa, C., Kent, D.V. and Roche, H. (2015). 3.3-million-year-old stone tools from Lomekwi 3, West Turkana, Kenya. *Nature*, 521(7552), 310-315.

Harvey, P. H., and Clutton-Brock, T. H. (1985). Life history variation in primates. *Evolution*, *39*(3), 559-581.

Hébert, D., Lebrun, R., and Marivaux, L. (2012). Comparative three-dimensional structure of the trabecular bone in the talus of primates and its relationship to ankle joint loads generated during locomotion. *The Anatomical Record: Advances in Integrative Anatomy and Evolutionary Biology*, *295*(12), 2069-2088.

Hildebrand, T., & Rüegsegger, P. (1997). A new method for the model-independent assessment of thickness in three-dimensional images. *Journal of microscopy*, *185*(1), 67-75.

Holliday, T.W. and Friedl, L., 2013. Hominoid humeral morphology: 3D morphometric analysis. *American journal of physical anthropology*, *152*(4), 506-515.

Huiskes, R. (2000). If bone is the answer, then what is the question?. *Journal of anatomy*, 197(2), 145-156.

Huiskes, R., Ruimerman, R., Van Lenthe, G. H., and Janssen, J. D. (2000). Effects of mechanical forces on maintenance and adaptation of form in trabecular bone. *Nature*, 405(6787), 704-706.

Hunt, K. D., Cant, J. G., Gebo, D. L., Rose, M. D., Walker, S. E., and Youlatos, D. (1996). Standardized descriptions of primate locomotor and postural modes. *Primates*, 37(4), 363-387.

Inouye, S. E. (1992). Ontogeny and allometry of African ape manual rays. *Journal of Human Evolution*, 23(2), 107-138.

Inouye, S. E. (1994). Ontogeny of knuckle-walking hand postures in African apes. *Journal of Human Evolution*, *26*(5-6), 459-485.

Isler, K. (2005). 3D-kinematics of vertical climbing in hominoids. *American Journal of Physical Anthropology*, 126(1), 66-81.

Judex, S., Donahue, L. R., and Rubin, C. (2002). Genetic predisposition to low bone mass is paralleled by an enhanced sensitivity to signals anabolic to the skeleton. *The FASEB Journal*, *16*(10), 1280-1282.

Kabel, J., Van Rietbergen, B., Odgaard, A., and Huiskes, R. (1999). Constitutive relationships of fabric, density, and elastic properties in cancellous bone architecture. *Bone*, *25*(4), 481-486.

Kerley, E. R. (1966). Skeletal age changes in the chimpanzee. *Tulane Studies Zool.*, 13, 71-82.

Kim, C. H., Takai, E., Zhou, H., Von Stechow, D., Müller, R., Dempster, D. W., and Guo, X. E. (2003). Trabecular bone response to mechanical and parathyroid hormone stimulation: the role of mechanical microenvironment. *Journal of bone and mineral research*, *18*(12), 2116-2125.

Kivell, T. L. (2007). *Ontogeny of the hominoid midcarpal joint and implications for the origin of human bipedalism*. PhD thesis, University of Toronto.

Kivell, T.L., (2016). A review of trabecular bone functional adaptation: what have we learned from trabecular analyses in extant hominoids and what can we apply to fossils?. *Journal of Anatomy*, *228*(4), 569-594.

Kivell, T. L., Lemelin, P., Richmond, B. G., and Schmitt, D. (2016). *The evolution of the primate hand*. Springer, New York.

Kivell, T. L., and Schmitt, D. (2009). Independent evolution of knuckle-walking in African apes shows that humans did not evolve from a knuckle-walking ancestor. *Proceedings of the National Academy of Sciences*, 106(34), 14241-14246.

Knigge, R.P., Tocheri, M.W., Orr, C.M. and Mcnulty, K.P., (2015). Three-dimensional geometric morphometric analysis of talar morphology in extant gorilla taxa from highland and lowland habitats. *The Anatomical Record*, *298*(1), pp.277-290.

Kothari, M., Keaveny, T. M., Lin, J. C., Newitt, D. C., Genant, H. K., and Majumdar, S. (1998). Impact of spatial resolution on the prediction of trabecular architecture parameters. *Bone*, *22*(5), 437-443.

Kuo, S., Desilva, J. M., Devlin, M. J., Mcdonald, G., and Morgan, E. F. (2013). The effect of the Achilles tendon on trabecular structure in the primate calcaneus. *The Anatomical Record*, *296*(10), 1509-1517.

Kuykendall, K. L. (2003). Reconstructing australopithecine growth and development: What do we think we know?. In Thompson, J.L., Krovitz, G.E., and Nelson, A.J. *Patterns of Growth and Development in the Genus Homo*, Cambridge University Press, pp. 191-218.

Langdahl, B., Ferrari, S., and Dempster, D. W. (2016). Bone modeling and remodeling: potential as therapeutic targets for the treatment of osteoporosis. *Therapeutic advances in musculoskeletal disease*, 8(6), 225-235.

Lanyon, L.E., 1974. Experimental support for the trajectorial theory of bone structure. *The Journal of bone and joint surgery*, 56(1), 160-166.

Lanyon, L.E. and Baggott, D.G., 1976. Mechanical function as an influence on the structure and form of bone. *The Journal of bone and joint surgery. British volume*, *58*(4), 436-443.

Lanyon, L.E. and Rubin, C.T., 1984. Static vs dynamic loads as an influence on bone remodelling. *Journal of biomechanics*, *17*(12), 897-905.

Latimer, B., and Lovejoy, C. O. (1990). Metatarsophalangeal joints of Australopithecus afarensis. *American Journal of Physical Anthropology*, 83(1), 13-23.

Lazenby, R. A., Skinner, M. M., Hublin, J. J., and Boesch, C. (2011). Metacarpal trabecular architecture variation in the chimpanzee (Pan troglodytes): Evidence for locomotion and tool-use?. *American Journal of Physical Anthropology*, *144*(2), 215-225.

Leakey, L., Tobias, P., and Napier, J. (1964). A new species of the genus Homo from Olduvai Gorge. *Nature*, 202(3), 7–9.

Leigh, S. R., and Shea, B. T. (1996). Ontogeny of body size variation in African apes. *American Journal of Physical Anthropology*, *99*(1), 43-65.

Lordkipanidze, D., Jashashvili, T., Vekua, A., Ponce de León, M., Zollikofer, C.P., Rightmire, G.P., Pontzer, H., Ferring, R., Oms, O., Tappen, M. and Bukhsianidze, M. (2007). Postcranial evidence from early Homo from Dmanisi, Georgia. *Nature*, 449, 305–310.

Lovejoy, C. O., McCollum, M. A., Reno, P. L., and Rosenman, B. A. (2003). Developmental biology and human evolution. *Annual Review of Anthropology*, *32*(1), 85-109.

MacLatchy, L. and Müller, R., (2002). A comparison of the femoral head and neck trabecular architecture of Galago and Perodicticus using micro-computed tomography (μCT). *Journal of human evolution*, *43*(1), 89-105.

Maga, M., Kappelman, J., Ryan, T.M. and Ketcham, R.A., (2006). Preliminary observations on the calcaneal trabecular microarchitecture of extant large-bodied hominoids. *American Journal of Physical Anthropology*, *129*(3), 410-417.

Majumdar, S., Kothari, M., Augat, P., Newitt, D. C., Link, T. M., Lin, J. C., Lang, A., T., Lu, A. Y., ,and Genant, H. K. (1998). High-resolution magnetic resonance imaging: three-dimensional trabecular bone architecture and biomechanical properties. *Bone*, *22*(5), 445-454.

Marchi, D. (2005). The cross-sectional geometry of the hand and foot bones of the Hominoidea and its relationship to locomotor behavior. *Journal of Human Evolution*, 49(6), 743-761.

Marieb, E.N., Wilhelm, P.B., and Mallatt, J.B. (2014). *Human Anatomy*. Pearson, UK.

Marzke, M. W., and Marzke, R. F. (1987). The third metacarpal styloid process in humans: origin and functions. *American Journal of Physical Anthropology*, 73(4), 415-431.

Matarazzo, S.A., (2013). Manual pressure distribution patterns of knuckle-walking apes. *American journal of physical anthropology*, *152*(1), 44-50.

Matarazzo, S.A., (2015). Trabecular architecture of the manual elements reflects locomotor patterns in primates. *PloS one*, *10*(3).

McFarlin, S. C., Bromage, T. G., Lilly, A. A., Cranfield, M. R., Nawrocki, S. P., Eriksen, A., and Mudakikwa, A. (2009, January). Recovery and preservation of a mountain gorilla skeletal resource in Rwanda. In *American Journal of Physical Anthropology*, 187-188.

McPherron, S. P., Alemseged, Z., Marean, C. W., Wynn, J. G., Reed, D., Geraads, D., Bobe, R., and Béarat, H. A. (2010). Evidence for stone-tool-assisted consumption of animal tissues before 3.39 million years ago at Dikika, Ethiopia. *Nature*, 466(7308), 857-860.

McPherron, S. P., Alemseged, Z., Marean, C., Wynn, J. G., Reed, D., Geraads, D., Bobe, R., and Béarat, H. (2011). Tool-marked bones from before the Oldowan change the paradigm. *Proceedings of the National Academy of Sciences*, 108(21), E116-E116.

Melillo, S. M. (2015). An alternative interpretation of the Australopithecus scapula. *Proceedings of the National Academy of Sciences*, 112(52), E7159-E7159.

Milovanovic, P., Djonic, D., Hahn, M., Amling, M., Busse, B. and Djuric, M., (2017). Region-dependent patterns of trabecular bone growth in the human proximal femur: A study of 3D bone microarchitecture from early postnatal to late childhood period. *American journal of physical anthropology*, *164*(2), 281-291.

Mullender, M., Van Rietbergen, B., Rüegsegger, P., and Huiskes, R. (1998). Effect of mechanical set point of bone cells on mechanical control of trabecular bone architecture. *Bone,* 22*(*2), 125-131.

Müller, R. (2005). Long-term prediction of three-dimensional bone architecture in simulations of pre-, peri-and post-menopausal microstructural bone remodeling. *Osteoporosis International*, 16(2), S25-S35.

Nafei, A., Kabel, J., Odgaard, A., Linde, F., and Hvid, I. (2000). Properties of growing trabecular ovine bone: PART II: architectural and mechanical properties. *The Journal of bone and joint surgery. British volume*, 82(6), 921-927.

Neufuss, J., Robbins, M. M., Baeumer, J., Humle, T., and Kivell, T. L. (2017). Comparison of hand use and forelimb posture during vertical climbing in mountain gorillas (Gorilla beringei beringei) and chimpanzees (Pan troglodytes). *American journal of physical anthropology*, 164(4), 651-664.

Nguyen, N. H., Pahr, D. H., Gross, T., Skinner, M. M., and Kivell, T. L. (2014). Micro-finite element (μFE) modeling of the siamang (Symphalangus syndactylus) third proximal phalanx: the functional role of curvature and the flexor sheath ridge. *Journal of human evolution*, *67*, 60-75.

van Noordwijk, M. A., and van Schaik, C. P. (2005). Development of ecological competence in Sumatran orangutans. *American Journal of Physical Anthropology*, 127(1), 79-94.

Nuzzo, S., Meneghini, C., Braillon, P., Bouvier, R., Mobilio, S. and Peyrin, F., (2003). Microarchitectural and physical changes during fetal growth in human vertebral bone. *Journal of bone and mineral research*, *18*(4), 760-768

Ortner, D. J. (2003). *Identification of pathological conditions in human skeletal remains*. Academic Press.

Ozcivici, E., and Judex, S. (2014). Trabecular bone recovers from mechanical unloading primarily by restoring its mechanical function rather than its morphology. *Bone, 67*, 122-129.

Pahr, D. H., and Zysset, P. K. (2008). Influence of boundary conditions on computed apparent elastic properties of cancellous bone. *Biomechanics and modeling in mechanobiology*, *7*(6), 463-476.

Panger, M. A., Brooks, A. S., Richmond, B. G., and Wood, B. (2002). Older than the Oldowan? Rethinking the emergence of hominin tool use. *Evolutionary Anthropology: Issues, News, and Reviews: Issues, News, and Reviews*, 11(6), 235-245.

Parr, W. C. H., Chamoli, U., Jones, A., Walsh, W. R., and Wroe, S. (2013). Finite element micro-modelling of a human ankle bone reveals the importance of the trabecular network to mechanical performance: new methods for the generation and comparison of 3D models. *Journal of biomechanics*, *46*(1), 200-205.

Parfitt, A. M. (2003). New concepts of bone remodeling: A unified spatial and temporal model with physiologic and pathophysiologic implications. In Agarwal, S. C., and Stout, S. D. (Eds.). (2003). *Bone loss and osteoporosis: an anthropological perspective*. Kluwer Academic/Plenum Publishers, pp. 3 – 17.

Patel, B. A., and Maiolino, S. A. (2016). Morphological diversity in the digital rays of primate hands. In Kivell, T. L., Lemelin, P., Richmond, B. G., and Schmitt, D. (2016). *The evolution of the primate hand*. Springer, New York, pp 55 – 100.

Perchalski, B., Placke, A., Sukhdeo, S.M., Shaw, C.N., Gosman, J.H., Raichlen, D.A. and Ryan, T.M., (2018). Asymmetry in the cortical and trabecular bone of the human humerus during development. *The Anatomical Record*, *301*(6), 1012-1025.

Pettersson, U., Nilsson, M., Sundh, V., Mellström, D., and Lorentzon, M. (2010). Physical activity is the strongest predictor of calcaneal peak bone mass in young Swedish men. *Osteoporosis international*, 21(3), 447-455.

Pontzer, H., Lieberman, D. E., Momin, E., Devlin, M. J., Polk, J. D., Hallgrimsson, B., and Cooper, D. M. L. (2006). Trabecular bone in the bird knee responds with high sensitivity to changes in load orientation. *Journal of Experimental Biology*, 209(1), 57-65.

Pouydebat, E. (2017) Introduction: The Necessity to Develop an Interdisciplinary Approach to Understand Grasping and Manipulation. *FOLIA PRIMATOLOGICA*, 88(2), 136-136.

Prakasam, G., Yeh, J. K., Chen, M. M., Castro-Magana, M., Liang, C. T., and Aloia, J. F. (1999). Effects of growth hormone and testosterone on cortical bone formation and bone density in aged orchiectomized rats. *Bone*, *24*(5), 491-497.

Rafferty, K. L., and Ruff, C. B. (1994). Articular structure and function in Hylobates, Colobus, and Papio. *American Journal of Physical Anthropology*, 94(3), 395-408.

Ragni, A. J. (2020). Trabecular architecture of the capitate and third metacarpal through ontogeny in chimpanzees (Pan troglodytes) and gorillas (Gorilla gorilla). *Journal of human evolution*, 138, 102702.

Randall, F. E. (1944). The Skeletal and Dental Development and Variability of the Gorilla"(Concluded)". *Human Biology*, *16*(1), 23 – 76.

Remis, M. (1995). Effects of body size and social context on the arboreal activities of lowland gorillas in the Central African Republic. *American Journal of Physical Anthropology*, *97*(4), 413-433.

Remis, M. J. (1998). The gorilla paradox. In Strasser, E., Fleagle, J., Rosenberger, A., and McHenry, H. (Eds) *Primate locomotion: Recent Advances.* Springer, Boston, MA, pp. 95-106.

Remis, M.J., Dierenfeld, E.S., Mowry, C.B. and Carroll, R.W., 2001. Nutritional aspects of western lowland gorilla (Gorilla gorilla gorilla) diet during seasons of fruit scarcity at Bai Hokou, Central African Republic. *International Journal of Primatology*, *22*(5), 807-836.

Raichlen, D. A. (2005). Ontogeny of limb mass distribution in infant baboons (Papio cynocephalus). *Journal of Human Evolution*, *49*(4), 452-467.

Raichlen, D. A., Gordon, A. D., Foster, A. D., Webber, J. T., Sukhdeo, S. M., Scott, R. S., Gosman, J.H., and Ryan, T. M. (2015). An ontogenetic framework linking locomotion and trabecular bone architecture with applications for reconstructing hominin life history. *Journal of human evolution*, 81, 1-12.

Richmond, B. G. (2006). Functional morphology of the midcarpal joint in knuckle-walkers and terrestrial quadrupeds. In Ishada, H., Tuttle, R., Pickford, M., Ogihara, N., and Nakatsukasa,M. *Human origins and environmental backgrounds*. Springer, Boston, MA, pp. 105 – 122.

Richmond, B. G. (2007). Biomechanics of phalangeal curvature. *Journal of Human Evolution*, 53(6), 678-690.

Richmond, B.G. and Strait, D.S. (2000). Evidence that humans evolved from a knuckle-walking ancestor. *Nature*, 404(6776), 382-385.

Robling, A. G., and Turner, C. H. (2002). Mechanotransduction in bone: genetic effects on mechanosensitivity in mice. *Bone*, *31*(5), 562-569.

Rolian, C. (2016). The role of genes and development in the evolution of the primate hand. In Kivell, T. L., Lemelin, P., Richmond, B. G., and Schmitt, D. (2016). *The evolution of the primate hand*. Springer, New York, pp. 101 – 130.

Rolian, C., Lieberman, D. E., and Zermeno, J. P. (2011). Hand biomechanics during simulated stone tool use. *Journal of Human Evolution*, 61(1), 26-41.

Rosas, A., Ríos, L., Estalrrich, A., Liversidge, H., García-Tabernero, A., Huguet, R., Cardoso, H., Bastir, M., Lalueza-Fox, C., de la Rasilla, M., and Dean, C. (2017). The growth pattern of Neandertals, reconstructed from a juvenile skeleton from El Sidrón (Spain). *Science*, *357*(6357), 1282-1287.

Rubin, C.T. and Lanyon, L.E., 1984. Regulation of bone formation by applied dynamic loads. *J Bone Joint Surg Am*, *66*(3), 397-402.

Rubin, C.T. and Lanyon, L.E., 1985. Regulation of bone mass by mechanical strain magnitude. *Calcified tissue international*, *37*(4), 411-417.

Rubin, C., Xu, G., and Judex, S. (2001). The anabolic activity of bone tissue, suppressed by disuse, is normalized by brief exposure to extremely low-magnitude mechanical stimuli. *The FASEB Journal*, *15*(12), 2225-2229.

Rubin, C., Turner, A. S., Müller, R., Mittra, E., McLeod, K., Lin, W., and Qin, Y. X. (2002). Quantity and quality of trabecular bone in the femur are enhanced by a strongly anabolic, noninvasive mechanical intervention. *Journal of bone and mineral research*, *17*(2), 349-357.

Ruff, C. (2003). Growth in bone strength, body size, and muscle size in a juvenile longitudinal sample. *Bone*, 33(3), 317-329.

Ruff, C.B., Burgess, M.L., Bromage, T.G., Mudakikwa, A. and McFarlin, S.C., (2013). Ontogenetic changes in limb bone structural proportions in mountain gorillas (Gorilla beringei beringei). *Journal of human evolution*, *65*(6), 693-703.

Ruff, C.B., Burgess, M.L., Ketcham, R.A. and Kappelman, J., (2016). Limb bone structural proportions and locomotor behavior in AL 288-1 (" Lucy"). *PLoS One*, *11*(11).

Ryan, T. M., and Ketcham, R. A. (2002). The three-dimensional structure of trabecular bone in the femoral head of strepsirrhine primates. *Journal of human evolution*, 43(1), 1-26.

Ryan, T. M., and Krovitz, G. E. (2006). Trabecular bone ontogeny in the human proximal femur. *Journal of human evolution*, 51(6), 591-602.

Ryan, T. M., Raichlen, D. A., and Gosman, J. H. (2017). Structural and mechanical changes in trabecular bone during early development in the human femur and humerus. In: Percival, C.J. and Richtsmeier, J.T., (Eds). *Building bones: Bone formation and development in anthropology*, Cambridge University Press. Pp. 281 – 302.

Ryan, T. M., and Shaw, C. N. (2012). Unique suites of trabecular bone features characterize locomotor behavior in human and non-human anthropoid primates. *PloS one*, *7*(7), e41037.

Ryan, T. M., and Shaw, C. N. (2013). Trabecular bone microstructure scales allometrically in the primate humerus and femur. *Proceedings of the Royal Society B: Biological Sciences*, *280*(1758), 20130172.

Ryan, T. M., and Van Rietbergen, B. (2005). Mechanical significance of femoral head trabecular bone structure in Loris and Galago evaluated using micromechanical finite element models. *American Journal of Physical Anthropology: The Official Publication of the American Association of Physical Anthropologists*, *126*(1), 82-96.

Ryan, T. M., and Walker, A. (2010). Trabecular bone structure in the humeral and femoral heads of anthropoid primates. *The Anatomical Record: Advances in Integrative Anatomy and Evolutionary Biology*, 293(4), 719-729.

Saers, J. P., Ryan, T. M., and Stock, J. T. (2019). Trabecular bone structure scales allometrically in the foot of four human groups. *Journal of human evolution*, *135*, 102654.

Saers, J. P., Ryan, T. M., and Stock, J. T. (2020). Baby steps towards linking calcaneal trabecular bone ontogeny and the development of bipedal human gait. *Journal of anatomy*, 236(3), 474-492.

Sarmiento, E. E. (1988). Anatomy of the hominoid wrist joint: its evolutionary and functional implications. *International Journal of Primatology*, *9*(4), 281-345.

Sarringhaus, L. A., MacLatchy, L. M., and Mitani, J. C. (2014). Locomotor and postural development of wild chimpanzees. *Journal of human evolution*, 66, 29-38.

Scherf, H., Harvati, K., and Hublin, J. J. (2013). A comparison of proximal humeral cancellous bone of great apes and humans. *Journal of human evolution*, 65(1), 29-38.

Scheuer, L., Black, S. and Christie, A., 2000. *Developmental Juvenile Osteology*. Academic Press.

Schilling, A. M., Tofanelli, S., Hublin, J. J., and Kivell, T. L. (2014). Trabecular bone structure in the primate wrist. *Journal of morphology*, 275(5), 572-585.

Schmitt, D., Zeininger, A., and Granatosky, M. C. (2016). Patterns, variability, and flexibility of hand posture during locomotion in primates. In Kivell, T. L., Lemelin, P., Richmond, B. G., and Schmitt, D. (2016). *The evolution of the primate hand*. Springer, New York, pp.345-369.

Schultz, A. H. (1940). Growth and development of the chimpanzee. *Contr. Embryol., 28*, 1-63.

Seto, H., Aoki, K., Kasugai, S. and Ohya, K., 1999. Trabecular bone turnover, bone marrow cell development, and gene expression of bone matrix proteins after low calcium feeding in rats. *Bone*, *25*(6), 687-695.

Shea, B. T. (1981). Relative growth of the limbs and trunk in the African apes. *American Journal of Physical Anthropology*, *56*(2), 179-201.

Shea, B.T., (1986). Ontogenetic approaches to sexual dimorphism in anthropoids. *Human Evolution*, *1*(2), 97.

Sinclair, K. D., Farnsworth, R. W., Pham, T. X., Knight, A. N., Bloebaum, R. D., and Skedros, J. G. (2013). The artiodactyl calcaneus as a potential 'control bone'cautions against simple interpretations of trabecular bone adaptation in the anthropoid femoral neck. *Journal of human evolution*, *64*(5), 366-379.

Skedros, J. G., and Baucom, S. L. (2007). Mathematical analysis of trabecular 'trajectories' in apparent trajectorial structures: the unfortunate historical emphasis on the human proximal femur. *Journal of theoretical biology*, *244*(1), 15-45.

Skinner, M. M., Stephens, N. B., Tsegai, Z. J., Foote, A. C., Nguyen, N. H., Gross, T., Pahr, D.H., Hublin, J.J., and Kivell, T. L. (2015). Human-like hand use in Australopithecus africanus. *Science*, 347(6220), 395-399.

Smith, B.H., 1989. Dental development as a measure of life history in primates. *Evolution*, *43*(3), 683-688.

Smith, B.H., 1991. Dental development and the evolution of life history in Hominidae. *American Journal of Physical Anthropology*, *86*(2), 157-174.

Smith, H.B., Crummett, T. L., and Brandt, K. L. (1994). Ages of eruption of primate teeth: a compendium for aging individuals and comparing life histories. *American journal of physical anthropology*, *37*(S19), 177-231.

Smith, B.H. and Tompkins, R.L., 1995. Toward a life history of the Hominidae. *Annual Review of Anthropology*, *24*(1), pp.257-279.

Sode, M., Burghardt, A. J., Nissenson, R. A., and Majumdar, S. (2008). Resolution dependence of the non-metric trabecular structure indices. *Bone*, *42*(4), 728-736.

Stephens, N.B., Kivell, T.L., Gross, T., Pahr, D.H., Lazenby, R.A., Hublin, J.J., Hershkovitz, I. and Skinner, M.M., (2016). Trabecular architecture in the thumb of Pan and Homo: implications for investigating hand use, loading, and hand preference in the fossil record. *American Journal of Physical Anthropology*, *161*(4), 603-619.

Stephens, N. B., Kivell, T. L., Pahr, D. H., Hublin, J. J., and Skinner, M. M. (2018). Trabecular bone patterning across the human hand. *Journal of Human Evolution*, *123*, 1-23.

Stern Jr, J. T. (2000). Climbing to the top: a personal memoir of Australopithecus afarensis. *Evolutionary Anthropology: Issues, News, and Reviews: Issues, News, and Reviews*, 9(3), 113-133.

Stern, J.T. and Susman, R.L., (1983). The locomotor anatomy of Australopithecus afarensis. *American Journal of Physical Anthropology*, *60*(3), 279-317.

Stewart, K. J. (1988). Suckling and lactational anoestrus in wild gorillas (Gorilla gorilla). *Reproduction*, 83(2), 627-634.

Stewart, K. J. (2001). Social relationships of immature gorillas and silverbacks. In Robbins, M.M., Sicotte, P., and Stewart, K.J. *Mountain gorillas: Three decades of research at Karisoke*. Cambridge University Press, pp. 183-213.

Stickens, D., and Evans, G. A. (1998). A sugar fix for bone tumours?. *Nature genetics*, *19*(2), 110-111.

Stoinski, T. S., Perdue, B., Breuer, T., and Hoff, M. P. (2013). Variability in the developmental life history of the genus Gorilla. *American journal of physical anthropology*, *152*(2), 165-172.

Su, A., and Carlson, K. J. (2017). Comparative analysis of trabecular bone structure and orientation in South African hominin tali. *Journal of Human Evolution*, 106, 1-18.

Su, A., Wallace, I. J., and Nakatsukasa, M. (2013). Trabecular bone anisotropy and orientation in an Early Pleistocene hominin talus from East Turkana, Kenya. *Journal of Human Evolution*, 64(6), 667-677.

Susman, R.L., (1979). Comparative and functional morphology of hominoid fingers. *American journal of physical anthropology*, *50*(2), pp.215-236

Swartz, S. M., Bertram, J. E., and Biewener, A. A. (1989). Telemetered in vivo strain analysis of locomotor mechanics of brachiating gibbons. *Nature*, *342*(6247), 270-272.

Swartz, S.M., Parker, A. and Huo, C., 1998. Theoretical and empirical scaling patterns and topological homology in bone trabeculae. *The Journal of experimental biology*, *201*(4),573-590.

Tanck, E., Hannink, G., Ruimerman, R., Buma, P., Burger, E. H., and Huiskes, R. (2006). Cortical bone development under the growth plate is regulated by mechanical load transfer. *Journal of anatomy*, *208*(1), 73-79.

Tanck, E., Homminga, J., van Lenthe, G. H., and Huiskes, R. (2001). Increase in bone volume fraction precedes architectural adaptation in growing bone. *Bone*, 28(6), 650-654.

Tardieu, C. (1999). Ontogeny and phylogeny of femoro-tibial characters in humans and hominid fossils: functional influence and genetic determinism. *American Journal of Physical Anthropology*, 110(3), 365-377.

Taylor, A. B. (1995). Effects of ontogeny and sexual dimorphism on scapula morphology in the mountain gorilla (Gorilla gorilla beringel). *American journal of physical anthropology*, *98*(4), 431-445.

Taylor, A. B. (1997). Relative growth, ontogeny, and sexual dimorphism in Gorilla (Gorilla gorilla gorilla and G. g. beringei): Evolutionary and ecological considerations. *American Journal of Primatology*, *43*(1), 1-31.

Thompson, N.E., Ostrofsky, K.R., McFarlin, S.C., Robbins, M.M., Stoinski, T.S. and Almécija, S., (2018). Unexpected terrestrial hand posture diversity in wild mountain gorillas. *American journal of physical anthropology*, *166*(1), 84-94

Thorpe, S. K., and Crompton, R. H. (2006). Orangutan positional behavior and the nature of arboreal locomotion in Hominoidea. *American Journal of Physical Anthropology: The Official Publication of the American Association of Physical Anthropologists*, 131(3), 384-401.

Tsegai, Z.J., Kivell, T.L., Gross, T., Nguyen, N.H., Pahr, D.H., Smaers, J.B. and Skinner, M.M., (2013). Trabecular bone structure correlates with hand posture and use in hominoids. *PLoS One*, *8*(11).

Tsegai, Z. J., Skinner, M. M., Gee, A. H., Pahr, D. H., Treece, G. M., Hublin, J. J., and Kivell, T. L. (2017). Trabecular and cortical bone structure of the talus and distal tibia in Pan and Homo. *American Journal of Physical Anthropology*, *163*(4), 784-805.

Tsegai, Z. J., Skinner, M. M., Pahr, D. H., Hublin, J. J., and Kivell, T. L. (2018a). Ontogeny and variability of trabecular bone in the chimpanzee humerus, femur and tibia. *American journal of physical anthropology*, *167*(4), 713-736.

Tsegai, Z. J., Skinner, M. M., Pahr, D. H., Hublin, J. J., and Kivell, T. L. (2018b). Systemic patterns of trabecular bone across the human and chimpanzee skeleton. *Journal of Anatomy*, 232(4), 641-656.

Turley, K. and Frost, S.R., 2013. The shape and presentation of the catarrhine talus: a geometric morphometric analysis. *The Anatomical Record*, *296*(6), 877-890.

Tuttle, R.H., (1969). Knuckle-walking and the problem of human origins. *Science*, *166*(3908), 953-961.

Ulrich, D., Van Rietbergen, B., Laib, A., and Ruegsegger, P. (1999). The ability of three-dimensional structural indices to reflect mechanical aspects of trabecular bone. *Bone*, 25(1), 55-60.

Van Rietbergen, B., Odgaard, A., Kabel, J., and Huiskes, R. (1996). Direct mechanics assessment of elastic symmetries and properties of trabecular bone architecture. *Journal of biomechanics*, *29*(12), 1653-1657.

Ward, C. V., Kimbel, W. H., and Johanson, D. C. (2011). Complete fourth metatarsal and arches in the foot of Australopithecus afarensis. *Science*, 331(6018), 750-753.

Wallace, I. J., Demes, B., and Judex, S. (2017). 10 Ontogenetic and Genetic Influences on Bone's Responsiveness to Mechanical Signals. In: Percival, C.J. and Richtsmeier, J.T., (Eds). *Building bones: Bone formation and development in anthropology*, Cambridge University Press. Pp. 233 – 253.

Ward, C.V., (2002). Interpreting the posture and locomotion of Australopithecus afarensis: where do we stand?. *American Journal of Physical Anthropology: The Official Publication of the American Association of Physical Anthropologists*, *119*(S35), 185-215.

Watts, D. P., and Pusey, A. E. (1993). Behavior of juvenile and adolescent great apes. In M. E. Pereira, M.E., and Fairbanks, L.A. (Eds.) *Juvenile Primates; Life History, Development and Behavior.* New York: Oxford University Press, pp. 148–167

Wolschrijn, C. F., and Weijs, W. A. (2004). Development of the trabecular structure within the ulnar medial coronoid process of young dogs. *The Anatomical Record Part A: Discoveries in Molecular, Cellular, and Evolutionary Biology*, 278(2), 514-519.

Wickham, H. (2009). ggplot2: elegant graphics for data analysis (use R!). *Springer, New York, 10*, 978-0.

Wunderlich, R. E., and Jungers, W. L. (2009). Manual digital pressures during knuckle-walking in chimpanzees (Pan troglodytes). *American Journal of Physical Anthropology*, 139(3), 394-403.

Young, N. M., Capellini, T. D., Roach, N. T., and Alemseged, Z. (2015). Fossil hominin shoulders support an African ape-like last common ancestor of humans and chimpanzees. *Proceedings of the National Academy of Sciences*, 112(38), 11829-11834.

Zeininger, A.D., 2013. *Ontogeny of bipedalism: pedal mechanics and trabecular bone morphology* (PhD dissertation).

Zeininger, A., Patel, B. A., Zipfel, B., and Carlson, K. J. (2016). Trabecular architecture in the StW 352 fossil hominin calcaneus. *Journal of human evolution*, *97*, 145-158.

Zeininger, A., Richmond, B. G., and Hartman, G. (2011). Metacarpal head biomechanics: A comparative backscattered electron image analysis of trabecular bone mineral density in Pan troglodytes, Pongo pygmaeus, and Homo sapiens. *Journal of human evolution*, *60*(6), 703-710.

Zihlman, A., Bolter, D., and Boesch, C. (2004). Wild chimpanzee dentition and its implications for assessing life history in immature hominin fossils. *Proceedings of the National Academy of Sciences*, *101*(29), 10541-10543.

8 Appendix

Table 6. Summary table of trabecular bone results for the base (Prox-) and metaphysis (Dist-).

Specimen	Subspecies	AgeGroups	ProxBVTV	DistBVTV	ProxDA	DistDA	ProxTbth	DistTbth	ProxTbN	DistTbN	ProxTbSp	DistTbSp
PC_M476	Ggg	1	0.152151	0.177615	0.549537	0.430809	0.127355	0.121918	1.092508	1.061209	0.78797	0.820404
MGSP_GP133	Gbb	1	0.137868	0.144235	0.38939	0.480123	0.156104	0.145673	1.180499	1.049042	0.690995	0.807578
MGSP_GP140	Gbb	1	0.168491	0.202416	0.410154	0.547729	0.107579	0.108533	2.035549	1.600343	0.383689	0.516333
MGSP_GP113	Gbb	1	0.252842	0.274633	0.426498	0.563335	0.109543	0.106598	2.670683	2.469726	0.264893	0.298305
PC_M117	Ggg	2	0.175266	0.229046	0.43115	0.502742	0.175831	0.17026	0.897223	1.150291	0.93872	0.699085
PC_M690	Ggg	2	0.22776	0.292916	0.545743	0.481938	0.179102	0.206636	0.719501	1.352789	1.21075	0.532578
MGSP_GP014	Gbb	2	0.265497	0.348762	0.35321	0.463147	0.236759	0.230653	0.750264	1.506165	1.096105	0.433285
MGSP_GP114	Gbb	2	0.210853	0.22739	0.343019	0.418198	0.216439	0.196115	1.019893	1.221925	0.764056	0.622266
MGSP_GP194	Gbb	2	0.199518	0.220426	0.351979	0.463335	0.23148	0.205409	0.871686	1.330316	0.915722	0.546292
MGSP_GP195	Gbb	2	0.17659	0.217653	0.329863	0.427907	0.161684	0.173416	1.362739	1.5782	0.572132	0.460217
ZMB_7907	Ggg	2	0.199452	0.176966	0.380617	0.388801	0.181719	0.165267	1.329056	0.879855	0.570695	0.971284
PC_MER_33_756	Ggg	2	0.250544	0.332791	0.379239	0.394857	0.188643	0.21353	0.912811	1.509492	0.906874	0.448944

PC_MER_34_887	Ggg	2	0.181804	0.266842	0.411332	0.331745	0.158366	0.158758	1.136626	1.655112	0.721431	0.44543
MGSP_GP009	Gbb	3	0.203637	0.291769	0.354719	0.370358	0.229521	0.211319	0.663578	1.437834	1.277461	0.484171
MGSP_GP025	Gbb	3	0.241388	0.268295	0.364374	0.42752	0.201653	0.189007	0.85602	1.570746	0.966544	0.447633
MGSP_GP071	Gbb	3	0.232693	0.318898	0.400119	0.458275	0.244562	0.22831	0.575563	1.484219	1.492868	0.445445
MGSP_GP125	Gbb	3	0.270568	0.31869	0.302684	0.427542	0.245379	0.228023	0.830355	1.451012	0.958925	0.461151
ZMB_30306	Ggg	3	0.237096	0.276295	0.352076	0.383993	0.234076	0.227162	0.701476	1.3322	1.191488	0.523476
MGSP_GP165	Gbb	3	0.271676	0.345043	0.349535	0.412942	0.204457	0.184223	0.942987	1.990428	0.856003	0.318181
PC_MER_409	Ggg	3	0.306414	0.330438	0.415865	0.361068	0.231984	0.186691	0.746618	1.778086	1.107389	0.375711
PC_MER_333	Ggg	3	0.319241	0.330438	0.462001	0.361068	0.204441	0.186691	1.308762	1.778086	0.559639	0.375711
PC_MER_33_471	Ggg	3	0.273163	0.288882	0.360809	0.442826	0.224115	0.204441	0.83861	1.308762	0.968334	0.559639
PC_MER_35_29	Ggg	3	0.329619	0.208376	0.483752	0.442005	0.235217	0.14286	0.860208	1.752841	0.927292	0.427642
PC_MER_35_99	Ggg	3	0.338109	0.34561	0.35953	0.509382	0.234079	0.213985	0.967748	1.478303	0.799248	0.462466
PC_MER_35_141	Ggg	3	0.307378	0.303925	0.471669	0.366007	0.196464	0.192466	1.120861	1.516808	0.695707	0.466813
PC_CAMI14	Ggg	4	0.343072	0.273474	0.379458	0.450541	0.308288	0.218918	0.697965	1.169552	1.124448	0.63611

PC_CAMI107	Ggg	4	0.363146	0.37394	0.39548	0.408655	0.37923	0.256334	0.52603	1.31644	1.52178	0.50328
MGSP_GP004	Gbb	4	0.265303	0.29971	0.30291	0.400013	0.28084	0.235656	0.79953	1.36806	0.96988	0.49530
MGSP_GP030	Gbb	4	0.308865	0.25527	0.31998	0.451817	0.44638	0.333404	0.71115	0.55098	0.95977	1.48153
MGSP_GP038	Gbb	4	0.304523	0.28872	0.28124	0.374537	0.35608	0.251044	0.54536	1.12917	1.47755	0.63456
MGSP_GP075	Gbb	4	0.304989	0.32256	0.30427	0.424944	0.26204	0.245059	1.16562	1.45936	0.59586	0.44017
MGSP_GP147	Gbb	4	0.293185	0.29373	0.28466	0.428202	0.35221	0.270349	0.75939	1.22360	0.96462	0.54690
ZMB_10493	Ggg	4	0.344044	0.28057	0.3262	0.471538	0.27069	0.235119	0.9087	1.13814	0.82978	0.64350
ZMB_31617	Gbb	4	0.433675	0.46912	0.33627	0.407561	0.29677	0.274203	1.11977	1.52350	0.59625	0.38217
MGSP_GP026	Gbb	5	0.39853	0.35206	0.35994	0.364175	0.41313	0.322172	0.71809	1.01703	0.97944	0.66108
MGSP_GP167	Gbb	5	0.337741	0.32653	0.30324	0.32469	0.35092	0.285056	0.67053	1.11603	1.14042	0.61097
MGSP_GP116	Gbb	5	0.249116	0.20233	0.32446	0.296143	0.26855	0.21424	0.68043	1.05577	1.20110	0.73293
MGSP_GP078	Gbb	5	0.238878	0.22437	0.31908	0.312261	0.29012	0.263228	0.57139	0.94034	1.45996	0.80020
MGSP_GP124	Gbb	5	0.33277	0.28637	0.39132	0.392083	0.38073	0.332855	0.68986	0.90723	1.06882	0.76939
MGSP_GP131	Gbb	5	0.267657	0.09442	0.32600	0.360762	0.30920	0.261385	0.63063	0.87718	1.27649	0.87862

MGSP_GP139	Gbb	5	0.336542	0.318334	0.364308	0.360394	0.333838	0.292009	0.767299	1.116998	0.969434	0.603248
MGSP_GP190	Gbb	5	0.305823	0.279481	0.335261	0.35451	0.469742	0.333654	0.420972	0.870788	1.905713	0.814731
ZMB_31624	Gbb	5	0.369409	0.246999	0.380805	0.358192	0.270603	0.23208	0.948253	1.135861	0.783968	0.648309
MGSP_GP191	Gbb	5	0.350039	0.281775	0.326926	0.421297	0.486124	0.330214	0.603001	0.827246	1.172248	0.878615
PC_MER_95	Ggg	5	0.343104	0.176308	0.296711	0.374282	0.333307	0.304962	0.681045	0.767242	1.135025	0.998408
PC_MER_135	Ggg	5	0.359652	0.279327	0.414241	0.454052	0.33799	0.325335	0.683358	0.784143	1.125371	0.949943
PC_MER_300	Ggg	5	0.341634	0.271905	0.339907	0.334447	0.320927	0.297914	1.291267	0.855435	1.291267	0.871083
PC_MER_372	Ggg	5	0.373076	0.19601	0.362456	0.441012	0.388363	0.304378	0.590095	0.819402	1.30628	0.916024
PC_MER_962	Ggg	5	0.312572	0.216028	0.384735	0.479492	0.334251	0.288336	0.565445	0.843694	1.434269	0.896929
PC_MERI_29	Ggg	5	0.408073	0.146204	0.391799	0.397196	0.304641	0.260518	0.924349	1.008188	0.777201	0.73136
PC_MER_138	Ggg	5	0.33442	0.195003	0.361032	0.400993	0.279835	0.246535	0.772172	0.943833	1.015213	0.812975
PC_ZII_64	Ggg	5	0.398353	0.301281	0.325428	0.501631	0.422586	0.275056	0.716373	0.996634	0.973334	0.728321

Table 7. Summary results of trabecular parameters epiphysis (head).

Specimen	Subspecies	AgeGroups	BVTV	DA	TbTh	TbN	TbSp
PC_CAMI14	Ggg	4	0.324406	0.298934	0.240313	1.056334	0.706357
PC_CAMI107	Ggg	4	0.346689	0.321596	0.316351	0.888947	0.808576
MGSP_GP026	Gbb	5	0.118112	0.434347	0.341677	0.961372	0.698502
MGSP_GP030	Gbb	4	0.365407	0.327652	0.380183	0.854302	0.790363
MGSP_GP038	Gbb	4	0.037664	0.463572	0.260363	1.12945	0.625023
MGSP_GP075	Gbb	4	0.332333	0.28168	0.243275	1.375853	0.483547
MGSP_GP147	Gbb	4	0.348055	0.249654	0.299976	1.08928	0.618062
MGSP_GP167	Gbb	5	0.06848	0.451282	0.287599	1.114294	0.60983
MGSP_GP116	Gbb	5	0.279258	0.245676	0.246521	1.070681	0.687464
MGSP_GP078	Gbb	5	0.061005	0.411377	0.28781	0.998545	0.713647
MGSP_GP124	Gbb	5	0.14591	0.448495	0.342374	0.922403	0.741751
MGSP_GP131	Gbb	5	0.072803	0.437483	0.267983	0.976567	0.756012
MGSP_GP139	Gbb	5	0.086578	0.417203	0.302946	1.105362	0.601735
MGSP_GP190	Gbb	5	0.066319	0.324002	0.378713	0.8319	0.823355
ZMB_7907	Ggg	2	0.245512	0.314923	0.163117	1.577958	0.470613
ZMB_10493	Ggg	4	0.295225	0.33286	0.260331	0.846263	0.921335
ZMB_30306	Ggg	3	0.268886	0.304268	0.201697	1.19655	0.63404
ZMB_31624	Gbb	5	0.334645	0.266111	0.245745	1.174957	0.60535
MGSP_GP191	Gbb	5	0.087117	0.421774	0.354056	0.826298	0.856161
PC_MER_95	Ggg	5	0.079072	0.444238	0.306582	0.87971	0.830156
PC_MER_135	Ggg	5	0.111565	0.471221	0.339202	0.794352	0.919685
PC_MER_300	Ggg	5	0.112954	0.49127	0.311094	0.91043	0.787289
PC_MER_372	Ggg	5	0.049194	0.236713	0.312212	0.872792	0.833537
PC_MER_962	Ggg	5	0.062946	0.505019	0.304134	0.8431	0.881965
PC_MERI_29	Ggg	5	0.112671	0.545344	0.257263	1.104159	0.648404

PC_MER_138	Ggg	5	0.096243	0.496296	0.250615	1.025834	0.724201
PC_ZII_64	Ggg	5	0.122731	0.399737	0.326923	0.952144	0.723339
MGSP_GP165	Gbb	3	0.271792	0.295245	0.204441	1.308762	0.559639
PC_MER_409	Ggg	3	0.35924	0.306576	0.204945	1.571336	0.431456
PC_MER_333	Ggg	3	0.296779	0.379776	0.198197	1.230034	0.614788
PC_MER_35_29	Ggg	3	0.298918	0.39831	0.210777	1.224097	0.606152
PC_MER_35_141	Ggg	3	0.278176	0.31844	0.17942	1.390127	0.539939

Table 8. Summary table ratios base/growth plate (Prox/Dist)

Specimen	Subspecies	AgeGroups	ProxDistBVTV	ProxDistDA	ProxDistTbth	ProxDistTbN	ProxDistTbSp
PC_M117	Ggg	2	0.7652	0.857597	1.032718	0.779996	1.342784
PC_M476	Ggg	1	0.856634	1.275593	1.044599	1.029494	0.960466
PC_CAMI14	Ggg	4	1.254496	0.842227	1.408233	0.59678	1.767694
PC_M690	Ggg	2	0.777561	1.132393	0.866754	0.531865	2.273376
PC_CAMI107	Ggg	4	0.971124	0.96776	1.479453	0.399587	3.023686
MGSP_GP004	Gbb	4	0.885178	0.757253	1.191775	0.584426	1.958158
MGSP_GP009	Gbb	3	0.697939	0.957773	1.086135	0.461512	2.638449
MGSP_GP014	Gbb	2	0.761256	0.76263	1.026473	0.498129	2.529757
MGSP_GP026	Gbb	5	1.131982	0.988396	1.282329	0.70607	1.481574
MGSP_GP030	Gbb	4	1.209912	0.708227	1.338881	1.290701	0.647826
MGSP_GP038	Gbb	4	1.054735	0.750911	1.4184	0.482978	2.328464
MGSP_GP025	Gbb	3	0.899711	0.852297	1.06691	0.544977	2.159231
MGSP_GP071	Gbb	3	0.729678	0.873098	1.071184	0.387788	3.351407
MGSP_GP075	Gbb	4	0.9455	0.716024	1.069315	0.798721	1.35371
MGSP_GP114	Gbb	2	0.927275	0.820231	1.103633	0.834661	1.227862

MGSP_GP125	Gbb	3	0.849001	0.707963	1.076116	0.572259	2.079416
MGSP_GP133	Gbb	1	0.955857	0.811021	1.071611	1.125312	0.855638
MGSP_GP140	Gbb	1	0.8324	0.748827	0.991208	1.271945	0.743104
MGSP_GP147	Gbb	4	0.998121	0.664782	1.302829	0.620618	1.763778
MGSP_GP167	Gbb	5	1.034312	0.933955	1.231067	0.600818	1.866574
MGSP_GP194	Gbb	2	0.905147	0.759664	1.126923	0.655248	1.676249
MGSP_GP195	Gbb	2	0.811337	0.770875	0.93235	0.863476	1.243179
MGSP_GP116	Gbb	5	1.231187	1.09565	1.253541	0.644482	1.638767
MGSP_GP078	Gbb	5	1.064623	1.021857	1.102187	0.607646	1.824483
MGSP_GP124	Gbb	5	1.162008	0.998072	1.143834	0.760401	1.389186
MGSP_GP131	Gbb	5	2.834707	0.903648	1.182963	0.718929	1.452835
MGSP_GP139	Gbb	5	1.057198	1.01086	1.143248	0.68693	1.607023
MGSP_GP190	Gbb	5	1.094253	0.945703	1.407872	0.483438	2.33907
MGSP_GP113	Gbb	1	0.920654	0.757095	1.027625	1.081368	0.887994
ZMB_7907	Ggg	2	1.127064	0.978951	1.099544	1.510541	0.587567
ZMB_10493	Ggg	4	1.226193	0.691779	1.151287	0.798405	1.289476
ZMB_30306	Ggg	3	0.858126	0.916881	1.030438	0.526555	2.276108
ZMB_31617	Gbb	4	0.924442	0.825081	1.082332	0.734998	1.56016
ZMB_31624	Gbb	5	1.495589	1.063131	1.16599	0.834831	1.209251
MGSP_GP191	Gbb	5	1.242264	0.775999	1.472148	0.728925	1.334199
PC_MER_95	Ggg	5	1.946049	0.792747	1.092946	0.887654	1.136835
PC_MER_135	Ggg	5	1.287566	0.912321	1.038899	0.871472	1.184672
PC_MER_300	Ggg	5	1.256446	1.016325	1.077249	1.509486	1.482371
PC_MER_372	Ggg	5	1.903352	0.821873	1.275922	0.720153	1.426033
PC_MER_962	Ggg	5	1.446905	0.80238	1.159244	0.670201	1.599089
PC_MERI_29	Ggg	5	2.791121	0.986412	1.169366	0.916842	1.062679

PC_MER_138	Ggg	5	1.714948	0.900345	1.135073	0.818124	1.248763
PC_ZII_64	Ggg	5	1.322198	0.64874	1.536363	0.718793	1.336408
MGSP_GP165	Gbb	3	0.787369	0.846451	1.109836	0.473761	2.690297
PC_MER_409	Ggg	3	0.927296	1.151764	1.242608	0.4199	2.947446
PC_MER_333	Ggg	3	0.966115	1.27954	1.095077	0.736051	1.489547
PC_MER_33_471	Ggg	3	0.945587	0.814787	1.096229	0.640766	1.730282
PC_MER_33_756	Ggg	2	0.752857	0.960446	0.883449	0.604714	2.020015
PC_MER_34_887	Ggg	2	0.681317	1.239904	0.997528	0.686736	1.619628
PC_MER_35_29	Ggg	3	1.581847	1.094449	1.646487	0.490751	2.168383
PC_MER_35_99	Ggg	3	0.978296	0.705816	1.093903	0.654634	1.72823
PC_MER_35_141	Ggg	3	1.011361	1.288688	1.020768	0.73896	1.490336

Table 9. Summary table ratios base/epiphysis (prox/head)

Specimen	Subspecies	AgeGroups	ProxHeadBVTV	ProxHeadDA	ProxHeadTbth	ProxHeadTbN	ProxHeadTbSp
PC_CAMI14	Ggg	4	1.057539	1.26937	1.282859	0.660743	1.591896
PC_CAMI107	Ggg	4	1.047469	1.229742	1.198774	0.591749	1.882059
MGSP_GP026	Gbb	5	3.37417	0.828713	1.209125	0.746949	1.402201
MGSP_GP030	Gbb	4	0.845263	0.976612	1.174143	0.832439	1.214346
MGSP_GP038	Gbb	4	8.085168	0.606689	1.36763	0.482859	2.363997
MGSP_GP075	Gbb	4	0.917721	1.080197	1.077155	0.847202	1.232277
MGSP_GP147	Gbb	4	0.842353	1.140222	1.174157	0.697151	1.560723
MGSP_GP167	Gbb	5	4.931987	0.671966	1.220181	0.601758	1.870064
MGSP_GP116	Gbb	5	0.892064	1.320719	1.089393	0.533677	1.747148
MGSP_GP078	Gbb	5	3.915705	0.775653	1.008049	0.57223	2.045784
MGSP_GP124	Gbb	5	2.280652	0.872534	1.112032	0.747901	1.440951

MGSP_GP131	Gbb	5	3.676476	0.745176	1.153837	0.645768	1.688455
MGSP_GP139	Gbb	5	3.88714	0.873215	1.101975	0.694161	1.611064
MGSP_GP190	Gbb	5	4.611373	1.03475	1.240366	0.506037	2.314569
ZMB_7907	Ggg	2	0.812392	1.208603	1.114035	0.842263	1.212663
ZMB_10493	Ggg	4	1.165362	0.979992	1.03979	1.07378	0.900632
ZMB_30306	Ggg	3	0.881771	1.157125	1.160537	0.586249	1.879201
ZMB_31624	Gbb	5	1.103883	1.431001	1.101156	0.807053	1.295066
MGSP_GP191	Gbb	5	4.018052	0.775121	1.373016	0.729762	1.369191
PC_MER_95	Ggg	5	4.339117	0.66791	1.087172	0.77417	1.412081
PC_MER_135	Ggg	5	3.223699	0.87908	0.996425	0.860271	1.223649
PC_MER_300	Ggg	5	3.024541	0.691894	1.031608	1.418305	1.640145
PC_MER_372	Ggg	5	7.583786	1.531204	1.243908	0.6761	1.567154
PC_MER_962	Ggg	5	4.965732	0.761823	1.099027	0.670673	1.62622
PC_MERI_29	Ggg	5	3.62181	0.718444	1.184163	0.837153	1.198637
PC_MER_138	Ggg	5	3.474743	0.727453	1.116593	0.752726	1.401838
PC_ZII_64	Ggg	5	3.245741	0.814105	1.292618	0.752379	1.345613
MGSP_GP165	Gbb	3	0.999573	1.183881	1.000079	0.720518	1.529561
PC_MER_409	Ggg	3	0.852951	1.356483	1.131934	0.475149	2.56663
PC_MER_333	Ggg	3	1.075686	0.950057	1.031505	1.064005	0.910296
PC_MER_35_29	Ggg	3	1.102707	1.214511	1.115952	0.702729	1.318561
PC_MER_35_141	Ggg	3	1.104977	1.481186	1.094992	0.806302	1.288493

Table 10. Summary table ratios metaphysis/epiphysis (Dist/head)

Specimen	Subspecies	AgeGroups	DistHeadBVTV	DistHeadDA	DistHeadTbth	DistHeadTbN	DistHeadSp
PC_CAMI14	Ggg	4	0.842999	1.507159	0.910971	1.10718	0.90055

PC_CAMI107	Ggg	4	1.078615	1.270709	0.810282	1.480902	0.622439
MGSP_GP026	Gbb	5	2.980764	0.838443	0.942913	1.057896	0.946426
MGSP_GP030	Gbb	4	0.698616	1.378954	1.174143	0.644951	1.874496
MGSP_GP038	Gbb	4	7.665594	0.807937	0.964206	0.999753	1.015261
MGSP_GP075	Gbb	4	0.97062	1.508606	1.007332	1.060698	0.910296
MGSP_GP147	Gbb	4	0.843938	1.715182	0.901237	1.123316	0.884875
MGSP_GP167	Gbb	5	4.768377	0.719484	0.991158	1.001566	1.00187
MGSP_GP116	Gbb	5	0.724556	1.205421	0.869053	0.98608	1.066136
MGSP_GP078	Gbb	5	3.67802	0.759063	0.91459	0.941717	1.121295
MGSP_GP124	Gbb	5	1.962682	0.872534	1.112032	0.747901	1.037263
MGSP_GP131	Gbb	5	1.296951	0.824631	0.975379	0.898236	1.162179
MGSP_GP139	Gbb	5	3.676834	0.863834	0.963898	1.010526	1.002515
MGSP_GP190	Gbb	5	4.214173	1.09416	0.881021	1.046746	0.989525
ZMB_7907	Ggg	2	0.720804	1.234591	1.013179	0.557591	2.063871
ZMB_10493	Ggg	4	0.95039	1.416626	0.903155	1.344906	0.698448
ZMB_30306	Ggg	3	1.027554	1.262022	1.126256	1.113368	0.82562
ZMB_31624	Gbb	5	0.738093	1.346025	0.944396	0.966725	1.070966
MGSP_GP191	Gbb	5	3.234458	0.998869	0.932661	1.001148	1.026227
PC_MER_95	Ggg	5	2.229706	0.842526	0.994717	0.872153	1.202675
PC_MER_135	Ggg	5	2.503715	0.963565	0.959116	0.987147	1.032901
PC_MER_300	Ggg	5	2.407219	0.68078	0.957632	0.939595	1.106434
PC_MER_372	Ggg	5	3.984437	1.863066	0.97491	0.938829	1.09896
PC_MER_962	Ggg	5	3.431968	0.949453	0.948055	1.000704	1.016967
PC_MERI_29	Ggg	5	1.297619	0.72834	1.012654	0.913083	1.127939
PC_MER_138	Ggg	5	2.02615	0.807971	0.983719	0.920064	1.122581
PC_ZII_64	Ggg	5	2.454808	1.254903	0.84135	1.046726	1.006888

MGSP_GP165	Gbb	3	1.269511	1.398642	0.901105	1.520848	0.568547
PC_MER_409	Ggg	3	0.919825	1.177744	0.910934	1.131576	0.870798
PC_MER_333	Ggg	3	1.113414	0.950739	0.941948	1.445558	0.611123
PC_MER_35_29	Ggg	3	0.697101	1.109701	0.677778	1.352109	0.705504
PC_MER_35_141	Ggg	3	1.092564	1.149375	1.072714	1.091129	0.864566